A UNIVERSAL INVARIANT OF FOUR-DIMENSIONAL 2-HANDLEBODIES AND THREE-MANIFOLDS

I. Bobtcheva

Dipartimento di Scienze Matematiche
Università Politecnica delle Marche – Italia

bobtchev@dipmat.univpm.it

R. Piergallini

Dipartimento di Matematica e Informatica
Università di Camerino – Italia

riccardo.piergallini@unicam.it

Abstract

In [2] it is shown that up to certain set of local moves, connected simple coverings of B^4 branched over ribbon surfaces, bijectively represent connected orientable 4-dimensional 2-handlebodies up to 2-deformations (handle slides and creations/cancellations of handles of index ≤ 2). We factor this bijective correspondence through a map onto the closed morphisms in a universal braided category $\mathcal{H}^r$ freely generated by a Hopf algebra object H. In this way we obtain a complete algebraic description of 4-dimensional 2-handlebodies. This result is then used to obtain an analogous description of the boundaries of such handlebodies, i.e. 3-dimensional manifolds, which resolves for closed manifolds the problem posed by Kerler in [13] (cf. [21, Problem 8-16 (1)]).

Keywords: 3-manifold, 4-manifold, handlebody, branched covering, ribbon surface, Kirby calculus, braided Hopf algebra, quantum invariant.

AMS Classification: 57M12, 57M27, 57N13, 57R56, 57R65, 16W30, 17B37, 18D35.

1. Introduction

During the last twenty years the developments in the quantum theory have build a bridge between two distinct areas of mathematics: the topology of low dimensions (2, 3 and 4) and the theory of Hopf algebras. An important result in this direction is the one of Shum [27], which states that the category of framed tangles is equivalent to the universal monoidal tortile category generated by a single object. Since the category of representations of a wide class of Hopf algebras, the so called ribbon Hopf algebras, is a tortile monoidal category (cf. [25, 16] etc.), the result of Shum implies that the subcategory generated by any representation of such a Hopf algebra produces an invariant of framed tangles. Framed tangles and links are interesting and rich object of study by themselves, but through surgery they are also the

main tool of describing 3- and 4-dimensional manifolds. Actually, 4-dimensional 2-handlebodies modulo 2-deformations (handle slidings and addition/deletion of canceling handles of indices ≤ 2), bijectively correspond to the equivalence classes of Kirby link diagrams modulo Kirby calculus moves (cf. [6] and Section 2 below), while 3-dimensional manifolds bijectively correspond to the equivalence classes of framed links modulo the Fenn-Rourke move [5]. Reshetikhin and Turaev [25] used this last fact to construct invariants of 3-manifolds, by showing that some finite dimensional Hopf algebras have a finite subset of representations S, such that a proper linear combination of the framed link invariants corresponding to the elements of S, is also invariant under the Fenn-Rourke move. On the other hand, Hennings [9] defined invariants of 3-manifolds starting directly with a unimodular ribbon Hopf algebra and a trace function on it. Eventually Lyubashenko and Kerler [12] constructed 3-manifold invariants (2+1 topological quantum field theory) out of a Hopf algebra in a linear abelian braided monoidal category with certain coends, and showed that Reshetikhin-Turaev's and Hennings' invariants are particular cases of such more general approach (cf. [10]).

All these results lead Kerler to define in [13] a surjective functor from a braided monoidal category $\mathcal{A}lg$, freely generated by a Hopf algebra object, to the category of 3-dimensional relative cobordisms $\mathcal{C}ob^{2+1}$. Moreover he asked what additional relations should be introduced in $\mathcal{A}lg$, so that the functor above defines an equivalence between the quotient of $\mathcal{A}lg$ by these relations and $\mathcal{C}ob^{2+1}$ (cf. [21, Problem 8-16 (1)]). Finding these relations would complete the characterization of $\mathcal{C}ob^{2+1}$ in purely algebraic terms.

In the present work we propose two new relations such that the corresponding functor on the quotient induces a bijective map between the closed morphisms of the algebraic category and the set of closed connected orientable 3-manifolds, obtaining in this way an algebraic characterization of such manifolds.

Our approach is independent of Kerler's work. Actually, we obtain the result for 3-manifolds as a consequence of the algebraic description of 4-dimensional 2-handlebodies modulo 2-deformations.

In particular, we construct a bijective correspondence between the set of equivalence classes of connected 4-dimensional 2-handlebodies modulo 2-deformations and the set of closed morphisms of a universal category $\mathcal{H}^r$. The objects of $\mathcal{H}^r$ are the elements of the free $(\diamond, \mathbf{1})$-algebra on a single object H and $\mathcal{H}^r$ is universal with respect to the properties that:

a) H is a unimodular braided Hopf algebra;

b) there is a special morphism $v : H \to H$ which makes H into a ribbon algebra as defined in 6.2 (over the trivial groupoid: one object and one relation).

We point out the following differences between $\mathcal{H}^r$ and the algebra $\mathcal{A}lg$ proposed by Kerler in [13].

Firstly, since we are interested in 4-dimensional 2-handlebodies, we do not require that the Hopf copairing $\mathbf{1} \to H \diamond H$ is non-degenerate. Such condition is equivalent to the requirement that the algebra integral and cointegral are dual with respect to this copairing (cf. (34) in [13]) and is necessary only when one restricts to 3-manifolds (cf. 6.9).

Secondly, we introduce the ribbon morphism as a morphism $v : H \to H$ instead of $v_K : \mathbf{1} \to H$ as it is done in [13]. These two ways are equivalent, being v obtainable by taking the product of v_K with the identity morphism on H and then composing with the multiplication. However, viewing the ribbon morphism as a morphism from the algebra to itself allows to talk about its propagation through the diagrams, which is a main tool in the proofs.

Besides these cosmetic differences, the new relations with respect to the ones given by Kerler are (*r10*) and (*r11*) in 6.2. The first one describes the propagation of the ribbon morphism through the copairing, and the second one relates the copairing and the braiding morphism.

Before stating the main results, we would like to sketch our approach to the problem. In [13] Kerler constructs a functor from the algebraic category to the category of Kirby tangles (similar map is presented also in [8]). The main difficulty in going the other way consists in the fact that the elementary morphisms in the universal braided Hopf algebra are local (involve only objects which are "close" to each other), while handle slides in general are not. So, to be able to go naturally from the topological category to the algebra, one would like to have an alternative description of the topological objects in which the moves of equivalence are more similar to the algebraic ones. For 4-dimensional 2-handlebodies such description is given in [2] in terms of simple coverings of B^4 branched over ribbon surfaces.

In particular, starting from a surgery description of a connected 4-dimensional 2-handlebody M as an ordinary Kirby diagram K (with a single 0-handle), in order to obtain a description of M as a simple covering of B^4 of degree $n \geq 4$ branched over a ribbon surface, one first stabilizes with $n-1$ pairs of canceling 0/1-handles. This transforms K into a generalized Kirby diagram $\widetilde{K}$, which represents the attaching maps of the 1- and 2-handles on the boundary of the n 0-handles. The generalized Kirby diagrams differ from the ordinary ones by the fact that in them each side of the spanning disks of the dotted components and each component of the framed ones, after cutting them at the intersections with those disks, carries a label from $\{1, 2, \ldots, n\}$, indicating the 0-handle where it lives. Examples of generalized Kirby tangles are shown in the right column of Figure 1, while the precise definition can be found in Section 2. By using the extra 0-handles, $\widetilde{K}$ can be symmetrized and the resulting diagram is interpreted as a labeled ribbon surface F_K in B^4, that is the branching surface of an n-fold covering. Moreover, if we change M by 2-deformation, i.e. change K by Kirby calculus moves, F_K changes by a sequence of local moves (1-isotopy and ribbon moves). The correspondence $K \mapsto F_K$ between labeled ribbon surfaces modulo 1-isotopy and ribbon moves, and generalized Kirby diagrams modulo Kirby calculus moves, is invertible (for the definition of the inverse $F \mapsto K_F$, see Section 2 in [2] and Section 4 below).

Therefore, in order to obtain the desired algebraic description of 4-dimensional 2-handlebodies it is enough to factor the correspondence $F \mapsto K_F$ through a map onto the morphisms of the algebraic category and since the equivalence moves on ribbon surfaces are local, this should be relatively easy to do. Yet, there is a price to pay: we will need a family of ribbon Hopf algebras $\mathcal{H}_n^r$, which generalize $\mathcal{H}^r = \mathcal{H}_1^r$ and describe 4-dimensional 2-handlebodies with n 0-handles. Then we will also need a "reduction" map, which is the algebraic analog of canceling pairs of 0/1-handles.

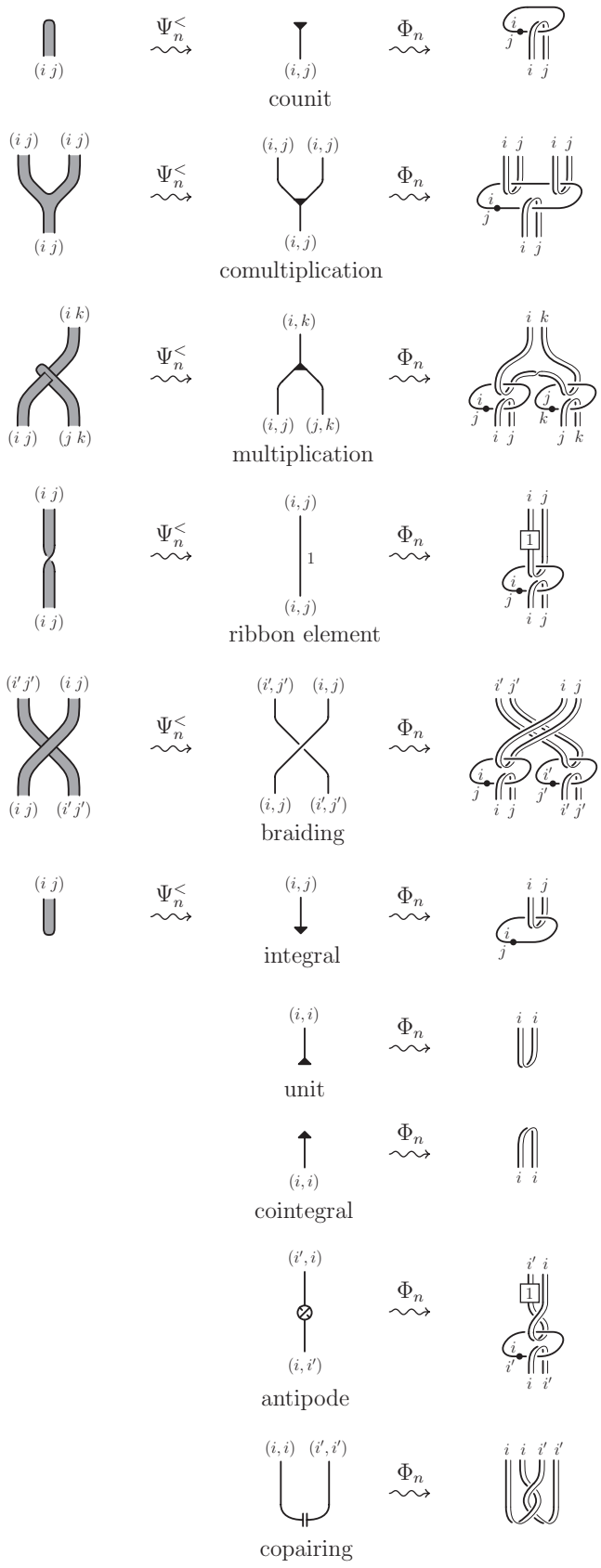
(i j)
Ψ≤n
(i, j)
Φn
counit
(i j) (i j)
(i j)
(i, j) (i, j)
(i, j)
comultiplication
(i k)
(i j) (j k)
(i, k)
(i, j) (j, k)
multiplication
(i j)
(i j)
(i, j)
1
(i, j)
ribbon element
(i′ j′) (i j)
(i j) (i′ j′)
(i′, j′) (i, j)
(i, j) (i′, j′)
braiding
integral
(i, i)
unit
(i, i)
cointegral
(i′, i)
(i, i′)
antipode
(i, i) (i′, i′)
copairing

FIGURE 1.

As one may expect, the construction of this map is the main technical difficulty to be overcome.

We now proceed with some more details and list the main results. Given a groupoid $\mathcal{G}$, we define a ribbon Hopf $\mathcal{G}$-algebra in a braided monoidal category (generalizing the concept of group Hopf algebra described in [29]) and introduce the universal category $\mathcal{H}^r(\mathcal{G})$ freely generated by a ribbon Hopf $\mathcal{G}$-algebra. Our basic example of a braided monoidal category with a ribbon Hopf $\mathcal{G}$-algebra in it, is the category of admissible generalized Kirby tangles $\mathcal{K}_n$ with n labels (equiv. n 0-handles) modulo slides of handles of index ≤ 2 and creations/cancellations of pairs of 1/2-handles. In this case, $\mathcal{G} = \mathcal{G}_n$ is the groupoid with objects $1, 2, \ldots, n$ and a single morphism, denoted by (i, j) between any i and j. In particular, if $\mathcal{H}^r_n = \mathcal{H}^r(\mathcal{G}_n)$ we have the following theorem, which extends results of Habiro [8] and Kerler [13].

THEOREM 1.1. *There is a braided monoidal functor* $\Phi_n : \mathcal{H}^r_n \to \mathcal{K}_n$.

The elementary morphisms in $\mathcal{H}^r_n$ and their images under Φ_n are presented on the right in Figure 1 (one needs to add the inverses of the braiding, the antipode and the ribbon morphism, but this is straightforward).

Another class of braided monoidal categories that we introduce are the categories $\mathcal{S}_n$ of *ribbon surface tangles* (rs-tangles) labeled by transpositions in the symmetric group Σ_n.

A smooth compact surface $F \subset B^4$ with $\operatorname{Bd} F \subset S^3 = R^3 \cup \infty$ is called a *ribbon surface* if the Euclidean norm restricts to a Morse function on F with no local maxima in $\operatorname{Int} F$. Then an rs-tangle should be thought as a slice of a ribbon surface. We present ribbon surfaces and rs-tangles through their projections in R^3. In particular, the objects in $\mathcal{S}_n$ are intervals labeled by transpositions in Σ_n, while any morphism is a composition of juxtapositions of the elementary morphisms presented on the left in Figures 1 and 2 (the transpositions $(i\ j)$ and $(k\ l)$ in Figure 2 are assumed to be disjoint, i.e. $\{i, j\} \cap \{k, l\} = \emptyset$). The relations in the category are given by 1-isotopy moves, which are special type of isotopy moves, and the two

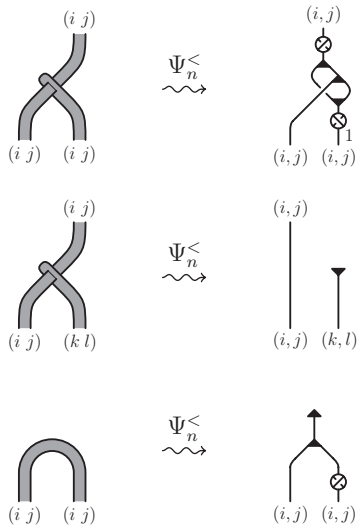

FIGURE 2. ($(i\ j)$ and $(k\ l)$ disjoint)

ribbon moves presented in Figure 3, where $(i\ j)$ and $(k\ l)$ are disjoint. It is not known if 1-isotopy coincides with isotopy of ribbon surfaces, for some discussions of this problem we refer the reader to [2].

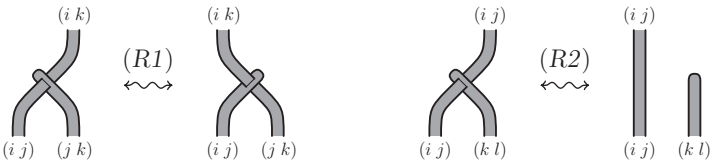

FIGURE 3. Ribbon relations in $\mathcal{S}_n$ ($(i\ j)$ and $(k\ l)$ disjoint).

Observe that each morphism in the monoidal categories we are considering is a composition of products (juxtapositions) of elementary ones and any elementary morphism involves some set of labels, which are morphisms in a given connected groupoid $\mathcal{G}$ ($\mathcal{G} = \mathcal{G}_n$ for $\mathcal{K}_n$ and $\mathcal{H}^r_n$, while $\mathcal{G} = \Sigma_n$ for $\mathcal{S}_n$). Then we call a morphism *complete* if the labels occurring in it together with the identities of $\mathcal{G}$ generate all $\mathcal{G}$, i.e. any element of $\mathcal{G}$ which is not an identity can be obtained as a product of those labels or their inverses. As it will be shown later, for each one of the categories used, the notion of completeness is well-posed, i.e it is preserved by equivalence of morphisms. In particular, a generalized Kirby diagram is complete if and only if it describes a connected 2-handlebody. Analogously, a labeled ribbon surface is complete if and only if it describes a connected branched covering.

Given such a monoidal category $\mathcal{C}$, we denote by $\widehat{\mathcal{C}}$ the set of *closed* morphisms, i.e. the ones having $\mathbf{1}$ (the empty object in $\mathcal{H}^r_n$ and $\mathcal{K}_n$) as source and target, and by $\widehat{\mathcal{C}}^c \subset \widehat{\mathcal{C}}$ the set of closed complete morphisms.

For $m < n$, there is an injection $\uparrow^n_m : \widehat{\mathcal{K}}^c_m \to \widehat{\mathcal{K}}^c_n$ which sends $K \in \mathcal{K}^c_m$ to its disjoint union with $n - m$ dotted components of labels $(m, m+1), (m+1, m+2), \ldots, (n-1, n)$. We call $\uparrow^n_m K$ the n-stabilization of K. In the handlebody, described by K, this corresponds to the creation of $n-m$ pairs of canceling 0/1-handles. As it is well known (cf. Section 2), any connected handlebody with n 0-handles is equivalent (through 1- and 2-handle slides) to the n-stabilization of a 2-handlebody with $m < n$ 0-handles. Therefore the stabilization map is invertible, and its inverse $\downarrow^n_m : \widehat{\mathcal{K}}^c_n \to \widehat{\mathcal{K}}^c_m$ will be called a reduction map.

The next theorem states the existence of analogous maps between the closed complete morphisms in $\mathcal{H}^r_m$ and $\mathcal{H}^r_n$ with $m < n$. Hopefully without causing a confusion, we use for these maps the same notation as for the corresponding maps between generalized Kirby diagrams.

THEOREM 1.2. *Given $m < n$, there exist a stabilization map $\uparrow^n_m : \widehat{\mathcal{H}}^{r,c}_m \to \widehat{\mathcal{H}}^{r,c}_n$ and a reduction map $\downarrow^n_m : \widehat{\mathcal{H}}^{r,c}_n \to \widehat{\mathcal{H}}^{r,c}_m$ which are the inverse of each another, such that $\Phi_n \circ \uparrow^n_m = \uparrow^n_m \circ \Phi_m$.*

One can also define a stabilization map $\uparrow^n_m : \widehat{\mathcal{S}}^c_m \to \widehat{\mathcal{S}}^c_n$ between the corresponding sets of labeled ribbon surfaces, by sending $F \in \widehat{\mathcal{S}}^c_m$ to the disjoint union of F and $n - m$ disks labeled by the permutations $(m\ m{+}1), (m{+}1\ m{+}2), \ldots, (n{-}1\ n)$, and we denote by $\uparrow^n_m F$ the n-stabilization of F. Proposition 4.2 in [2] states that this map is invertible for $n > m \geq 3$ (that is any $F' \in \widehat{\mathcal{S}}^c_n$ is equivalent through 1-isotopy

and ribbon moves to the n-stabilization of a surface $F \in \widehat{\mathcal{S}}^c_m$). The inverse is called again a reduction map and is denoted by $\downarrow^n_m : \widehat{\mathcal{S}}^c_n \to \widehat{\mathcal{S}}^c_m$.

Recall that our goal is to factor the bijective correspondence $F \mapsto K_F$ between the set $\widehat{\mathcal{S}}^c_n$ of complete labeled ribbon surfaces and the set $\widehat{\mathcal{K}}^c_n$ of complete generalized Kirby diagrams with $n \geq 4$, through a map onto the closed complete morphisms in the universal algebraic category $\widehat{\mathcal{H}}^{r,c}_n$. This is done by defining a functor $\mathcal{S}_n \to \mathcal{H}^r_n$ and then composing it with Φ_n. Observe that the objects in $\mathcal{S}_n$ and $\mathcal{H}^r_n$ are not the same: in $\mathcal{S}_n$ they are intervals labeled by simple permutations, i.e. unordered pairs of indices, while in $\mathcal{H}^r_n$ they are intervals labeled by morphisms in $\mathcal{G}_n$, i.e. ordered pairs of indices. Then, any functor $\mathcal{S}_n \to \mathcal{H}^r_n$ requires a choice of an ordering of the indices. However, its restriction to the closed morphisms is independent on such a choice, as indicated in the next theorem.

THEOREM 1.3. *Let $<$ denote a strict total order on the set of objects of $\mathcal{G}_n$. Then there exists a braided monoidal functor $\Psi^<_n : \mathcal{S}_n \to \mathcal{H}^r_n$. Moreover, if $<'$ is another strict total order on the set of objects of $\mathcal{G}_n$, there is a natural equivalence $\tau : \Psi^<_n \to \Psi^{<'}_n$ which is identity on the empty set. In particular, the restriction of $\Psi^<_n$ to $\widehat{\mathcal{S}}_n$ is independent on $<$ and is denoted by Ψ_n.*

On the left in Figures 1 and in Figure 2 we present the images under $\Psi^<_n$ of the elementary morphisms with some choices of labels. We assume $i < j < k$ and $i' < j'$ in Figure 1, and $i < j$, $k < l$, $\{k, l\} \cap \{i, j\} = \emptyset$ in Figure 2. The images under $\Psi^<_n$ of elementary morphisms with different orderings of the labels are similar (see Section 9).

The following theorem summarizes and completes the algebraic description of 4-dimensional 2-handlebodies.

THEOREM 1.4. *For $n \geq 4$ there is a commutative diagram of bijective maps:*

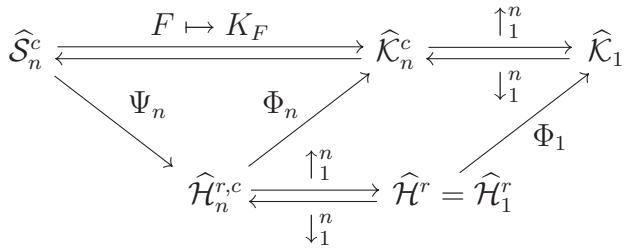

Observe that, since $F \mapsto K_F$ is a bijective map, the commutativity of the diagram implies that Ψ_n is injective and Φ_n is surjective. Therefore to prove the bijectivity of all maps in the diagram it is enough to show that Ψ_n is also surjective when $n \geq 4$.

In order to deal with 3-manifolds we basically need to quotient all the categories involved in Theorem 1.4 by some additional relations. Indeed, according to Kirby [14], we can think of closed connected 3-manifolds as connected 4-dimensional 2-handlebodies modulo 1/2-handle trading and positive/negative blowups. The quotient category of $\mathcal{K}_n$ modulo these extra relations is denoted by $\partial\mathcal{K}_n$. Analogously, following [2], one can introduce in $\mathcal{S}_n$ the additional local relations presented in Figure 4. Those relations preserve up to isotopy the boundary of the ribbon surface while changing its Euler characteristic. Let $\partial\mathcal{S}_n$ denote the quotient of $\mathcal{S}_n$ modulo

these additional relations. Then Theorem 2 in [2] states that $F \mapsto K_F$ defines a bijective correspondence between $\partial\widehat{\mathcal{S}}_n^c$ and $\partial\widehat{\mathcal{K}}_n^c$ for $n \geq 4$.

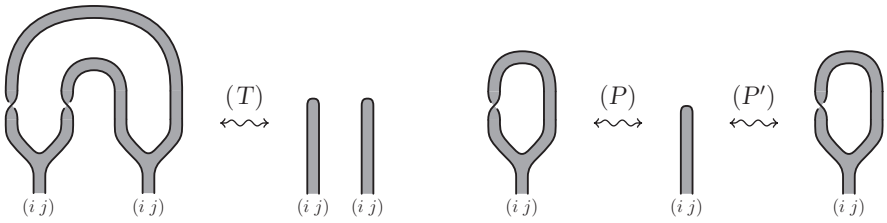

FIGURE 4. Additional relations in $\partial\mathcal{S}_n$.

In the same spirit, in Paragraph 6.9 we introduce two additional relations in $\mathcal{H}_n^r$: the first one states the duality of the algebra integral andcointegral with respect to the copairing, and the second one is a normalization in sense that a specific closed morphism is sent to the trivial morphism on $\mathbf{1}$. Let $\partial\mathcal{H}_n^r$ denote the quotient of $\mathcal{H}_n$ modulo these two relations and put $\partial\widehat{\mathcal{H}}^r = \partial\widehat{\mathcal{H}}_1^r$. Then the algebraic description of 3-manifolds follows from our last theorem.

THEOREM 1.5. *The braided monoidal functors Φ_n and Ψ_n induce well defined functors $\partial\Phi_n : \partial\mathcal{H}_n^r \to \partial\mathcal{K}_n$ and $\partial\Psi_n : \partial\mathcal{S}_n \to \partial\mathcal{H}_n^r$ between the quotient categories. Moreover, $\uparrow_m^n$ and $\downarrow_m^n$ induce well defined bijective maps $\partial\uparrow_m^n : \partial\widehat{\mathcal{H}}_m^{r,c} \to \partial\widehat{\mathcal{H}}_n^{r,c}$ and $\partial\downarrow_m^n : \partial\widehat{\mathcal{H}}_n^{r,c} \to \partial\widehat{\mathcal{H}}_m^{r,c}$, for any $m < n$. Consequently, the commutative diagram in Theorem 1.4 induces an analogous commutative diagram of bijective maps between the corresponding quotient sets.*

Comments and open questions

a) The proofs of all theorems are constructive, i.e. the functors Φ_n, Ψ_n and the map $\downarrow_m^n$ are explicitly defined. Moreover, once we know that Φ_1 is a bijection on the set of closed morphisms, it is easy to describe its inverse, i.e. the map which associates to each surgery description of a 4-dimensional 2-handlebody a morphism in $\widehat{\mathcal{H}}^r$, without passing through $\widehat{\mathcal{S}}_n^c$ (cf. 7.3).

b) The reader might wonder why we have introduced the general concept of a groupoid ribbon Hopf algebra, even if it is being used only in the case of a specific and very simple groupoid. The reasons are two. The first one is that working with the general case does not make heavier the algebraic part, actually it makes it easier to follow. The second one is that, in our believe, the group ribbon Hopf algebra (which is another particular case of the construction) should be useful in finding an algebraic description of other types of topological objects, for example the group manifolds studied in [29].

c) The only reason for which our result concerns closed 3-manifolds and not cobordisms, is because it is based on the result of [2], where the map $F \mapsto K_F$ is defined and shown to be a bijection only for surfaces/links and not for tangles. Nevertheless, the whole spirit of the present work (observe that the factorization of $F \mapsto K_F$ is done through functors defined on the categories of tangles), suggests that these functors themselves are probably equivalences of categories, i.e. that $\partial\mathcal{H}^r$ is indeed the category which represents the algebraic characterization of the 3-dimensional relative cobordisms (see [13]).

d) By restricting the map $\downarrow_1^2 \circ \Psi_2$ to double branched coverings of B^4, i.e. to ribbon surfaces labeled with the single permutation (1 2), one obtains an invariant of ribbon surfaces embedded in R^4 under 1-isotopy taking values in $\mathcal{H}^r$.

e) Obviously, given any particular braided (selfdual) ribbon Hopf algebra over a ring, Theorem 1.4 (resp. Theorem 1.5) can be used to construct particular invariants of 4-dimensional 2-handlebodies (resp. 3-manifolds). All examples of such algebras that we know are simply braidings of (ordinary) finite-dimensional unimodular ribbon Hopf algebras, therefore the resulting invariants are the HKR-type invariants from [1] (for the definition of the braided Hopf algebra associated to an ordinary ribbon Hopf algebra, see for example Lemma 3.7 in [29]). Nevertheless, we do not know if any finite-dimensional braided ribbon Hopf algebra is a braiding of an ordinary one.

Contents

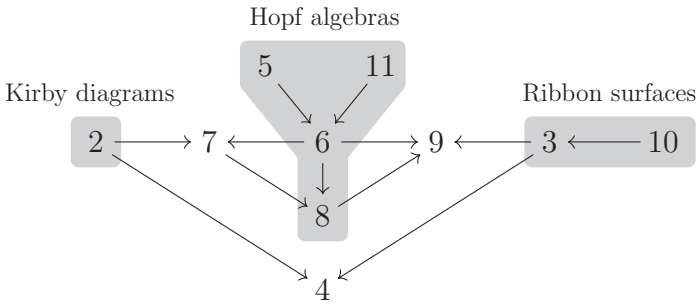

Table of interdependence of sections

2. The category $\mathcal{K}_n$ of admissible generalized Kirby tangles

In this section we review the concept of generalized Kirby diagram from [2].

2.1. A *Kirby diagram* describes an orientable 4-dimensional 2-handlebody $H^0 \cup H^1_1 \cup \ldots \cup H^1_p \cup H^2_1 \cup \ldots \cup H^2_q$ with only one 0-handle, by encoding 1- and 2-handles in a suitable link $K \subset S^3 \cong \operatorname{Bd} H^0$. Namely, K has p dotted components spanning disjoint flat disks which represent the 1-handles and q framed components which determine the attaching maps of the 2-handles. We refer to [14] or [6] for details and basic facts about Kirby diagrams, limiting ourselves to recall here only the ones relevant for our purposes.

The assumption of having only one 0-handle, is crucial in order to make a natural convention on the framings, that allows to express them by integers fixing as zero the homologically trivial ones.

However, we renounce this advantage on the notation for framings in favour of more flexibility in the representation of multiple 0-handles. The reason is that an n-fold covering of B^4 branched over a ribbon surface turns out to have a natural handlebody structure with n 0-handles.

We call a generalized Kirby diagram a representation of an orientable 4-dimensional 2-handlebody with multiple 0-handles. It is essentially defined by identifying the boundaries of all 0-handles with S^3 (where the diagram takes place), and by putting labels in the diagram in order to keep trace of the original 0-handle where each part of it is from. If there is only one 0-handle, the labels can be omitted and we have an ordinary Kirby diagram.

More precisely, a *generalized Kirby diagram* representing an orientable 4-dimensional handleboby $H^0_1 \cup \ldots \cup H^0_n \cup H^1_1 \cup \ldots \cup H^1_p \cup H^2_1 \cup \ldots \cup H^2_q$ consists of the following data: a boxed label indicating the number n of 0-handles; p dotted unknots spanning disjoint flat disks, each side of which has a label from $\{1, \ldots, n\}$; q integer framed disjoint knots transversal with respect to those disks, with a label from $\{1, \ldots, n\}$ for each component of the complement of the intersections with the disks. The labeling must be admissible in the sense that all the framed arcs coming out from one side of a disks have the same label of that side (cf. Figure 5). This rule makes the labeling redundant and sometimes we omit the superfluous labels. Moreover, the framings are always drawn as parallel curves, i.e. the undotted components represent embeddings of $S^1 \times I$ in R^3.

To establish the relation between a generalized Kirby diagram and the handlebody it represents, we first convert the dot notation for the 1-handles into a ball notation, as shown in Figure 5. Here, the two balls, together with the relative framed arcs, are symmetric with respect to the horizontal plane containing the disk and squeezing them vertically on the disk we get back the original diagram. After

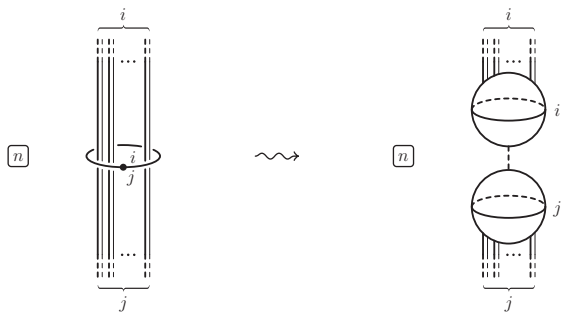

FIGURE 5. One-handle notation.

that, we take a disjoint union of n 4-balls $H^0_1 \cup \ldots \cup H^0_n$, which are going to be the 0-handles, and draw on the boundary of each H^0_i the portion of the diagram labeled with i. Then, we attach to $H^0_1 \cup \ldots \cup H^0_n$ a 1-handle between each pair of balls (possibly lying in different 0-handles), according to the diffeomorphism induced by the above symmetry, so that we can join longitudinally along the handle the corresponding framed arcs. Of course, the result turns out to be defined only up to 1-handle full twists. At this point, we have a 1-handlebody $H^0_1 \cup \ldots \cup H^0_n \cup H^1_1 \cup \ldots \cup H^1_p$ with q framed loops in its boundary and we use such framed loops as attaching instructions for the 2-handles $H^2_1, \ldots, H^2_q$.

We observe that any orientable 4-dimensional 2-handlebody can be represented, up to isotopy, by a generalized Kirby diagram. In fact, in order to reverse our construction, we only need that the identification of the boundaries of the 0-handles with S^3 is injective on the attaching regions of 1- and 2-handles and that the attaching maps of the 2-handles run longitudinally along the 1-handles. These properties can be easily achieved by isotopy.

The above construction gives isotopic handlebody structures if and only if the starting generalized Kirby diagrams are equivalent up to *labeled isotopy*, generated by labeled diagram isotopy, preserving all the intersections between loops and disks (as well as labels), and by the three moves described in Figure 6. Here, in the last move we assume $k \neq l$, so that the crossing change at the bottom of the figure preserves the isotopy class of the framed link in $H^0_1 \cup \ldots \cup H^0_n \cup H^1_1 \cup \ldots \cup H^1_p$. It is due to this crossing change that the framing convention usually adopted for ordinary Kirby diagrams cannot be extended to generalized Kirby diagrams. On the contrary, the other two moves make sense whatever are i, j and k. In particular, if $i = j = k$ they reduce to the ordinary ones. Actually, this is the only relevant case for the second move, usually referred to as "sliding a 2-handle over a 1-handle", since the other cases can be obtained by crossing changes. Moreover, even this ordinary case becomes superfluous in the context of 2-deformations, since it can be realized by addition/deletion of canceling 1/2-handles and 2-handle slides (cf. [6]).

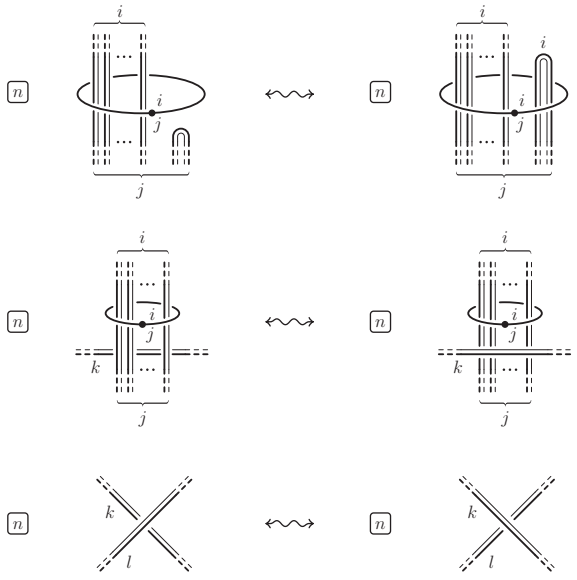

FIGURE 6. Labeled isotopy moves ($k \neq l$ in the last crossing change).

The following Figures 7 and 8 represent 2-deformations of 4-dimensional 2-handlebodies in terms of generalized Kirby diagrams. Namely: the moves in Figure 7 correspond to addition/deletion of canceling 0/1-handles and 1/2-handles, where $i \leq n$ and the canceling framed component in the bottom move is assumed to be closed; the moves in Figure 8 correspond to 1- and 2-handle slidings (in the low left corner of the figure we assume that the two framed segments correspond to different components of the link). Except for the addition/deletion of canceling 0/1-handles, which does not make sense for ordinary Kirby diagrams, the rest of the moves reduce to the ordinary ones if $i = j = k$.

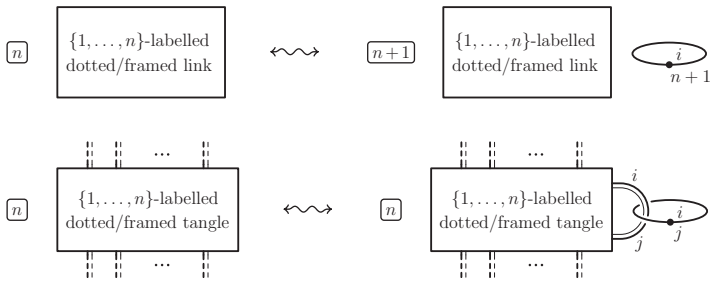

FIGURE 7. Addition/deletion of canceling pairs of handles.

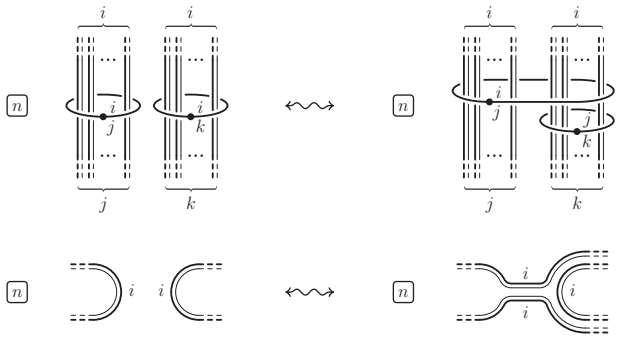

FIGURE 8. Handle slidings.

The 1-handle sliding is included for the sake of completeness, but it can be generated by addition/deletion of canceling 1/2-handles and 2-handle sliding, just like in the ordinary case (cf. [6]).

Summing up, two generalized Kirby diagrams represent 2-equivalent 4-dimensional 2-handlebodies if and only if they can be related by the first and third moves in Figure 6 (labeled isotopy), the two moves in Figure 7 (addition/deletion of canceling handles) and the second move in Figure 8 (2-handle sliding).

Of these, only the first move in Figure 6 and the second ones in Figures 7 and 8 (for $i = j = n = 1$) make sense in the case of ordinary Kirby diagrams. Actually, such three moves suffice to realize 2-equivalence of 4-dimensional 2-handlebodies with only one 0-handle, since any extra 0-handle occurring during a 2-deformation can be eliminated by a suitable fusion of 0-handles.

2.2. Given any generalized Kirby diagram K representing a connected handlebody with n 0-handles, we can use 2-deformation moves to transform it into an ordinary one, by reducing the number of 0-handles to 1. In fact, assuming $n > 1$,

we can eliminate the n-th 0-handle as follows. Since the handlebody is connected, there exists at least one dotted component such that one side of its spanning disk is labeled by n, and the other one is labeled by $i \neq n$. We may assume that all such disks lie in the xy plane with the side labeled n facing up. Moreover, by changing the crossings of framed components with different labels and by isotopy we may also assume that the diagram intersects the xy plane only in these spanning disks and that all dotted and framed components above the xy plane contain only the label n. Now we choose one of the components in the xy plane, say U of label (i_0, n), and slide it over all dotted components in this plane changing their labels from (i, n) to (i, i_0) (cf. the top move in Figure 8). Then we pull U up until it becomes disjoint from the rest of the diagram and this changes the labels of the dotted components above the plane from (n, n) to (i_0, i_0). The resulting diagram is the disjoint union of U and a diagram K^U which does not contain the label n. Finally we cancel the n-th 0-handle with the one handle represented by U. An example of such reduction is presented in Figure 9, where the 1-handle U is the one in the upper right corner of the diagram. Observe that if we had chosen another 1-handle, for example the one in the lower left corner, we would obtain the diagram on the right in Figure 10 which, as it is shown in the figure (and as it should be), is equivalent to the previous one through 1-handle slides.

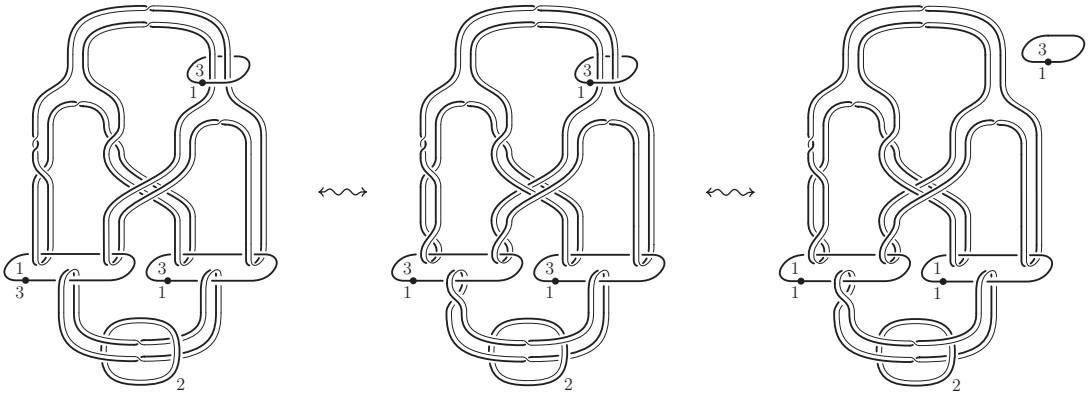

FIGURE 9.

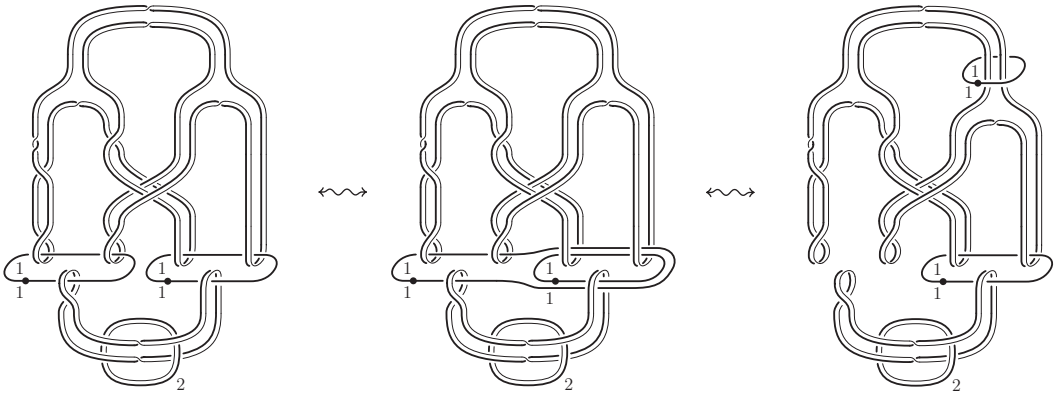

FIGURE 10.

2.3. Now we introduce the notion of an admissible generalized Kirby tangle and organize such tangles into a monoidal category.

We recall that a *braided monoidal* category $(\mathcal{C}, \diamond, \mathbf{1}, \iota_A, {}_A\iota, \alpha, \gamma)$ is a category $\mathcal{C}$ equipped with a functor $\diamond : \mathcal{C} \times \mathcal{C} \to \mathcal{C}$, an object $\mathbf{1} \in \mathcal{C}$ and natural isomorphisms:

$$\begin{aligned} \iota_A &: \mathbf{1} \diamond A \to A, \\ {}_A\iota &: A \diamond \mathbf{1} \to A, \\ \alpha_{A,B,C} &: (A \diamond B) \diamond C \to A \diamond (B \diamond C) \quad \text{(associativity)}, \\ \gamma_{A,B} &: A \diamond B \to B \diamond A \quad \text{(commutativity or braiding)}, \end{aligned}$$

which satisfy a well known set of axioms (see for example [27]). $\diamond$ is called the product of the category. In the category of generalized Kirby tangles this product will be given by the juxtaposition of diagrams. This is possible only if the number of the 0-handles (labels) is fixed; otherwise the equivalence move presented on the top in Figure 7 would violate the monoidal structure. So, in what follows we assume that the box of all diagrams contains a fixed n, and therefore we omit it.

A *generalized Kirby tangle* is a slice of a generalized Kirby diagram, i.e. the intersection of a generalized Kirby diagram K with $R^2 \times [0,1]$, where the dotted components of K (and their spanning disks) do not intersect $R^2 \times \{0,1\}$, while the framed components of K intersect $R^2 \times \{0,1\}$ transversely. Two generalized Kirby tangles are equivalent if they can be transformed into each other through ambient isotopy of $R^2 \times [0,1]$, the first and the third moves in Figure 6, the lower move in Figure 7, and the second move in 8, leaving $R^2 \times \{0,1\}$ fixed. Moreover, in the move in Figure 8 we assume that the two segments belong to different components of the tangle and that the component over which the sliding is done is closed.

We define the category $\mathcal{K}_n$ of (n-labeled) *admissible* generalized Kirby tangles as follows. An object of $\mathcal{K}_n$ is an ordered set of pairs of intervals $\{(I_1^+, I_1^-), \dots, (I_s^+, I_s^-)\}$ in $R^1 \subset R^2$, each one labeled with pair of numbers (i_k^+, i_k^-), $1 \le i_k^+, i_k^- \le n$. To simplify the notation we will often denote such object simply by the ordered sequence of labels. A morphism in $\mathcal{K}_n$ is given by a generalized Kirby tangle each component of which is either closed or intersects at most one of the planes $R^2 \times \{0\}$ and $R^2 \times \{1\}$ in a pair of intervals (I_k^+, I_k^-), in such a way that the label of each interval coincides with the label of the framed component to which it belongs. Moreover, any open component has a half-integer framing. The composition of two morphisms is obtained by identifying the target of the first one with the sourse of the second and rescaling. Observe that our notion of admissible tangles is more restrictive than the one in [19] and [12], but this is all we need. $\mathcal{K}_n$ is a braided monoidal category with respect to juxtaposition of diagrams. In particular, $\mathbf{1}$ is the empty set, the identity on (i,j) and the braiding morphisms $\gamma_{(i,j),(i',j')}$ and $\gamma^{-1}_{(i',j'),(i,j)}$ are presented in Figure 11, while ι_A, ${}_A\iota$ and the associativity morphisms are the identities.

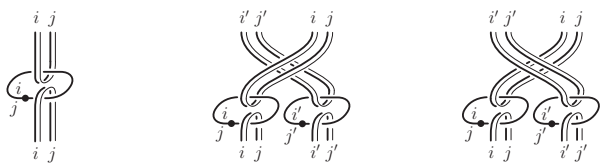

FIGURE 11. Identity and the braiding morphisms in $\mathcal{K}_n$.

We recall from the Introduction that a morphism K in $\mathcal{K}_n$ is closed if it has the empty object as sourse and target. Moreover, K is complete if the labels of the dotted components (taken as ordered pairs of indices) together with the identities (i,i), $i=1,\dots,n$, generate all the groupoid $\mathcal{G}_n$. Equivalently, K is complete if and only if the graph having n ordered vertices and one edge connecting the i-th and the j-th vertex for any dotted component of label (i,j), is connected. To see that the notion of completeness is well-posed with respect to equivalences of morphisms, we observe that the only move in which a dotted component may appear or disappear is the bottom move in Figure 7 where if there $i \neq j$, neccesarily the cancelling framed component passes through other 1-handes, the corresponding edges of which connect the i-th and the j-th vertex of the graph. In particular, removing or adding the edge corresponding to the cancelling dotted component does not change the connectedness of the graph.

Let $\widehat{\mathcal{K}}^c_n$ denote the set of closed complete morphisms in $\mathcal{K}_n$. Of course, a closed morphism is complete if and only if the corresponding handlebody is connected. Then the stabilization with an 1-handle of label $(n+1,n)$ shown in the upper part of Figure 7 defines a bijective map $\uparrow^{n+1}_n : \widehat{\mathcal{K}}^c_n \to \widehat{\mathcal{K}}^c_{n+1}$, while the procedure of reducing the number of 0-handles given in 2.2 represents its inverse $\downarrow^{n+1}_n : \widehat{\mathcal{K}}^c_{n+1} \to \widehat{\mathcal{K}}^c_n$. Observe that $\uparrow^{n+1}_n K \in \widehat{\mathcal{K}}^c_{n+1}$ and $K \in \widehat{\mathcal{K}}^c_n$ describe the same 4-dimensional 2-handlebody up to 2-deformation.

2.4. Even if it is irrelevant for the present work, we would like to point out that the category $\mathcal{K}_n$ is equivalent to the category of n-labeled $3+1$ cobordisms $\mathcal{C}ob_n$ (for $n=1$ see Section 1 in [11]). The objects in $\mathcal{C}ob_n$ are oriented 3-dimensional 1-handlebodies with n 0-handles. Given two such handlebodies M_s and M_r respectively with s and r 1-handles, let $N(M_s,M_r)$ denote the 3-dimensional 1-handlebody obtained from $M_s \sqcup M_r$ by attaching for any $i \leq n$ a single 1-handle connecting the i-th 0-handles of M_s and M_r. We can cancel the new 1-handles against some of the 0-handles thinking of $N(M_s,M_r)$ as a 3-dimensional 1-handlebody with n 0-handles as well. Then a morphism $W : M_s \to M_r$ is a relative (4-dimensional) 2-handlebody build on $N(M_s,M_r)$. Note that the term relatitve handlebody build on M, is usually limited to the case when M is a closed 3-manifold, but the generalization is straightforward: we attach 1- and 2-handles on $N(M_s,M_r)\times\{1\} \subset N(M_s,M_r)\times[0,1]$. Then $W_1, W_2 : M_s \to M_r$ are called 2-equivalent if they are obtained from each other by a 2-deformation, i.e. changing the attaching maps of the handles through isotopy or adding/deleting a canceling pair of 1/2-handles. Obviously these handle moves are limited to $N(M_s,M_r)\times\{1\}$. The composition of two relative cobordims $W : M_s \to M_r$ and $W' : M_r \to M_t$ is obtained by gluing through an orientation reversing homeomorphism $M_r\times\{0\} \subset N(M_s,M_r)\times[0,1]$ and $M_r\times\{0\} \subset N(M_r,M_t)\times[0,1]$ and canonically identifying the resulting manifold as $N(M_s,M_t)\times[0,1]$ on which we have attached r 4-dimensional 1-handles.

Any morphism $K : \{(i_1^+,i_1^-),\dots,(i_s^+,i_s^-)\} \to \{(j_1^+,j_1^-),\dots,(j_r^+,j_r^-)\}$ can be easily seen as describing a cobordism $W(K) : M_s \to M_r$ by composing it (if necessary) with the identity morphisms as shown in Figure 12.

2.5. The main theorem of Kirby calculus [14] asserts that two orientable 4-dimensional 2-handlebodies have diffeomorphic boundaries and the same signature if and only if they are related by 2-deformations and 1/2-handle trading, while two

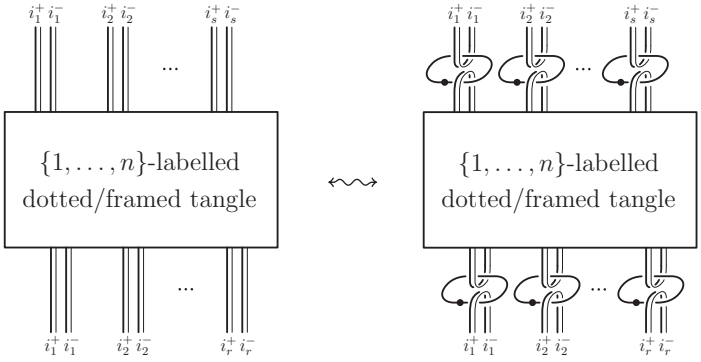

FIGURE 12. Identifying a morphism in $\mathcal{K}_n$ as relative cobordism.

orientable 4-dimensional 2-handlebodies have diffeomorphic boundaries if and only if they are related by 2-deformations, positive/negative blowing up/down and 1/2-handle trading.

In terms of generalized Kirby diagrams these last three modifications can be realized by the moves in Figure 13. These moves essentially coincide with the corresponding ones for ordinary Kirby diagrams (with $i = n = 1$), being the involved labels all the same.

As it is shown in Figure 14 (a), modulo 2-deformations, 1/2-handle trading is equivalent to 1/2-handle trading for a canceling pair, which is the move presented

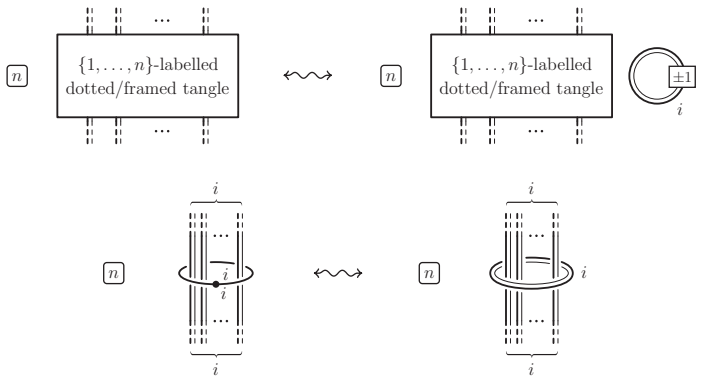

FIGURE 13. Blowing up/down and 1/2-handle trading.

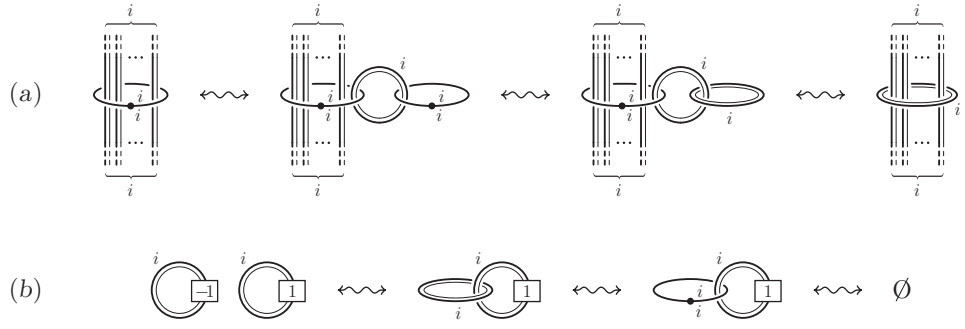

FIGURE 14. Reducing blowing up/down and 1/2-handle trading to special cases.

in Figure 15 (a). Moreover, the relation in Figure 14 (b) implies that in $\partial^\star K_n$ a negative blow up can be obtained through 2-deformations and 1/2-handle trading from the positive one (Figure 15 (b)). Therefore we define the category $\partial^\star\mathcal{K}_n$ to be the $\mathcal{K}_n$ modulo the relation in Figure 15 (a), while $\partial\mathcal{K}_n$ to be the $\mathcal{K}_n$ modulo the relations in Figure 15 (a) and (b). From [14] and the discussion above it follows that the closed morphisms $\partial^\star\widehat{\mathcal{K}}_n$ in $\partial^\star\mathcal{K}_n$ describe framed 3-manifolds, while the closed morphisms $\partial\widehat{\mathcal{K}}_n$ in $\partial\mathcal{K}_n$ describe 3-manifolds.

(a) (b)

FIGURE 15. Additional relations in $\partial^\star\mathcal{K}_n$ and $\partial\mathcal{K}_n$.

3. The category $\mathcal{S}_n$ of labeled rs-tangles

We review the notion of ribbon surface and 1-isotopy of such surfaces from [2]. A smooth compact surface $F \subset B^4$ with $\operatorname{Bd} F \subset S^3$ is called a *ribbon surface* if the Euclidean norm restricts to a Morse function on F with no local maxima in $\operatorname{Int} F$. Assuming $F \subset R^4_- \subset R^4_- \cup \{\infty\} \simeq B^4$, this property is topologically equivalent to the fact that the fourth Cartesian coordinate restricts to a Morse height function on F with no local maxima in $\operatorname{Int} F$. Such a surface $F \subset R^4_-$ can be horizontally (preserving the height function) isotoped to make its orthogonal projection into R^3 a self-transversal immersed surface, whose double points form disjoint arcs as in Figure 16 (a).

(a) (b)

FIGURE 16.

We refer to such a projection as a *3-dimensional diagram* of F. Actually, any immersed compact surface $F \subset R^3$ with no closed components and all self-intersections of which are as above, is the diagram of a ribbon surface uniquely determined up to vertical isotopy. This can be obtained by pushing $\operatorname{Int} F$ down inside $\operatorname{Int} R^4_-$ in such a way that all self-intersections disappear.

In, [BP] we introduced *1-isotopy* between ribbon surfaces, to be generated by 3-dimensional diagram isotopy in R^3 (that means isotopy preserving ribbon intersections) and the 1-isotopy moves depicted in Figure 17.

Since a ribbon surface F has no closed components, any 3-dimensional diagram of it, considered as a 2-dimensional complex in R^3, collapses to a graph G. We choose

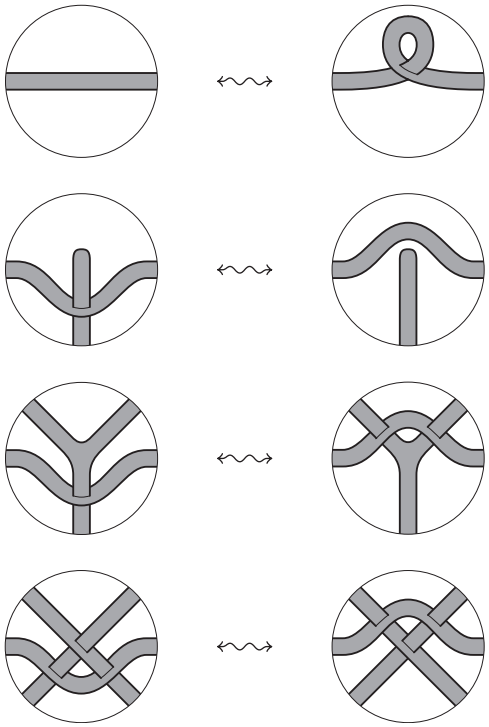

FIGURE 17. 1-isotopy moves.

G to be the projection in R^3 of a smooth simple spine $\widetilde{G}$ of F (simple means that all the vertices have valency one or three), which meets at exactly one point each arc projecting to a ribbon intersection of the 3-dimensional diagram of F as shown in Figure 16 (b). The inverse image in $\widetilde{G}$ of such a point consists of a single uni-valent vertex and a point in the interior of an edge, while the restriction of the projection to $\widetilde{G}$ with such uni-valent vertices removed, is injective.

Therefore, G turns out to have only vertices of valency 1 and 3. We call *singular vertices* the tri-valent vertices located at the ribbon intersections, and *flat vertices* all the other vertices. Moreover, we assume that G has distinct tangent lines at each flat tri-valent vertex while the tangent lines to two of the edges at a singular vertex coincide (since those two edges form a unique edge of $\widetilde{G}$) and differ from the tangent line to the third edge at such vertex.

Up to a further horizontal isotopy, we can contract the 3-dimensional diagram of F to a narrow regular neighborhood of the graph G. Moreover, by considering a planar diagram of G, we can assume that the diagram of F is contained in the projection plane, except for a finite number of positive/negative ribbon half-twists, ribbon intersections and ribbon crossings, as the ones depicted in Figure 18.

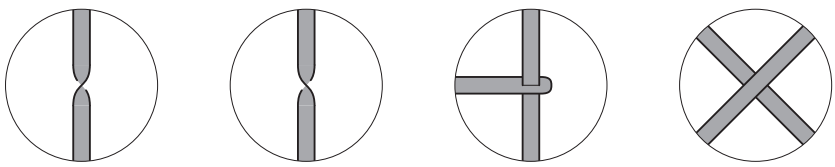

FIGURE 18.

In this way we get a new diagram of F, consisting of a certain number of regions as the ones presented in Figures 18 and 19, suitably connected by flat bands contained in the projection plane. We call such diagram a *planar diagram* of F.

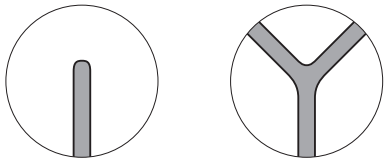

FIGURE 19.

Actually, a planar diagram of F arises as a diagram of the pair (F, G) and this is the right way to think of it. However, we omit to draw the graph G in the pictures of a planar diagram, since it can be trivially recovered, up to diagram isotopy, as the core of the diagram itself. In particular, the singular vertices and the projection crossings are located at the centers of the third circle in Figure 18, while the flat vertices of G are located at the centers of the circles in Figure 19. To be precise, there are two choices in recovering the graph G at a singular vertex, as shown in Figure 20. They give the same graph diagram of each other, but differ for the way the graph is embedded in the 3-dimensional diagram of the surface. We consider the move depicted in Figure 20 as an equivalence move for the pair (F, G). Up to this move, G is uniquely determined also as a graph in the 3-dimensional diagram of F.

FIGURE 20.

Like the 3-dimensional diagrams, also the planar ones uniquely determine the ribbon surface F up to vertical isotopy. Here, by vertical isotopy we mean an isotopy which preserves the first 2 coordinates. In other words, the 3-dimensional height functions (as well as the 4-dimensional one) is left undetermined for a planar diagram. Of course, such height function is required to be consistent with the restrictions deriving from the local configurations in Figure 18.

In the following, *ribbon surfaces will be always represented by planar diagrams and considered up to vertical isotopy* (preserving the first 2 coordinates).

By a *ribbon surface tangle* (or simply *rs-tangle*) we mean the intersection of a pair (F, G), consisting of a ribbon surface F and its core graph G, with $R^2 \times [0, 1] \subset R^3$, where F intersects transversely $R^2 \times \{0, 1\}$ in some sets of arcs, called boundary arcs, and G intersects transversely $R^2 \times \{0, 1\}$ in some set of points, one for each boundary arc, different from its vertices.

Two rs-tangles are *1-isotopic* if they are related by 1-isotopy inside $R^2 \times [0, 1]$ leaving fixed a small regular neighborhood of the boundary arcs. The rs-tangles form a category $\mathcal{S}$ whose objects are sets of intervals in R^2, and whose morphisms are

rs-tangles in which source and target are respectively given by the intersection of the rs-tangle with $R^2 \times \{0\}$ and $R^2 \times \{1\}$. Then the composition of two morphisms is obtained by identifying the target of the first one with the source of the second and rescaling. We also define the product of two rs-tangles by horizontal juxtaposition.

PROPOSITION 3.1. *$\mathcal{S}$ is equivalent to the category of planar diagrams, whose objects are finite sequences of disjoint intervals in R, and whose morphisms are iterated products and compositions of the elementary planar diagrams presented in Figure 21, modulo plane isotopies preserving the y-coordinate and the moves presented in Figures 22–25, where D and D' in moves (I1), (I8) and (I9) correspond to any of the elementary diagrams in Figure 21.*

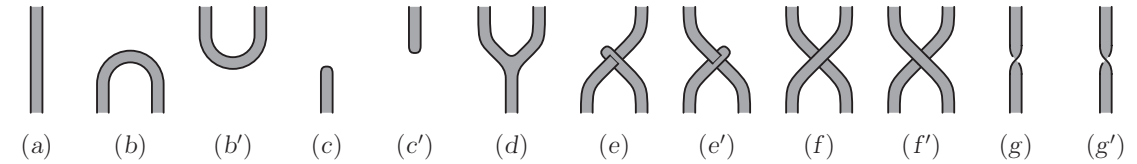

FIGURE 21. Elementary diagrams in $\mathcal{S}$

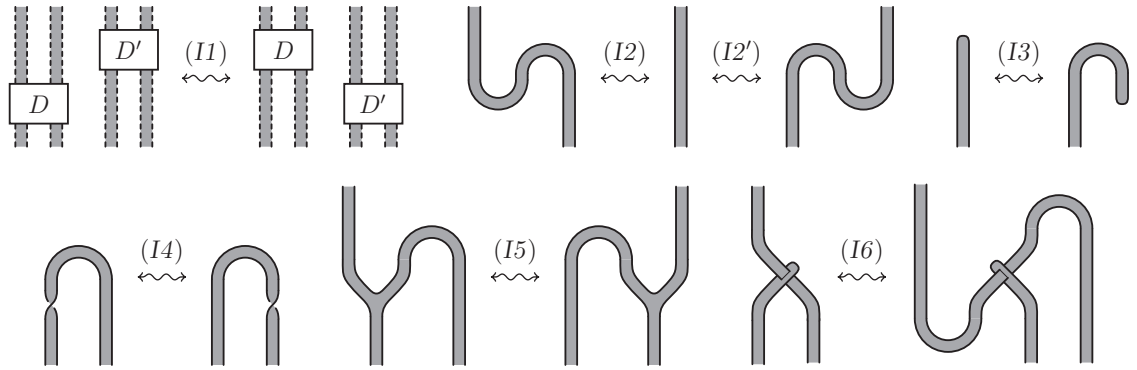

FIGURE 22. Planar isotopy relations in $\mathcal{S}$

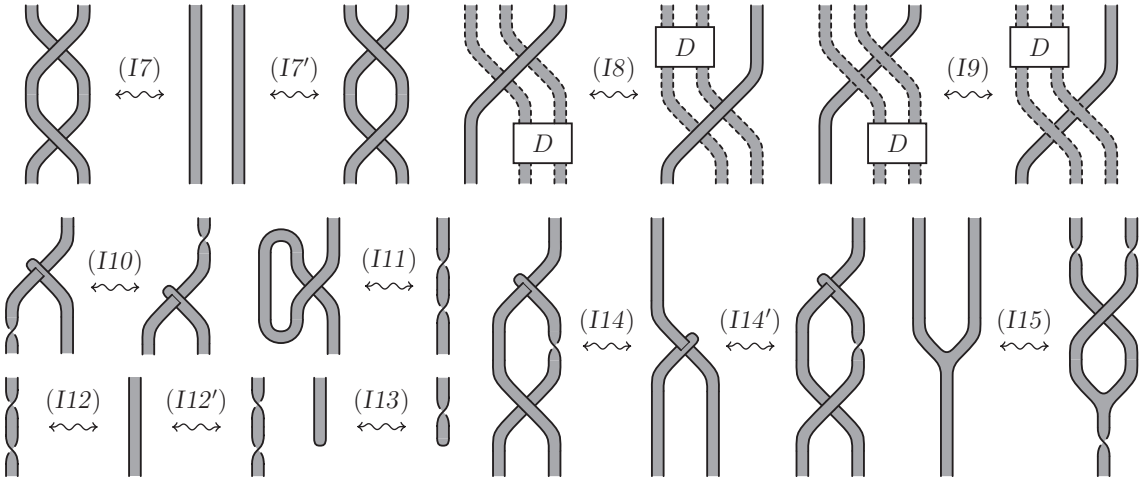

FIGURE 23. 3-dimensional isotopy relations in $\mathcal{S}$

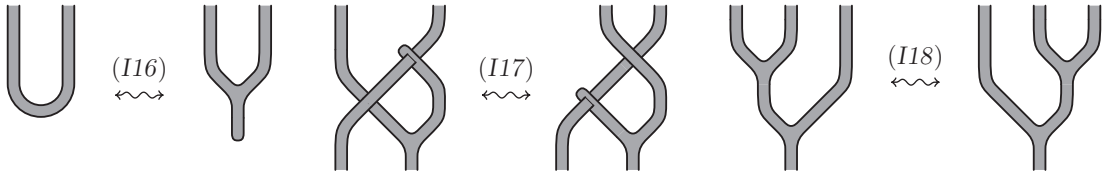

FIGURE 24. Graph changing relations in $\mathcal{S}$

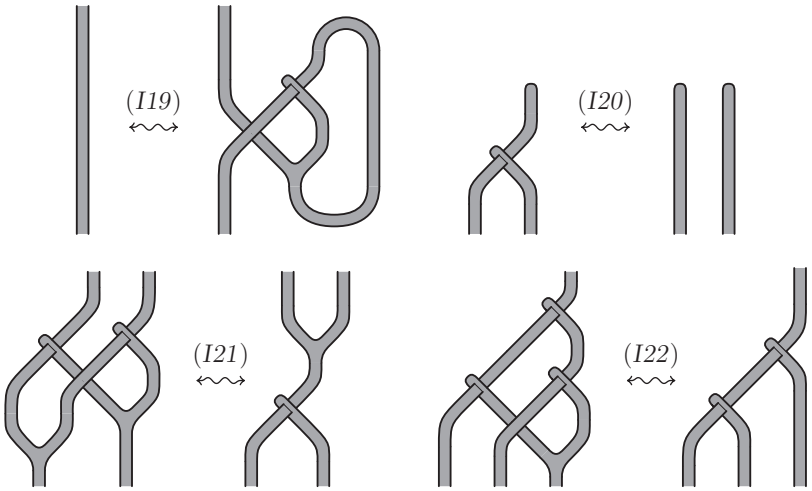

FIGURE 25. 1-isotopy relations in $\mathcal{S}$

The proof of Proposition 3.1 is technical but quite standard and the details are presented in Appendix I (p. 76). Here, we only make few observations: moves (*I1*) to (*I6*) come from isotopy of (oriented with respect to the y-axis) planar diagrams in the projection plane (but suffice for that only up to the subsequent moves); moves (*I7*) to (*I15*) describe the changes under 3-dimensional isotopies preserving the ribbon intersections; moves (*I16*) to (*I18*) describe the changes which occur in the planar diagram when one changes the core graph G of F; moves (*I19*) to (*I22*) represent in terms of standard planar diagrams the 1-isotopy moves in Figure 17.

3.2. Proposition 3.1 implies that $\mathcal{S}$ is a braided monoidal category with respect to juxtaposition of diagrams: $\mathbf{1}$ is again the empty set, the braiding morphisms $\gamma_{I,I'}$ and $\gamma^{-1}_{I,I'}$ are presented in Figure 19 (f) and (f'), while ι_A, ${}_A\iota$ and the associativity morphisms are the identities. In fact, as we will show, $\mathcal{S}$ carries also autonomous and tortile structures. Recall from [27] that an *autonomous* braided monoidal category $(\mathcal{C}, \diamond, \mathbf{1}, \iota_A, {}_A\iota, \alpha, \gamma, \Lambda, \lambda)$ is a braided monoidal category $\mathcal{C}$ in which every object A has a right dual $(A^*, \Lambda_A, \lambda_A)$, where the morphisms

$$\Lambda_A : \mathbf{1} \to A^* \diamond A \quad (\textit{coform})$$
$$\lambda_A : A \diamond A^* \to \mathbf{1} \quad (\textit{form})$$

are such that the compositions

$$A \xrightarrow{{}^A\iota^{-1}} A \diamond \mathbf{1} \xrightarrow{\mathrm{id}\diamond\Lambda_A} A \diamond (A^* \diamond A) \xrightarrow{\alpha^{-1}} (A \diamond A^*) \diamond A \xrightarrow{\lambda_A\diamond\mathrm{id}} \mathbf{1} \diamond A \xrightarrow{\iota_A} A,$$
$$A^* \xrightarrow{\iota_A^{-1}} \mathbf{1} \diamond A^* \xrightarrow{\Lambda_A\diamond\mathrm{id}} (A^* \diamond A) \diamond A^* \xrightarrow{\alpha} A^* \diamond (A \diamond A^*) \xrightarrow{\mathrm{id}\diamond\lambda_A} A^* \diamond \mathbf{1} \xrightarrow{{}^A\iota} A^*,$$

are the identities. Then, given any morphism $F : A \to B$ in $\mathcal{C}$, we define its *dual* $F^* : B^* \to A^*$ as follows:

$$F^* = {}_A\iota^{-1} \circ (\mathrm{id}_{A^*} \diamond \lambda_B) \circ \alpha_{A^*,B,B^*} \circ ((\mathrm{id}_{A^*} \diamond F) \diamond \mathrm{id}_{B^*}) \circ (\Lambda_A \diamond \mathrm{id}_{B^*}) \circ \iota^{-1}_{B^*}.$$

A *twist* for a braided monoidal category is a family of natural isomorphisms $\theta_A : A \to A$ such that $\theta_{\mathbf{1}} = \mathrm{id}_{\mathbf{1}}$ and $\theta_{A\diamond B} = \gamma_{B,A} \circ (\theta_B \diamond \theta_A) \circ \gamma_{A,B}$.

An autonomous braided monoidal category is called *tortile* (the terminology is from [27]) if it is equipped with a distinguished twist such that $\theta_{A^*} = (\theta_A)^*$ for any object A.

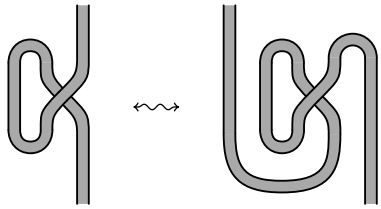

FIGURE 26.

A classical example of tortile category is the category $\mathcal{T}$ of framed tangles. We remind that $\mathcal{T}$ has the same objects as $\mathcal{S}$, but the morphisms are compositions of products of the elementary diagrams (a), (b), (b'), (f) and (f') in Figure 19 modulo the relations $(I1)$, $(I2\text{-}2')$, $(I7\text{-}7')$, $(I8)$, $(I9)$ and the relation in Figure 26. The autonomous structure on $\mathcal{T}$ is determined by $A^* = A$ for any object A, while λ_I and Λ_I for a single interval I are represented by the diagrams (b) and (b') in Figure 19 and then extended to any other object by requiring that $\Lambda_{A\diamond B} = (\mathrm{id}_B \diamond \Lambda_A \diamond \mathrm{id}_B) \circ \Lambda_B$ and $\lambda_{A\diamond B} = \lambda_A \circ (\mathrm{id}_A \diamond \lambda_B \diamond \mathrm{id}_A)$. Then the conditions on the form and coform in 3.2 reduce to relations $(I2\text{-}2')$. The twist is defined by $\theta_A = (\lambda_A \diamond \mathrm{id}_A) \circ (\mathrm{id}_A \diamond \gamma_{A,A}) \circ (\Lambda_A \diamond \mathrm{id}_A)$. In particular, θ_I is presented on the left in Figure 26 while the relation in the same figure represents the condition $\theta_{I^*} = (\theta_I)^*$. The fact that this condition is satisfied for any object A and that $\theta_{A\diamond B} = \gamma_{B,A} \circ (\theta_B \diamond \theta_A) \circ \gamma_{A,B}$, is a straightforward application of the relations $(i7\text{-}9)$.

PROPOSITION 3.3. *$\mathcal{S}$ is a tortile category and the map which sends any tangle in $\mathcal{T}$ to the corresponding rs-tangle in $\mathcal{S}$ defines a functor $\mathcal{T} \mapsto \mathcal{S}$ which is a strict tortile functor.*

Proof. In order to show that the map is a functor we only need to observe that the relation in Figure 26 is satisfied in $\mathcal{S}$. Indeed, this follows easily by applying $(I11)$, $(I4)$ and $(I2)$. Now we define the form, coform and the twist in $\mathcal{S}$ to be equal to the images of the correspoinding morphisms in $\mathcal{T}$. Those would make $\mathcal{S}$ into a tortile category if the twist is natural in $\mathcal{S}$, i.e if for any morphism $F : A \to B$ in $\mathcal{S}$, $\theta_B \circ F = F \circ \theta_A$. This follows from the naturality of the twist in $\mathcal{T}$ and relations $(I13\text{-}15)$. □

3.4. An rs-tangle labeled in the symmetric group Σ_n, is an rs-tangle in which each boundary arc and each connected component of its 3-dimensional diagrams with double points removed, is labeled by a transposition in Σ_n, according to the following

rules: the label of any boundary arc coincides with the label of the component to which it belongs; at any ribbon intersection, the label of the ribbon entering into a disk, gets conjugated by the label of this disk.

Then the category $\mathcal{S}_n$ of *labeled rs-tangles*, is defined to have as objects the finite sets $\{I_i, (k_i\ l_i)\}_i$ of intervals $I_i \subset R^2$ labeled by transpositions $(k_i\ l_i) \in \Sigma_n$, and as morphisms the equivalence classes of labeled rs-tangles modulo the labeled version of the defining relations of $\mathcal{S}$ and the relations $(R1)$ and $(R2)$ presented in Figure 3, where i, j, k and l are all distinct.

A labeling of a planar diagram of an rs-tangle induces a labeling of the planar diagram of its core graph. We call a singular vertex of such graph uni-, bi- or tri-colored according to how many different transpositions appear as labels of the edges attached to it. Then move $(R1)$ in Figure 3 states that a tri-colored singular vertex carries a cyclic symmetry, while move $(R2)$ allows to create or remove in $\mathcal{S}_n$ bi-colored singular vertices.

$\mathcal{S}_n$ is also a monoidal tortile category, where the product corresponds to disjoint union, the identity corresponds to the empty set and the tortile structure is induced by that of $\mathcal{S}$.

We recall that a morphism in $\mathcal{S}_n$ is called complete if the transpositions occuring as labels of any planar diagram of it generate all Σ_n. Notice that this property does not depend on the choice of the planar diagram representation of the morphism, being invariant under the defining relations in Figures 22–25.

As already mentioned in the Introduction, one can define a stabilization map $\uparrow_n^{n+1} : \widehat{\mathcal{S}}_n^c \to \widehat{\mathcal{S}}_{n+1}^c$ by sending a ribbon surface to its disjoint union with a disk labeled $(n\ n+1)$. Moreover, according to Proposition 4.2 in [2], $\uparrow_n^{n+1}$ is invertible for $n > m \geq 3$ and its inverse $\downarrow_n^{n+1} : \widehat{\mathcal{S}}_{n+1}^c \to \widehat{\mathcal{S}}_n^c$ is called a reduction map.

Finally, we define $\partial^\star \mathcal{S}_n$ to be quotient of $\mathcal{S}_n$ modulo the relation (T) in Figure 4, and $\partial \mathcal{S}_n$ to be quotient of $\partial^\star \mathcal{S}_n$ modulo the relations (P) and (P') presented in the same figure.

4. From labeled ribbon surfaces to Kirby diagrams

In this section we recall from Section 2 of [2], the definition of the bijective map $F \mapsto K_F$ sending any labeled ribbon surface F to a generalized Kirby diagram K_F in $\mathcal{K}_n$.

The main idea is that an 1-handlebody structure on the labeled ribbon surface F, representing a n-fold simple branched covering $p : M \to B^4$, naturally induces a 2-handlebody structure on M defined up to 2-deformations. In particular, the construction of K_F requires to make some choices:

a) a choice of an adapted 1-handlebody structure on F, i.e. a decomposition

$$F = D_1 \cup \ldots \cup D_p \cup B_1 \cup \ldots \cup B_q,$$

where the D_h's are disjoint flat disks (the 0-handles of F) and the B_h's are disjoint bands attached to $F_0 = D_1 \cup \ldots \cup D_p$ (the 1-handles of F); in particular, any ribbon intersection occurs between a band and a disk;

b) a choice of orientations of the disks D_h;

c) for every ribbon intersection contained in a disk D_h, a choice of an arc α in D_h, joining the ribbon intersection with $\operatorname{Bd} D_h \cap \operatorname{Bd} F$; such arcs are taken disjoint from each other.

Then the following steps summarize the procedure defined in [2] for constructing K_F in the case when F is presented by a planar diagram. In particular, in this case a choice of an orientation of the projection plane induces an orientation of all disks (since they lie in this plane):

a) replace any disk D_h by a dotted unknot coinciding with $\operatorname{Bd} D_h$; if D_h is labeled $(i\ j) \in \Sigma_n$ with $i < j$, then assign to its upper side the label i and to its lower side, the label j;

b) cut any band B_h at the ribbon intersections by removing a small neighborhood of the intersection arc; then take two small positive and negative vertical shifts of the resulting pieces of B_h, disjoint from the original surface; if a piece is labeled $(i\ j) \in \Sigma_n$ with $i < j$, then label by i its upper shift and by j its lower shift; Figure 27 (*a*) shows how the two shifts look like in a neighborhood of a positive half-twist (in this figure, as well as in the next one, the projection plane is depicted from a perspective point of view);

c) connect the two shifts of any attaching arc of a band B_h by a band which forms a ribbon intersection with the attaching disk, as shown in Figure 27 (*b*);

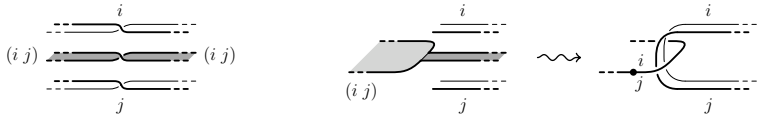

FIGURE 27. $(i < j)$

d) for each ribbon intersection of F contained in a disk D_h, connect in pairs the shifts approaching D_h from opposite sides, according to the following rule: if two shifts have the same label and this is different from the ones of D_h, then connect them with a flat band disjoint from D_h; if two shifts have different labels coinciding with the ones of D_h, then connect them by a band which forms

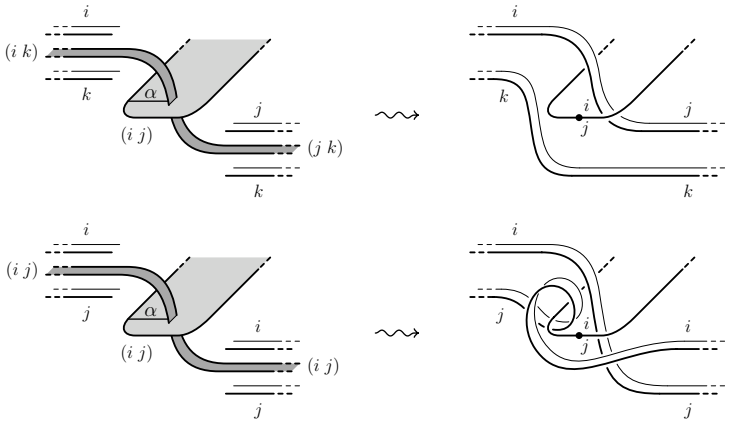

FIGURE 28. $(i < j < k)$

a ribbon intersection with D_h and is flat except for a twist around $\mathrm{Bd}\, D_h$ in the case when the two shifts approach D_h from the wrong sides with respect to the labeling; the whole construction is carried out in a regular neighborhood of the arc α and Figure 28 shows two special cases.

Lemma 2.3 and Proposition 2.4 in [2] state that K_F is well defined up to 2-deformation, i.e. making different choices of 1-handlebody structure, orientations or arcs, as well as changing F by 1-isotopy or ribbon moves, changes K_F only by 2-deformation. For more details on this point, as well as for the proof that the restriction of the map to the complete morphisms is bijective, we refer the interested reader to [2], observing that our final result relies on the bijectivity of the map, but does not need the explicit form of the inverse, which can be found in [2].

Instead, given any labeled ribbon surface $F \in \widehat{\mathcal{S}}^c_n$, we will need an explicit form for K_F, which requires a specific choice of adapted 1-handlebody structure for any such surface. Since the morphisms in $\widehat{\mathcal{S}}^c_n$ are compositions of the elementary morphisms presented by the planar diagrams in Figure 19, we can define an 1-handlebody structure on each morphism by indicating its intersection with the elementary morphisms. This is done in Figures 29, 30 and 31, where the disks are denoted with lighter gray and the bands with heavier gray color. Observe that there are two types of disks: the ones which deformation retract onto neighborhoods of the vertices of the core graph, and the others which divide the ribbons in such a way that none of them contains two boundary arcs. Moreover, since any band forms at most one ribbon intersection with any disk D_h, and in this case D_h has a single band attached to it, the choice of the arcs α is unique up to isotopy, so we omit it.

The application of the construction of K_F to the particular 1-handlebody structure of F chosen above is shown in Figures 29, 30 and 31, where for later use the image of the uni-colored singular vertex in Figure 31 has been transformed through the isotopy move presented in Figure 32. In particular, given $F \in \widehat{\mathcal{S}}^c_n$ as a compo-

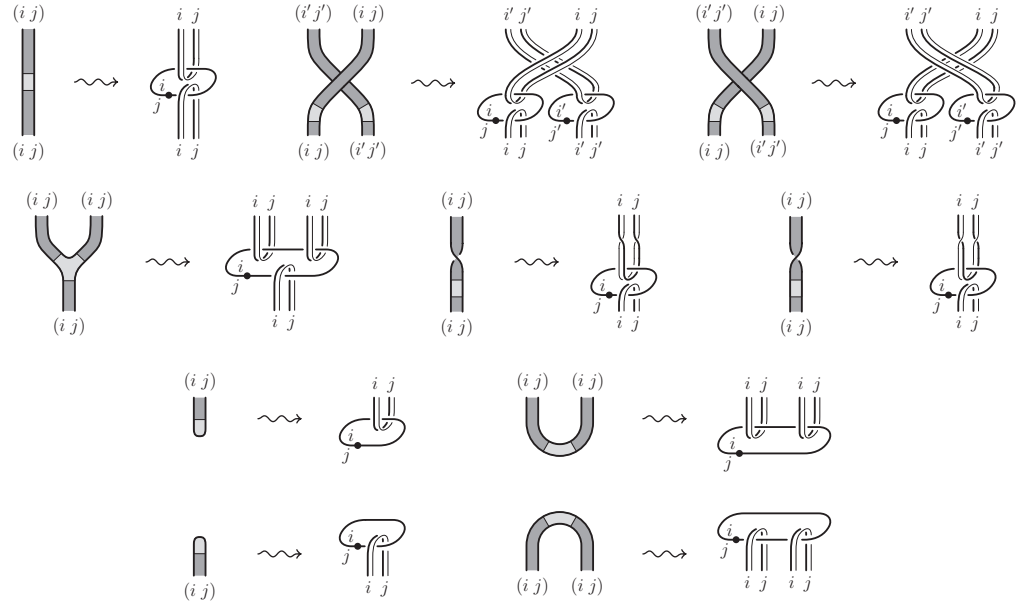

FIGURE 29. Definition of K_F ($i < j$ and $i' < j'$).

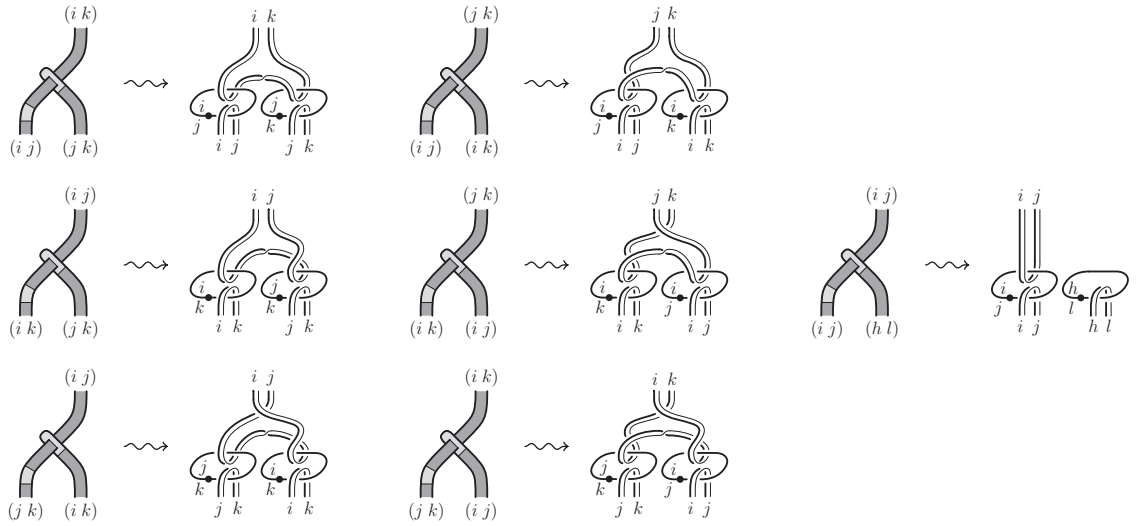

FIGURE 30. Definition of K_F ($i < j < k$, $h < l$ and $\{i, j\} \cap \{h, l\} = \emptyset$).

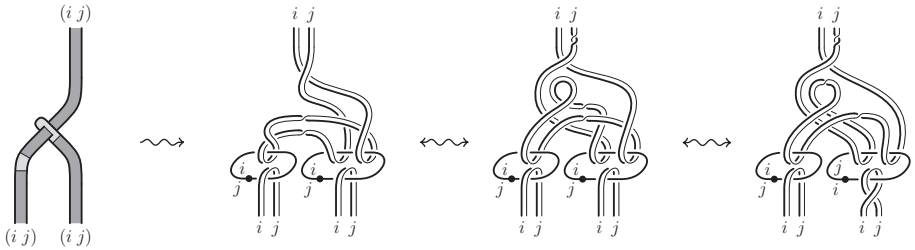

FIGURE 31. Definition of K_F ($i < j$).

sition of elementary diagrams, K_F is the formal composition of the corresponding generalized Kirby tangles on the right in those figures. Observe that the results in [2] assure us that such composition is well defined morphism in $\widehat{K}_n^c$. By proving Theorem 1.4, we will prove that the map $\mathcal{S}_n \to \mathcal{K}_n$ defined in Figures 29, 30 and 31 is a composition of two braided monoidal functors: $\Psi_n : \mathcal{S}_n \to \mathcal{H}_n$ and $\Phi_n : \mathcal{H}_n \to \mathcal{K}_n$, and therefore it is a braided monoidal functor itself.

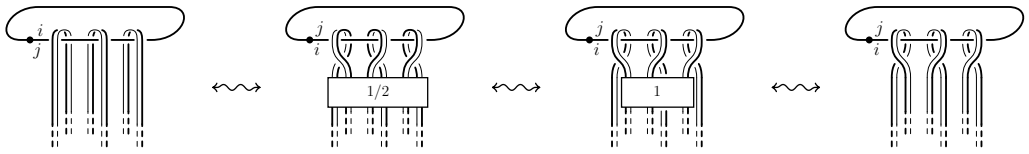

FIGURE 32. Reversing a dotted unknot in $\mathcal{K}_n$ ($i \neq j$)

5. The universal braided Hopf algebras $\mathcal{H}(\mathcal{G})$ and $\mathcal{H}^u(\mathcal{G})$

5.1. We remind that a groupoid $\mathcal{G}$ is a small category in which every morphism is invertible. Hopefully without causing a confusion, we will indicate by $\mathcal{G}$ also the set of the morphisms of $\mathcal{G}$, endowed with the partial binary operation given by the composition, for which we adopt the multiplicative notation from left to right. The identity of $i \in \operatorname{Obj} \mathcal{G}$ will be denoted by $1_i \in \mathcal{G}$, while the inverse of $g \in \mathcal{G}$ will be

denoted by $\overline{g} \in \mathcal{G}$. Moreover, given two objects $i, j \in \operatorname{Obj}\mathcal{G}$, we denote by $\mathcal{G}(i,j) \subset \mathcal{G}$ the subset of morphisms from i to j. Consequently, if $g \in \mathcal{G}(i,j)$ and $h \in \mathcal{G}(j,k)$ then $gh \in \mathcal{G}(i,k)$. In particular, $g\overline{g} = 1_i$ and $\overline{g}g = 1_j$, and sometimes the identity morphisms will be represented in this way. A groupoid is called *connected* if $\mathcal{G}(i,j)$ is non-empty for any $i, j \in \operatorname{Obj}\mathcal{G}$. Given two groupoids $\mathcal{G} \subset \mathcal{G}'$, we say that $\mathcal{G}$ is *full* in $\mathcal{G}'$ if $\mathcal{G}(i,j) = \mathcal{G}'(i,j)$ for all $i, j \in \operatorname{Obj}\mathcal{G}$.

We have the following basic examples of (connected) groupoids:

a) any group G, considered as a groupoid $\mathcal{G}$ with a single object $\mathbf{1}$, i.e. $\operatorname{Obj}\mathcal{G} = \{\mathbf{1}\}$ and $\mathcal{G}(\mathbf{1},\mathbf{1}) = G$;

b) the groupoid $\mathcal{G}_n$ with $n \in \mathbb{N}$, such that $\operatorname{Obj}\mathcal{G}_n = \{1, 2, \dots, n\}$ and $\mathcal{G}_n(i,j)$ consists of a unique arrow $(i,j) : i \to j$ for any $i, j \in \operatorname{Obj}\mathcal{G}$; in particular, the composition is given by $(i,j)(j,k) = (i,k)$ and $\overline{(i,j)} = (j,i)$.

The $\mathcal{G}_n$'s are exactly the groupoids which we will need later.

5.2. For a groupoid $\mathcal{G}$ and $x \in \mathcal{G}(i,k)$, define the functor $\_^x : \mathcal{G} \to \mathcal{G}$ as follows:

a) $k^x = i$ and $j^x = j$ if $j \in \operatorname{Obj}\mathcal{G} - \{k\}$;

b)
$$g^x = \begin{cases} xg\overline{x} & \text{if } g \in \mathcal{G}(k,k), \\ xg & \text{if } g \in \mathcal{G}(k,l) \text{ with } l \neq k, \\ g\overline{x} & \text{if } g \in \mathcal{G}(j,k) \text{ with } j \neq k, \\ g & \text{if } g \in \mathcal{G}(j,l) \text{ with } j, l \neq k. \end{cases}$$

Then the following statements hold:

c) $\overline{g^x} = \overline{g}^x$ for any $g \in \mathcal{G}$;

d) if $k \neq i$ then the image of the functor $\_^x$ is the full subgroupoid $\mathcal{G}^{\setminus k}$ of $\mathcal{G}$ with $\operatorname{Obj}\mathcal{G}^{\setminus k} = \operatorname{Obj}\mathcal{G} - \{k\}$ (we use the notation $\mathcal{G}^{\setminus k}$ instead of $\mathcal{G}^x$, to emphasize that this groupoid depends only on the target of x);

e) $\_^x$ restricts to the identity on $\mathcal{G}^{\setminus k}$ and to an equivalence of categories $\mathcal{G}^{\setminus i} \to \mathcal{G}^{\setminus k}$, whose inverse $\mathcal{G}^{\setminus k} \to \mathcal{G}^{\setminus i}$ is the corresponding restriction of $\_^{\overline{x}}$;

f) for any $x \in \mathcal{G}(i,k)$ and $y \in \mathcal{G}(j,k)$, there exists a natural transformation $N : \_^x \to \_^y$ such that $N(k) = x\overline{y}$ and $N(l) = 1_l$ if $l \neq k$.

5.3. Given a groupoid $\mathcal{G}$ and a braided monoidal category $\mathcal{C}$, a *Hopf $\mathcal{G}$-algebra* in $\mathcal{C}$ is a family of objects $H = \{H_g\}_{g\in\mathcal{G}}$ in $\mathcal{C}$, equipped with the following families of morphisms in $\mathcal{C}$ (here and in the sequel we will often write g instead of H_g. In particular we will use the notations $\mathrm{id}_g = \mathrm{id}_{H_g}$, $\gamma_{g,h} = \gamma_{H_g,H_h}$, ${}_g\iota = {}_{H_g}\iota$ and $\iota_g = \iota_{H_g}$; moreover, based on the MacLane's coherence result for monoidal categories (p. 161 in [17]), we will omit the associativity morphisms since they can be filled in a unique way):

a *comultiplication* $\Delta = \{\Delta_g : H_g \to H_g \diamond H_g\}_{g\in\mathcal{G}}$, such that for any $g \in \mathcal{G}$

$$(\Delta_g \diamond \mathrm{id}_g) \circ \Delta_g = (\mathrm{id}_g \diamond \Delta_g) \circ \Delta_g; \tag{a1}$$

a *counit* $\epsilon = \{\epsilon_g : H_g \to \mathbf{1}\}_{g\in\mathcal{G}}$, such that for any $g \in \mathcal{G}$

$$(\epsilon_g \diamond \mathrm{id}_g) \circ \Delta_g = \mathrm{id}_g = (\mathrm{id}_g \diamond \epsilon_g) \circ \Delta_g; \tag{a2-2'}$$

a *multiplication* $m = \{m_{g,h} : H_g \diamond H_h \to H_{gh}\}_{g,h,gh\in\mathcal{G}}$ ($m_{g,h}$ is defined when g and h are composable in $\mathcal{G}$), such that if $f, g, h, fgh \in \mathcal{G}$ then

$$m_{fg,h} \circ (m_{f,g} \diamond \mathrm{id}_h) = m_{f,gh} \circ (\mathrm{id}_f \diamond m_{g,h}), \tag{a3}$$

$$(m_{g,h} \diamond m_{g,h}) \circ (\mathrm{id}_g \diamond \gamma_{g,h} \diamond \mathrm{id}_h) \circ (\Delta_g \diamond \Delta_h) = \Delta_{gh} \circ m_{g,h}, \tag{a5}$$

$$\epsilon_{gh} \circ m_{g,h} = \epsilon_g \diamond \epsilon_h; \tag{a6}$$

a *unit* $\eta = \{\eta_i : \mathbf{1} \to H_{1_i}\}_{i\in \mathrm{Obj}\,\mathcal{G}}$, such that if $g \in \mathcal{G}(i, j)$ then

$$m_{g,1_j} \circ (\mathrm{id}_g \diamond \eta_j) = \mathrm{id}_g = m_{1_i,g} \circ (\eta_i \diamond \mathrm{id}_g), \tag{a4-4'}$$

$$\Delta_{1_i} \circ \eta_i = \eta_i \diamond \eta_i, \tag{a7}$$

$$\epsilon_{1_i} \circ \eta_i = \mathrm{id}_{\mathbf{1}}; \tag{a8}$$

an *antipode* $S = \{S_g : H_g \to H_{\bar{g}}\}_{g\in\mathcal{G}}$ and its inverse $\overline{S} = \{\overline{S}_g : H_g \to H_{\bar{g}}\}_{g\in\mathcal{G}}$, such that if $g \in \mathcal{G}(i, j)$ then

$$m_{\bar{g},g} \circ (S_g \diamond \mathrm{id}_g) \circ \Delta_g = \eta_{1_j} \circ \epsilon_g, \tag{s1}$$

$$m_{g,\bar{g}} \circ (\mathrm{id}_g \diamond S_g) \circ \Delta_g = \eta_{1_i} \circ \epsilon_g, \tag{s1'}$$

$$S_{\bar{g}} \circ \overline{S}_g = \overline{S}_{\bar{g}} \circ S_g = \mathrm{id}_g\,. \tag{s2-2'}$$

The definition above is a straightforward generalization of a categorical group Hopf algebra given in [29]. Observe that an ordinary braided Hopf algebra in $\mathcal{C}$ is a Hopf $\mathcal{G} = \mathcal{G}_1$-algebra, where $\mathcal{G}_1$ is the trivial groupoid with a single object and a single morphism. In particular, H_{1_i} is a braided Hopf algebra in $\mathcal{C}$ for any $i \in \mathrm{Obj}\,\mathcal{G}$.

5.4. Let $\mathcal{C}$ be a braided monoidal category and $H = \{H_g\}_{g\in\mathcal{G}}$ be a Hopf $\mathcal{G}$-algebra in $\mathcal{C}$. By a categorical *left* (resp. *right*) *cointegral* of H we mean a family $l = \{l_i : H_{1_i} \to \mathbf{1}\}_{i\in\mathrm{Obj}\,\mathcal{G}}$ of morphisms in $\mathcal{C}$, such that for any $i \in \mathrm{Obj}\,\mathcal{G}$

$$\begin{array}{c}(\mathrm{id}_{1_i} \diamond l_i) \circ \Delta_{1_i} = \eta_i \circ l_i : H_{1_i} \to H_{1_i} \\ (\text{resp. } (l_i \diamond \mathrm{id}_{1_i}) \circ \Delta_{1_i} = \eta_i \circ l_i : H_{1_i} \to H_{1_i}).\end{array} \tag{i1-1'}$$

On the other hand, by categorical *right* (resp. *left*) *integral* of H we mean a family $L = \{L_g : \mathbf{1} \to H_g\}_{g\in\mathcal{G}}$ of morphisms in $\mathcal{C}$, such that if $g, h, gh \in \mathcal{G}$ then

$$\begin{array}{c}m_{g,h} \circ (L_g \diamond \mathrm{id}_h) = L_{gh} \circ \epsilon_h : H_h \to H_{gh} \\ (\text{resp. } m_{g,h} \circ (\mathrm{id}_g \diamond L_h) = L_{gh} \circ \epsilon_h : H_g \to H_{gh}).\end{array} \tag{i2-2'}$$

If l (resp. L) is both right and left categorical cointegral (integral) of H, we call it simply a cointegral (integral) of H.

5.5. Given a groupoid $\mathcal{G}$, let $\mathcal{H}(\mathcal{G})$ be the free braided monoidal category with a Hopf $\mathcal{G}$-algebra $H = \{H_g\}_{g\in\mathcal{G}}$ in it and with a left cointegral l and a right integral L of H, such that for any $i \in \mathrm{Obj}\,\mathcal{G}$

$$l_i \circ L_{1_i} = \mathrm{id}_{\mathbf{1}} = l_i \circ S_{1_i} \circ L_{1_i}. \tag{i3-3'}$$

We refer to $\mathcal{H}(\mathcal{G})$ as the *universal Hopf $\mathcal{G}$-algebra*. In particular, if $\mathcal{C}$ is any braided monoidal category with a Hopf $\mathcal{G}$-algebra $A = \{A_g\}_{g\in\mathcal{G}}$ in it which has a

left cointegral and a right integral satisfying the condition above, then there exists a braided monoidal functor $\mathcal{H}(\mathcal{G}) \to \mathcal{C}$ sending H_g to A_g.

Analogously to [13], $\mathcal{H}(\mathcal{G})$ can be described as a category of planar diagrams in $R \times [0,1]$. The objects of $\mathcal{H}(\mathcal{G})$ are sequences of points in R labeled by elements in $\mathcal{G}$, and the morphisms are iterated products and compositions of the elementary diagrams presented in Figure 33, modulo the relations presented in Figures 34, 35, 36 and 37 and plane isotopies which preserve the y-coordinate. We remind that the composition of diagrams $D_2 \circ D_1$ is obtained by stacking D_2 on the top of D_1 and then rescaling, while the product $D_1 \diamond D_2$ is given by the horizontal juxtaposition of D_1 and D_2.

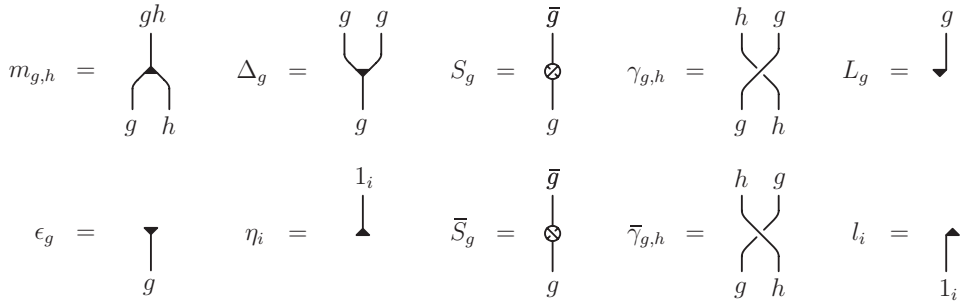

FIGURE 33. Elementary diagrams in $\mathcal{H}(\mathcal{G})$.

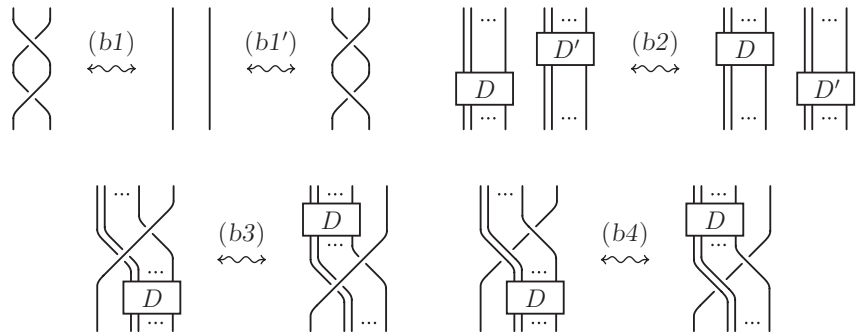

FIGURE 34. Braid axioms for $\mathcal{H}(\mathcal{G})$.

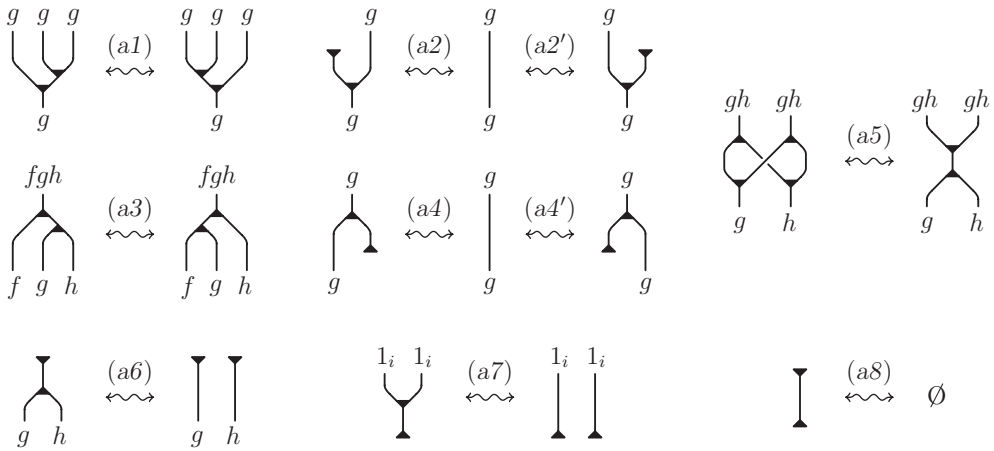

FIGURE 35. Bi-algebra axioms for $\mathcal{H}(\mathcal{G})$.

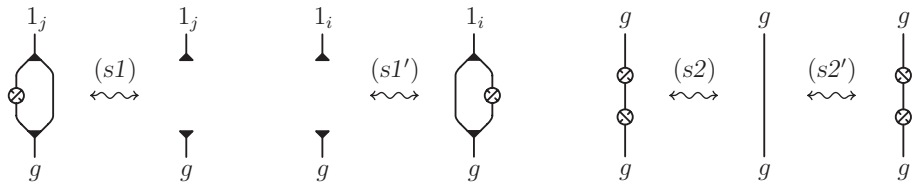

FIGURE 36. Antipode axioms for $\mathcal{H}(\mathcal{G})$ ($g \in \mathcal{G}(i,j)$).

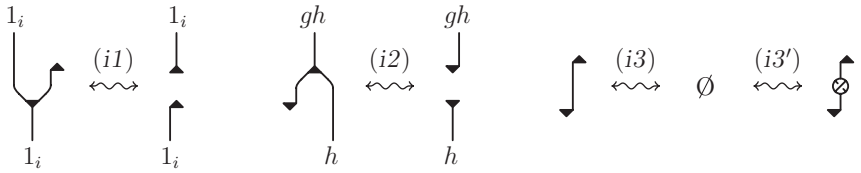

FIGURE 37. Integral axioms for $\mathcal{H}(\mathcal{G})$.

The plane diagrams and the relations between them listed above are going to be our main tool, so it would be useful to stop and reflect, trying to catch some general rules which would allow faster reading of the somewhat complicated compositions which will appear later. The first observation is that the plane diagrams used represent projections of embedded graphs in R^3 with uni-, bi- and tri-valent vertices and the projections of the edges do not contain local extremis. The vertices correspond to the defining morphisms in the algebra, and often we will call them with the name of the corresponding morphism. For example the bi-valent vertices (which have one incoming and one outgoing edge) will also be called antipode vertices. The uni-valent vertices are divided in unit vertices (corresponding to η and ϵ) and integral vertices (corresponding to l and Λ).

The notation for the vertices reflects their interaction in the relations and later their interpretation in terms of Kirby tangles. In particular, the uni- and tri-valent vertices are represented by small triangles which may point up (positively polarized) or down (negatively polarized). Then relations $(a8)$ and $(i3)$ can be summarized by saying that two uni-valent vertices of opposite polarizations, connected by an edge, annihilate each other. Analogously, relations $(a6)$, $(a7)$, $(i1)$ and $(i2)$ can be summarized by saying that a uni-valent vertex connected to a tri-valent vertex of opposite polarization, cancels this last one, creating two uni-valent vertices of the same polarization as its own.

Relations $(a2)$ and $(a4)$ can be put together as well, by saying that if a uni-valent vertex is connected to a tri-valent vertex of the same polarization, we can delete both vertices and the edge between them, fusing the remaining two edges into a single one. But we point out that there are two other possibilities to connect a uni- and tri-valent vertices of the same polarization, which do not appear in the relations above. Later, in Lemma 5.6 (cf. Figure 41), we will see that the diagrammatic language can be generalized to extend the statement to those two cases as well, but a "correction" appears.

The remaining three relations $(a1)$, $(a3)$ and $(a5)$ in Figure 35, concern the diagrams in which two tri-valent vertices are connected by a single edge. Observe that if the vertices have the same polarization, we can slide one through the other, while if they have opposite polarization, the diagram splits as shown in $(a5)$.

The proofs of most of our theorems require to show that some morphisms in the universal algebra are equivalent, meaning that the graph diagram of one of them can be obtained from the graph diagram of the other by applying a sequence of the defining relations (moves) in the algebra. We will outline the main steps in this procedure by drawing in sequence the intermedate diagrams, and for each step we will indicate in the corresponding order, the main moves needed to transform the diagram on the left into the one on the right. Actually, some steps can be understood more easily by starting from the diagram on the right and reading the moves in the reverse order. Notice, that the moves represent equivalences of diagrams and we use the same notation for them and their inverses. In the captions of the figures the reader will find (in square brackets) the reference to the pages where those moves are defined. For example, in the first step in Figure 38 we obtain the diagram on the left from the one on the right by first applying moves (*a1-3*) in Figure 35 on p. 29, then move (*s1*) in Figure 36 on p. 30 and finally moves (*a2-4′*) in Figure 35 on p. 29. To be precise, before applying (*s1*) and (*a4′*), we use the braid axioms in Figure 34, but this in general will not be indicated.

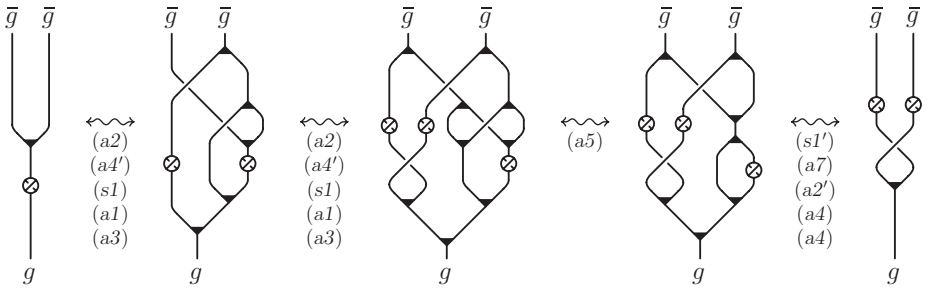

FIGURE 38. Proof of Lemma 5.6 [a/29, s/30].

In Figure 38 it is proved the first of the following properties of the antipode in $\mathcal{H}(\mathcal{G})$, which hold for any $g, h \in \mathcal{G}$ such that gh is defined and for any $i \in \mathcal{G}$:

$$\Delta_{\bar{g}} \circ S_g = (S_g \diamond S_g) \circ \gamma_{g,g} \circ \Delta_g : H_g \to H_{\bar{g}} \diamond H_{\bar{g}}, \tag{s3}$$

$$S_{gh} \circ m_{g,h} = m_{\bar{h},\bar{g}} \circ (S_h \diamond S_g) \circ \gamma_{g,h} : H_g \diamond H_h \to H_{\bar{h}\bar{g}}, \tag{s4}$$

$$S_{1_i} \circ \eta_i = \eta_i, \tag{s5}$$

$$\epsilon_{\bar{g}} \circ S_g = \epsilon_g. \tag{s6}$$

In terms of diagrams these relations are presented in Figure 39. They are analogous to the case of braided and group Hopf algebras (see [13] and [29]) and the rest of the proofs are left as an exercise.

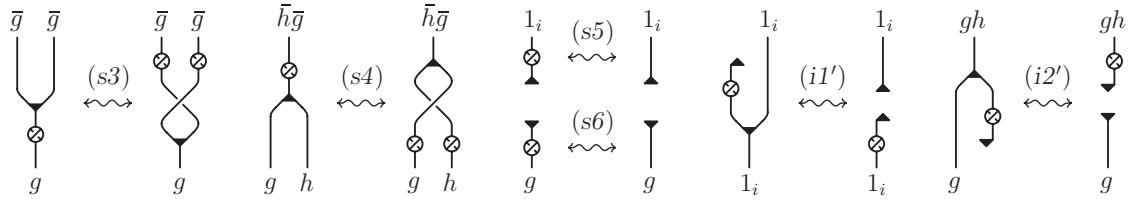

FIGURE 39. Properties of the antipode in $\mathcal{H}(\mathcal{G})$.

Using these properties one immediately sees that if $l = \{l_j : H_{1_j} \to \mathbf{1}\}_{j \in \mathrm{Obj}\,\mathcal{G}}$ is a left cointegral of H, then (cf. Figure 39):

$$l \circ S = \{l_j \circ S_{1_j} : H_{1_j} \to \mathbf{1}\}_{j \in \mathrm{Obj}\,\mathcal{G}} \text{ is a right cointegral of } H. \qquad (i1')$$

Analogously, if $L = \{L_g : \mathbf{1} \to H_g\}_{g \in \mathcal{G}}$ is a right integral of H, then (cf. Figure 39 again):

$$S \circ L = \{S_g \circ L_g : \mathbf{1} \to H_{\bar{g}}\}_{g \in \mathcal{G}} \text{ is a left integral of } H. \qquad (i2')$$

The next lemma extends Lemma 7 of [13] to possibly non-unimodular categories.

LEMMA 5.6. *$\mathcal{H}(\mathcal{G})$ is an autonomous category such that for every $g \in \mathcal{G}$ (cf. Figure 41):*

$$H_g^* = H_g,$$
$$\Lambda_{H_g} = \Lambda_g = \Delta_g \circ L_g, \qquad (f1)$$
$$\lambda_{H_g} = \lambda_g = l_{g\bar{g}} \circ m_{g,\bar{g}} \circ (\mathrm{id}_g \diamond S_g). \qquad (f2)$$

Proof of Lemma 5.6. Figure 40 shows that Λ_{H_g} and λ_{H_g} satisfy the relations in Paragraph 3.2. Then it suffices to observe that such relations propagate to Λ_A and λ_A for any object A in $\mathcal{H}(\mathcal{G})$, where Λ_A and λ_A are defined inductively by the following identities (observe that the definition is well-posed, giving equivalent results for different decompositions $A \diamond B = A' \diamond B'$):

$$(A \diamond B)^* = B^* \diamond A^*,$$
$$\Lambda_{A \diamond B} = (\mathrm{id}_{B^*} \diamond \Lambda_A \diamond \mathrm{id}_B) \circ \Lambda_B,$$
$$\lambda_{A \diamond B} = \lambda_A \circ (\mathrm{id}_A \diamond \lambda_B \diamond \mathrm{id}_{A^*}). \quad \square$$

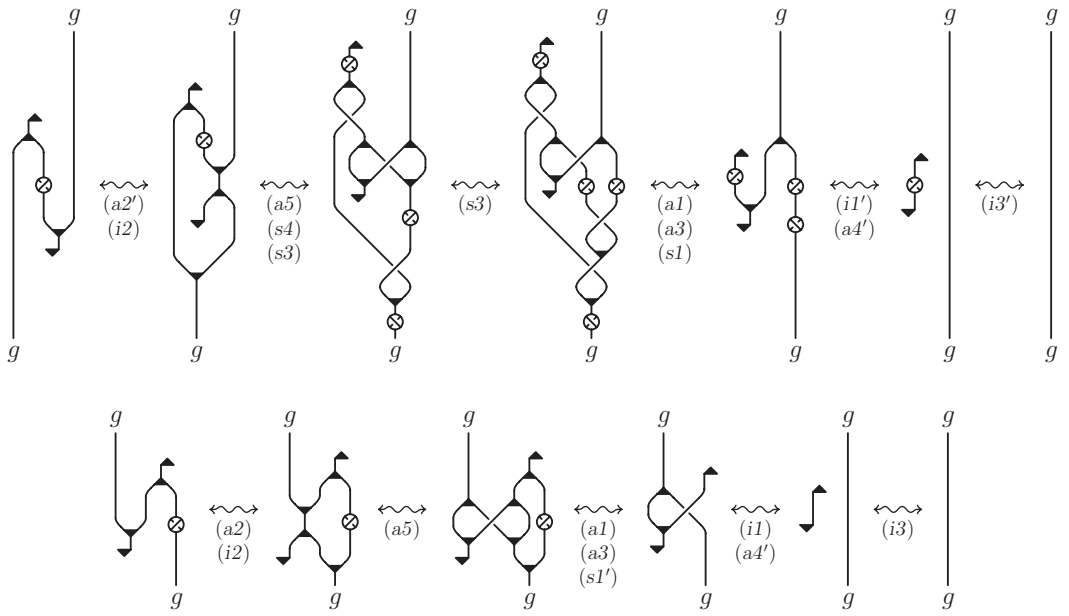

FIGURE 40. Proof of Lemma 5.6 [a/29, *i*/30-31, *s*/30-31].

To simplify notations we will often write λ_g and Λ_g instead of λ_{H_g} and Λ_{H_g}.

Lemma 5.6 implies that in the diagrams representing the morphisms of $\mathcal{H}(\mathcal{G})$, it is appropriate to use the notations (*f1*) and (*f2*) in Figure 41 for the coform and the form. In fact, the identities in Paragraph 3.2 reduce to the standard "pulling the string" (relation (*f3-3′*) in Figure 41), which together with the braid axioms in Figure 34 realize regular isotopy of strings.

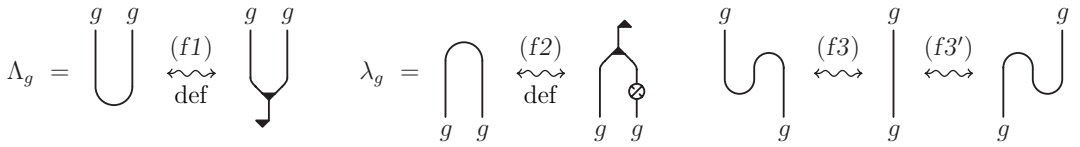

FIGURE 41. Coform and form in $\mathcal{H}(\mathcal{G})$.

Let $\mathrm{Mor}(A, B)$ denote the set of morphisms $A \to B$ in $\mathcal{H}(\mathcal{G})$. Then we define the "rotation" map

$$\mathrm{rot} : \mathrm{Mor}(H_g \diamond A, B \diamond H_h) \to \mathrm{Mor}(A \diamond H_h, H_g \diamond B)$$

by the equation

$$\mathrm{rot}(F) = (\mathrm{id}_{H_g \diamond B} \diamond \lambda_h) \circ (\mathrm{id}_g \diamond F \diamond \mathrm{id}_h) \circ (\Lambda_g \diamond \mathrm{id}_{A \diamond H_h}).$$

The following lemma shows that the negatively polarized tri-valent vertices are invariant under such rotation, while for the positively polarized tri-valent vertices this is equivalent to applying the antipode on the outgoing edge and its inverse on the right incoming edge.

LEMMA 5.7. *If $g, h, gh \in \mathcal{G}$ (g and h are composable) then (cf. Figure 42):*

$$\mathrm{rot}(\Delta_g) = \Delta_g : H_g \to H_g \diamond H_g, \tag{f4}$$

$$\mathrm{rot}(m_{g,h}) = \overline{S}_{\overline{g}} \circ m_{h,\overline{h}\overline{g}} \circ (\mathrm{id}_g \diamond S_{gh}) : H_h \diamond H_{gh} \to H_g. \tag{f5}$$

Proof. See Figure 43. □

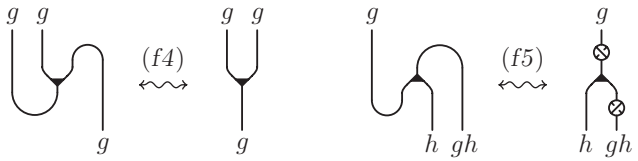

FIGURE 42. Properties of coform and form in $\mathcal{H}(\mathcal{G})$.

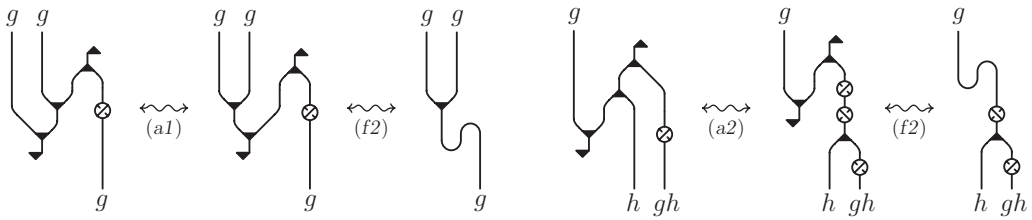

FIGURE 43. Proof of Lemma 5.7 [a/29, f/33].

5.8. A Hopf $\mathcal{G}$-algebra H in a braided monoidal category $\mathcal{C}$ is called *unimodular* if H has S-invariant integral and cointegral, i.e.

$$S_g \circ L_g = L_{\bar{g}}, \tag{i4}$$

$$l_{\bar{g}} \circ S_g = l_g. \tag{i5}$$

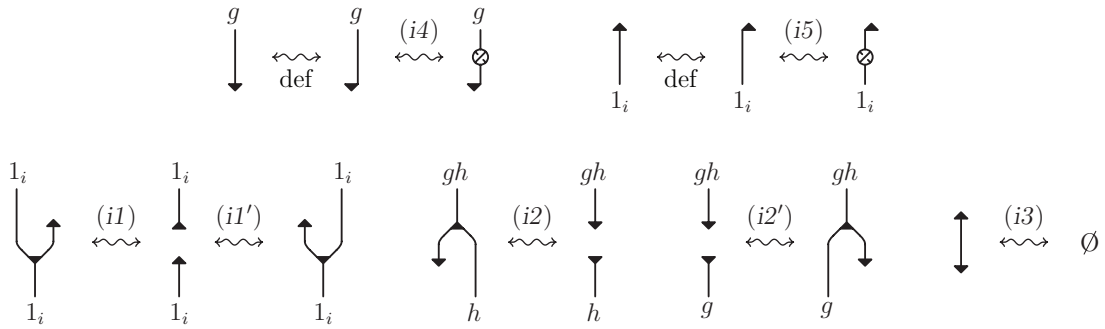

FIGURE 44. Integral axioms for $\mathcal{H}^u(\mathcal{G})$.

Given a groupoid $\mathcal{G}$, let $\mathcal{H}^u(\mathcal{G})$ be the quotient of $\mathcal{H}(\mathcal{G})$ modulo the relations (*i4*) and (*i5*) presented in Figure 44. We refer to $\mathcal{H}^u(\mathcal{G})$ as the *universal unimodular Hopf $\mathcal{G}$-algebra*. Moreover, in $\mathcal{H}^u(\mathcal{G})$ we change the notation for the integral vertices by connecting the edge to the middle point of the base of the triangle, to reflect that the corresponding integral is two-sided (cf. the bottom line in Figure 44).

Using the integral axioms (*i1*)-(*i5*) and (*a8*) in Figure 35, it is easy to see that the uni-valent vertices of the same polarization are dual to each other with respect to the form/coform as shown in Figure 45.

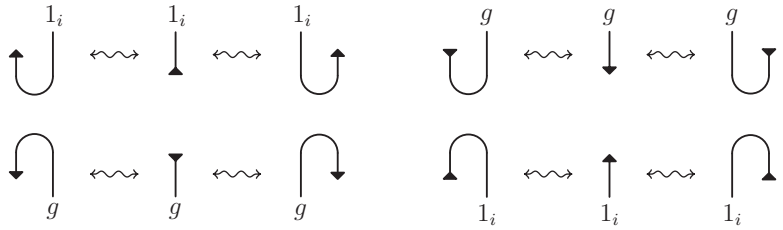

FIGURE 45. Duality of uni-valent vertices with the same polarization in $\mathcal{H}^u(\mathcal{G})$.

The next lemma is a version of Lemma 8 in [13], but for completeness we present the proof.

LEMMA 5.9. *$\mathcal{H}^u(\mathcal{G})$ is a tortile category where for any $g \in \mathcal{G}$ (cf. Figure 46):*

$$\theta_{H_g} = S_{\bar{g}} \circ S_g, \tag{f6-6′}$$

$$(\mathrm{id}_g \diamond S_g) \circ \Lambda_{\bar{g}} = (S_{\bar{g}} \diamond \mathrm{id}_g) \circ \Lambda_g, \tag{f7}$$

$$\lambda_g \circ (\mathrm{id}_g \diamond S_{\bar{g}}) = \lambda_{\bar{g}} \circ (S_g \diamond \mathrm{id}_{\bar{g}}). \tag{f8}$$

Proof. Define $\theta_A = (\lambda_{A^*} \diamond \mathrm{id}_A) \circ (\mathrm{id}_{A^*} \diamond \gamma_{A,A}) \circ (\Lambda_A \diamond \mathrm{id}_A)$ for any object A in $\mathcal{H}^u(\mathcal{G})$ (cf. Paragraph 3.2). In particular, θ_g is represented by the diagram on the left in move (*f6*) in Figure 46. This definition guarantees that $\theta_1 = \mathrm{id}_1$ and that

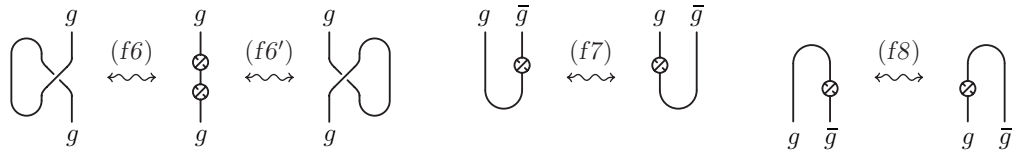

FIGURE 46. Additional properties of coform and form in $\mathcal{H}^u(\mathcal{G})$.

the identity $\theta_{A\diamond B} = \gamma_{B,A} \circ (\theta_B \diamond \theta_A) \circ \gamma_{A,B}$ holds, up to isotopy moves, for any two objects A, B in $\mathcal{H}^u(\mathcal{G})$. Therefore, in order to see that θ makes $\mathcal{H}^u(\mathcal{G})$ into a tortile category, it is enough to show its naturality and that $\theta_{A^*} = (\theta_A)^*$ for any A.

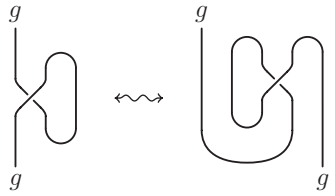

FIGURE 47.

We will first prove the last identity. Actually, through an induction argument, one can easily see that if this identity is true for $A = H_g$, then it is true for any other object A in $\mathcal{H}(\mathcal{G})$. As it is shown in Figure 47, the diagram on the right of move $(f6')$ in Figure 46 coincides with $(\theta_g)^*$ up to isotopy moves. In particular, the identity for $A = H_g$ would follow if we show $(f6)$ and $(f6')$. Now, in Figure 48 we prove moves $(f6)$ and $(f7)$. Then move $(f6')$ follows by applying $(f6)$ and $(f7)$ to right diagram in Figure 47.

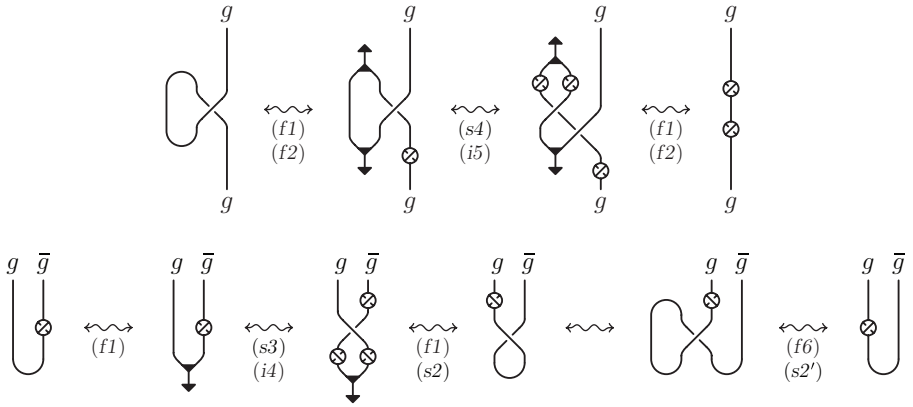

FIGURE 48. Proof of Lemma 5.9 [f/33, s/31-30].

It is left to show the naturality of θ, i.e. that for any morphism $F : A \to B$ in $\mathcal{H}^u(\mathcal{G})$ one has $\theta_B \circ F = F \circ \theta_A$. Actually, using the fact that $\theta_{A\diamond B} = \gamma_{B,A} \circ (\theta_B \diamond \theta_A) \circ \gamma_{A,B}$ and isotopy moves, one sees that it is enough to show this identity when F is any elementary morphism and in this case it follows from $(f6)$, $(s3\text{-}6)$ in Figure 39 and $(i4\text{-}5)$ in Figure 44.

To complete the proof of the theorem, observe that move $(f8)$ in Figure 46 follows from $(f7)$ and the properties $(f3\text{-}3')$ of the form and coform presented in Figure 41. □

6. The universal ribbon Hopf algebra $\mathcal{H}^r(\mathcal{G})$

6.1. Let $\mathcal{C}$ be a braided monoidal category and $(A, m^A, \eta^A, \Delta^A, \epsilon^A, S^A)$ and $(B, m^B, \eta^B, \Delta^B, \epsilon^B, S^B)$ be Hopf algebras in it (over the trivial groupoid). Then a morphism $\sigma_{A,B} : \mathbf{1} \to A \diamond B$ is called a *Hopf copairing* if the following conditions are satisfied:

$$(\Delta^A \diamond \mathrm{id}_B) \circ \sigma_{A,B} = (\mathrm{id}_{A\diamond A} \diamond m^B) \circ (\mathrm{id}_A \diamond \sigma_{A,B} \diamond \mathrm{id}_B) \circ \sigma_{A,B},$$
$$(\mathrm{id}_A \diamond \Delta^B) \circ \sigma_{A,B} = (m^A \diamond \mathrm{id}_{B\diamond B}) \circ (\mathrm{id}_A \diamond \sigma_{A,B} \diamond \mathrm{id}_B) \circ \sigma_{A,B},$$
$$(\epsilon^A \diamond \mathrm{id}_B) \circ \sigma_{A,B} = \eta^B \quad \text{and} \quad (\mathrm{id}_A \diamond \epsilon^B) \circ \sigma_{A,B} = \eta^A.$$

The Hopf copairing $\sigma_{A,B}$ is called *trivial* if $\sigma_{A,B} = \eta^A \diamond \eta^B$.

6.2. A unimodular Hopf $\mathcal{G}$-algebra H in a braided monoidal category $\mathcal{C}$ is called *ribbon* if there exists a family $v = \{v_g : H_g \to H_g\}_{g\in\mathcal{G}}$ of invertible morphisms in $\mathcal{C}$, called *ribbon morphisms*, such that:

$$\epsilon_g \circ v_g = \epsilon_g \quad (\epsilon\text{-invariance}), \tag{r2}$$
$$v_g \circ L_g = L_g \quad (L\text{-invariance}), \tag{r3}$$
$$S_g \circ v_g = v_{\bar{g}} \circ S_g \quad (S\text{-invariance}), \tag{r4}$$
$$m_{g,h} \circ (v_g \diamond \mathrm{id}_h) = v_{gh} \circ m_{g,h} = m_{g,h} \circ (\mathrm{id}_g \diamond v_h) \quad (\text{centrality}), \tag{r5-5'}$$
$$\gamma_{g,h} \circ (\mathrm{id}_g \diamond v_h) = (v_h \diamond \mathrm{id}_h) \circ \gamma_{g,h}, \tag{b3}$$
$$\overline{\gamma}_{g,h} \circ (\mathrm{id}_g \diamond v_h) = (v_h \diamond \mathrm{id}_h) \circ \overline{\gamma}_{g,h}; \tag{b4}$$

moreover, the family $\sigma = \{\sigma_{i,j} : \mathbf{1} \to H_{1_i} \diamond H_{1_j}\}_{i,j\in \mathrm{Obj}\,\mathcal{G}}$ of morphisms, defined by the identity

$$\sigma_{i,j} = \begin{cases} (v_{1_j}^{-1} \diamond (v_{1_j}^{-1} \circ S_{1_j})) \circ \Delta_{1_j} \circ v_{1_j} \circ \eta_j & \text{if } i = j, \\ \eta_i \diamond \eta_j & \text{if } i \neq j, \end{cases} \tag{r6-7}$$

satisfies the following properties:

$$\sigma_{i,j} \text{ is a Hopf copairing for any } i, j \in \mathrm{Obj}\,\mathcal{G} \tag{r8-8'-9-9'}$$
$$\Delta_g \circ v_g^{-1} = \mu_{g,g} \circ (v_g^{-1} \diamond v_g^{-1}) \circ \overline{\gamma}_{g,g} \circ \Delta_g : H_g \to H_g \diamond H_g, \tag{r10}$$
$$\begin{aligned}(m_{1_j,h} \diamond m_{g,1_i}) \circ (S_{1_j} \diamond (\mu_{h,g} \circ \overline{\gamma}_{g,h} \circ \mu_{g,h}) \diamond S_{1_i}) \circ (\rho^l_{g,j} \diamond \rho^r_{h,i}) = \\ = \gamma_{g,h} : H_g \diamond H_h \to H_h \diamond H_g,\end{aligned} \tag{r11}$$

where $\bar{g}g = 1_i$, $h\bar{h} = 1_j$ and:

$$\rho^r_{g,j} = (m_{g,1_i} \diamond \mathrm{id}_{1_j}) \circ (\mathrm{id}_g \diamond \sigma_{i,j}) : H_g \to H_g \diamond H_{1_j},$$
$$\rho^l_{h,i} = (\mathrm{id}_{1_i} \diamond m_{1_j,h}) \circ (\sigma_{i,j} \diamond \mathrm{id}_h) : H_h \to H_{1_i} \diamond H_h,$$
$$\mu_{g,h} = (m_{g,1_i} \diamond m_{1_j,h}) \circ (\mathrm{id}_g \diamond \sigma_{i,j} \diamond \mathrm{id}_h) : H_g \diamond H_h \to H_g \diamond H_h.$$

It is easy to check that $\rho^r_{g,j}$ (resp. $\rho^l_{g,j}$) make H_g into a right (resp. left) H_{1_j}-comodule. We will refer to the morphisms $\sigma_{i,j}$'s as *copairing morphisms* or simply *copairings*.

6.3. Given a groupoid $\mathcal{G}$, let $\mathcal{H}^r(\mathcal{G})$ be the free braided monoidal category with a ribbon Hopf $\mathcal{G}$-algebra H. We refer to $\mathcal{H}^r(\mathcal{G})$ as the *universal ribbon Hopf $\mathcal{G}$-algebra*. $\mathcal{H}^r(\mathcal{G})$ has the same objects as $\mathcal{H}(\mathcal{G})$ and its morphisms are iterated compositions and products of the elementary morphisms presented in Figures 33 and 49, modulo the relations presented in Figures 34 (where now D can be also a ribbon morphism), 35, 36, 44 and the additional relations presented in Figures 50 and 51, which express the ribbon axioms (*r6*)–(*r11*) in 6.2. Look at Figure 52 for the diagramatic presentations of the morphisms $\rho^r_{g,j}$, $\rho^l_{h,i}$, $\mu_{g,h}$ (here we also present the morphism $\mu^{-1}_{g,h}$ defined and shown to be the inverse of $\mu_{g,h}$ in Proposition 6.5).

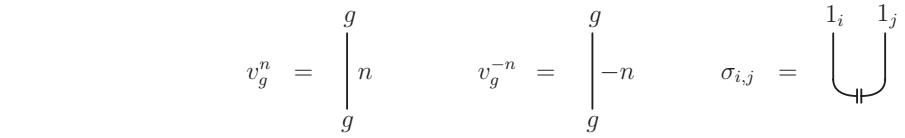

FIGURE 49. Additional elementary diagrams in $\mathcal{H}^r(\mathcal{G})$.

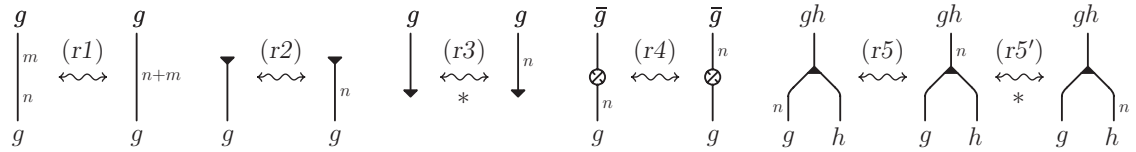

FIGURE 50. Additional axioms for $\mathcal{H}^r(\mathcal{G})$ – I.

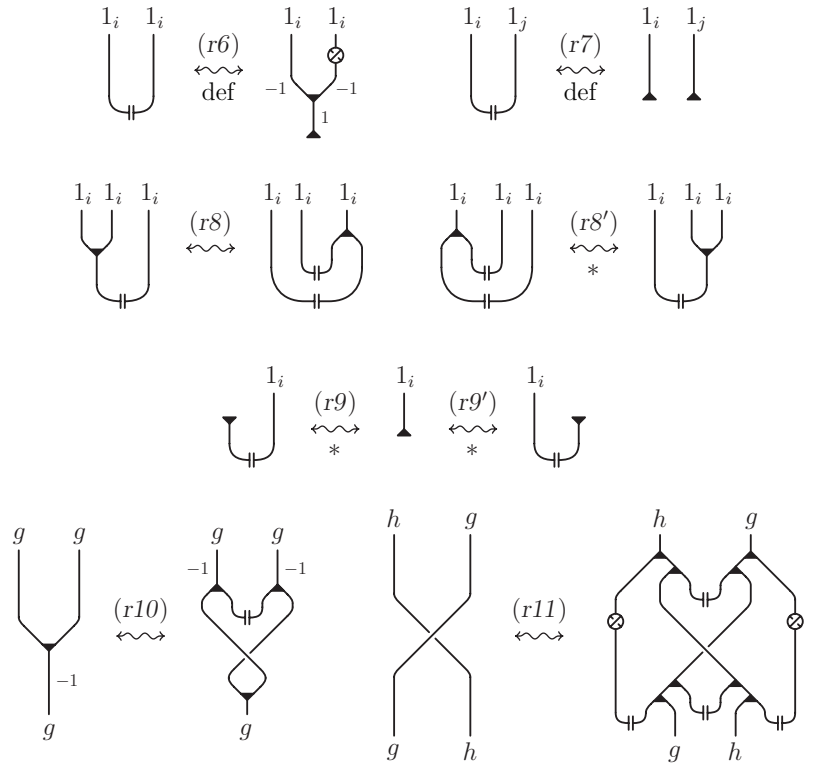

FIGURE 51. Additional axioms for $\mathcal{H}^r(\mathcal{G})$ – II ($i \neq j$).

We make here few useful observations about the axioms of the ribbon algebra and their diagramatic interpretation:

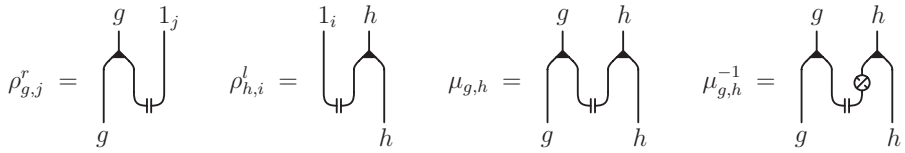

FIGURE 52.

a) In the diagrams v_g^n is interpreted as weight of an edge. Then relations (*r2*) and (*r3*) say that the weight of an edge attached to a negatively polarized uni-valent vertex can be changed arbitrarily, while (*r5-5′*) imply that the weight of one of the edges attached to a positevely polarized tri-valent vertex can be transferred to any other edge attached at that vertex.

b) In Figure 51, the relations (*r8-8′*) and (*r9-9′*) expressing the fact that $\sigma_{i,j}$ is a Hopf copairing, are shown only for $i = j$, since for $i \neq j$ the copairing is trivial and they follow from the rest of the axioms.

c) For some combinations of the labels, moves (*r10*) and (*r11*) simplify because trivial copairings appear. In particular, move (*r11*) reduces to a crossing change when $g \in \mathcal{G}(i,j)$ and $h \in \mathcal{G}(k,l)$ with $\{i,j\} \cap \{k,l\} = \emptyset$.

d) An interesting and important question is which of the axioms for v and σ in 6.2 are independent. In particular, the relations (*r3*), (*r5′*), (*r8′*) and (*r9-9′*) (marked with a star below the arrow), are consequences of the rest and have been listed as axioms only for convenience. In fact: (*r3*) can be obtained from (*r2*) by using (*r5*) and the duality of the negative uni-valent vertices (Figure 45); (*r9-9′*) immediately follow from the definition (*r6-7*) of the copairing, and the properties (*a2-2′*), (*s5-6*) and (*r2*) (Figures 35 and 39); (*r5′*) can be shown to be equivalent to (*r5*) by using property (*s4*) of the antipode (Figure 39). The proof that (*r8′*) derives from the rest of the axioms is presented in Appendix (Section 11). On the other hand, it seems unlikely that the relations (*r10*) and (*r11*), the new ones with respect to the relations in [13], are consequences of the rest, even if, as we will see later, they can be presented in different equivalent forms (cf. Corollary 6.6).

PROPOSITION 6.4. *Any functor $\varphi : \mathcal{G} \to \mathcal{G}'$ between groupoids which is injective on the set of objects can be extended to a functor $\Upsilon_\varphi : \mathcal{H}^r(\mathcal{G}) \to \mathcal{H}^r(\mathcal{G}')$. Moreover, if φ is faithful (an embedding) then Υ_φ is also faithful.*

In particular, when $\iota : \mathcal{G} \subset \mathcal{G}'$ is an inculsion of groupoids, we can identify $\mathcal{H}(\mathcal{G})$ and $\Upsilon_\iota(\mathcal{H}(\mathcal{G}))$ through the isomorphism of categories $\Upsilon_\iota : \mathcal{H}(\mathcal{G}) \to \Upsilon_\iota(\mathcal{H}(\mathcal{G}))$ and write $\mathcal{H}(\mathcal{G}) \subset \mathcal{H}(\mathcal{G}')$.

Proof. The extension Υ_φ of φ is formally defined as $\Upsilon_\varphi(m_{g,h}) = m_{\varphi(g),\varphi(h)}$, $\Upsilon_\varphi(\eta_i) = \eta_{\varphi(i)}$, etc. To see that Υ_φ is well defined, we need to check that all relations for $\mathcal{H}^r(\mathcal{G})$ are satisfied in the image. The only problem we might have would be with relation (*r7*) in Figure 51, if $i \neq j$ and $\varphi(i) = \varphi(j)$. But this cannot happen since φ is injective on objects. This concludes the first part of the proposition since the functoriality of Υ_φ is obvious.

At this point, it is left to show that when φ is injective on the set of morphisms, then Υ_φ is injective on morphisms as well. First of all, in this case φ induces an

isomorphism of categories $\widehat{\varphi} : \mathcal{G} \mapsto \mathcal{G}^\varphi$, where $\mathcal{G}^\varphi = \varphi(\mathcal{G})$. Then by definition, $\Upsilon_{\widehat{\varphi}} \circ \Upsilon_{\widehat{\varphi}^{-1}}$ and $\Upsilon_{\widehat{\varphi}^{-1}} \circ \Upsilon_{\widehat{\varphi}}$ are the identities; therefore $\Upsilon_{\widehat{\varphi}} : \mathcal{H}(\mathcal{G}) \mapsto \mathcal{H}(\mathcal{G}^\varphi)$ is an isomorphism of categories as well. Moreover, $\Upsilon_\varphi = \Upsilon_\iota \circ \Upsilon_{\widehat{\varphi}}$ where $\iota : \mathcal{G}^\varphi \subset \mathcal{G}'$ is the corresponding inclusion. Hence, the statement would follow if we show that the functor Υ_ι is injective on the set of morphisms.

Now let $F, F' : A \to B$ be two morphsims in $\mathcal{H}(\mathcal{G}^\varphi)$ such that $\Upsilon_\iota(F) = \Upsilon_\iota(F')$ in $\mathcal{H}(\mathcal{G}')$; in particular, F and F' are represented by two diagrams labeled in $\mathcal{G}^\varphi$, which are related by a sequence of moves in $\mathcal{H}(\mathcal{G}')$. Observe that when we apply a relation move to a diagram representing a morphism of $\mathcal{H}(\mathcal{G}')$, the only new labels that can appear are identities of $\mathcal{G}'$ and products of labels already occurring in it or their inverses. Since $\mathcal{G}^\varphi$ is a subcategory of $\mathcal{G}'$, this implies that the only labels not belonging to $\mathcal{G}^\varphi$ that can occur in the intermediate diagrams of the sequence are identities 1_i with $i \in \operatorname{Obj}\mathcal{G}' - \operatorname{Obj}\mathcal{G}^\varphi$. The parts of the graph diagram carrying such labels interact with the rest of the diagram only through move $(r7)$ in Figure 51; in particular, if to any intermediate diagram we apply move $(r7)$ to change back any trivial copairing into two units, the part of the graph labeled by 1_i's with $i \in \operatorname{Obj}\mathcal{G}' - \operatorname{Obj}\varphi(\mathcal{G})$, forms a component, disjoint from the rest. By deleting such component, we obtain a new sequence of diagrams between F and F' related by moves in $\mathcal{H}(\mathcal{G}^\varphi)$ which proves that $F = F'$ (in $\mathcal{H}(\mathcal{G}^\varphi)$). □

PROPOSITION 6.5. *For every $i, j \in \operatorname{Obj}\mathcal{G}$ and $g, h \in \mathcal{G}$, we have (cf. Figure 53):*

$$(S_{1_i} \diamond \mathrm{id}_j) \circ \sigma_{i,j} = (\mathrm{id}_i \diamond S_{1_j}) \circ \sigma_{i,j}, \tag{$p1$}$$

$$\mu_{g,h} \circ \mu_{g,h}^{-1} = \mathrm{id}_{g \diamond h} = \mu_{g,h}^{-1} \circ \mu_{g,h}, \tag{$p2$-$2'$}$$

with $\mu_{g,h}^{-1}$ defined by the following identity, where we are assuming $\bar{g}g = 1_i$ and $h\bar{h} = 1_j$ (cf. Figure 52):

$$\mu_{g,h}^{-1} = (m_{g,1_i} \diamond m_{1_j,h}) \circ (\mathrm{id}_g \diamond ((\mathrm{id}_{1_i} \diamond S_{1_j}) \circ \sigma_{i,j}) \diamond \mathrm{id}_h) : H_g \diamond H_h \to H_g \diamond H_h.$$

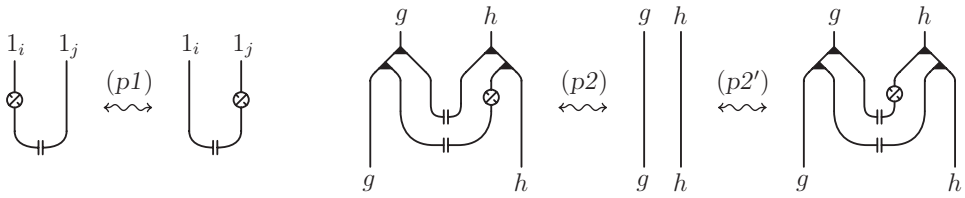

FIGURE 53. Some more relations in $\mathcal{H}^r(\mathcal{G})$ – I.

Proof. $(p2)$ is proved in Figure 54. The proof of $(p2')$ is analogous. To prove $(p1)$ let us consider the morphism $\overline{\mu}_{g,h}^{-1}$, which is the same as $\mu_{g,h}^{-1}$ but with the antipode moved to the left side of $\sigma_{i,j}$:

$$\overline{\mu}_{g,h}^{-1} = (m_{g,1_i} \diamond m_{1_j,h}) \circ (\mathrm{id}_g \diamond ((S_{1_i} \diamond \mathrm{id}_{1_j}) \circ \sigma_{i,j}) \diamond \mathrm{id}_h) : H_g \diamond H_h \to H_g \diamond H_h.$$

Then, by replacing $(r8')$, $(r9')$ and $(s1')$ in Figure 54 respectively with $(r8)$, $(r9)$ and $(s1)$, we obtain that $(p2)$ and $(p2')$ are still valid if $\mu_{g,h}^{-1}$ is replaced by $\overline{\mu}_{g,h}^{-1}$. Hence $\overline{\mu}_{g,h}^{-1}$ and $\mu_{g,h}^{-1}$ are equal, being both two-sided inverses of $\mu_{g,h}$. This gives $(p1)$. □

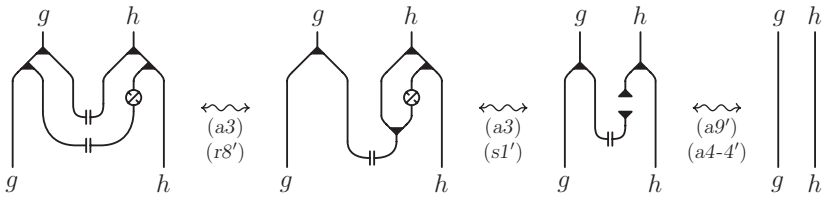

FIGURE 54. Proof of relation (*p2*) in Figure 53 [a/29, r/37, s/30].

In Figures 55 and 56 we list some more useful relations satisfied in $\mathcal{H}^r(\mathcal{G})$, but in order not to make this section excessively technical, we collect their proofs in Appendix (Section 11). We only point out that (*p3-3′*), (*p5-5′*) and (*p10-10′*) – (*p12*) follow directly from the definition of $\sigma_{i,j}$ and axioms (*r1*)–(*r5′*), but do not depend on the extra axioms in Figure 51, in particular on the fact that $\sigma_{i,j}$ is a Hopf copairing. Observe also that (*p1*) in Figure 53 and the moves in Figure 55 allow us to extend the notion of isotopy to $\mathcal{H}^r(\mathcal{G})$. As it is shown in Appendix 11, they imply that if a string connecting two polarized vertices, is divided by a copairing morphism, this morphisms can be shifted anywhere between those vertices. Therefore, we will

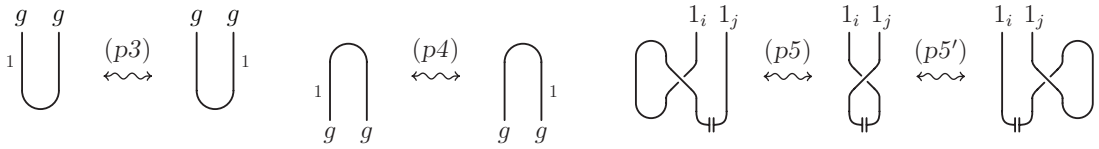

FIGURE 55. Additional isotopy relations in $\mathcal{H}^r(\mathcal{G})$.

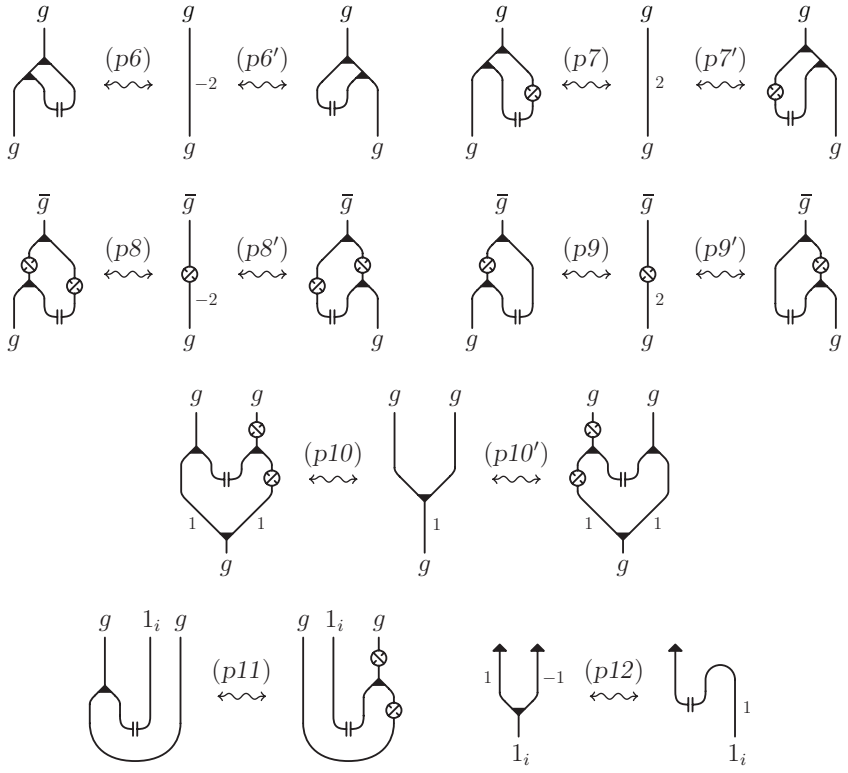

FIGURE 56. Some more relations in $\mathcal{H}^r(\mathcal{G})$ – II.

say that two graph diagrams in $\mathcal{H}^r(\mathcal{G})$ are *isotopic* or that one of them is obtained from the other through *isotopy* if it is obtained by applying a sequence of moves (*b1-4*) in Figure 34, (*f3-3′*) in Figure 41, (*f6*) ∘ (*f6′*) and (*f7-8*) in Figure 46, (*p1*) in Figure 53 and (*p3-5′*) in Figure 55.

An immediate consequence of Proposition 6.5 is the following.

COROLLARY 6.6. *The axiom* (*r10*) *can be replaced by either* (*r10′*), (*r12*) *or* (*r12′*) *in Figure 57, while axiom* (*r11*) *can be replaced by* (*r11′*) *in Figure 58.*

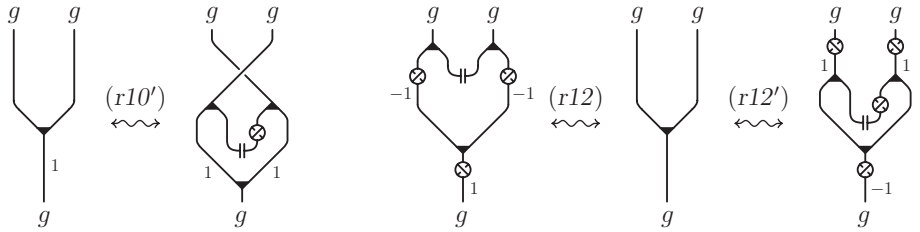

FIGURE 57. Equivalent presentations of (*r10*).

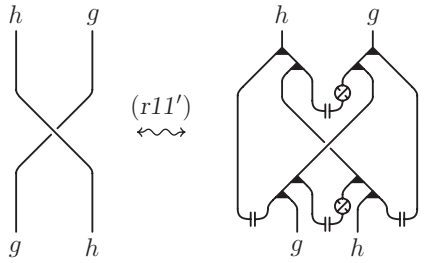

FIGURE 58. Equivalent presentation of (*r11*).

Proof. The equivalence between (*r10*) and (*r12*) derives from (*s3*) in Figure 39 after having composed both sides of (*r10*) on the bottom with v_g. (*r10′*) is obtained from (*r10*) by composing both sides on the bottom with v_g and on the top with the invertible morphism $\gamma_{g,g} \circ \mu_{g,g}^{-1} \circ (v_g \diamond v_g)$. Analogously, (*r12′*) is obtained from (*r12*) by replacing g with $\overline{g}$ and composing both sides on the bottom and on the top respectively with the invertible morphisms $S_g \circ v_g^{-1}$ and $(\overline{S}_g \diamond \overline{S}_g) \circ \mu_{g,g}^{-1} \circ (v_g \diamond v_g)$.

To see that (*r11*) and (*r11′*) are equivalent, it suffices to observe that the right sides of the two relations are inverse of each other by using (*p2-2′*). □

6.7. As we have seen at page 38 for move (*r11*), some relations involving the copairing simplify significantly for suitable choices of the labeling, due to the fact that $\sigma_{i,j}$ is trivial if $i \neq j$.

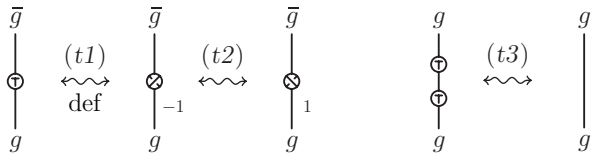

FIGURE 59. Additional relations for T_g – I ($g \in \mathcal{G}(i,j)$, $i \neq j$).

In particular, for $g \in \mathcal{G}(i,j)$ with $i \neq j$ relation $(p8)$ in Figure 56 implies that $S_g \circ v_g^{-1} = \overline{S}_g \circ v_g$ and in this case we define (cf. Figure 59)

$$T_g = S_g \circ v_g^{-1} = \overline{S}_g \circ v_g \quad \text{if } g \in \mathcal{G}(i,j) \text{ with } i \neq j. \tag{t1-2}$$

Then we have

$$T_{\overline{g}} \circ T_g = \mathrm{id}_g\,. \tag{t3}$$

For any object A in $\mathcal{H}^r(\mathcal{G})$, let $V_A : A \to A^*$ be the morphism in $\mathcal{H}^r(\mathcal{G})$, defined inductively by the following identities (the definition is well-posed, giving equivalent results for different decompositions $A \diamond B = A' \diamond B'$):

$$V_{\mathbf{1}} = \mathrm{id}_{\mathbf{1}}\,, \quad V_{H_g} = v_g \quad \text{and} \quad V_{A\diamond B} = (V_B \diamond V_A) \circ \gamma_{A,B}.$$

This morphism is obviously invertible and for any $F : A \to B$ we define:

$$\mathrm{rev}(F) = V_B^{-1} \circ F \circ V_A.$$

Proposition 6.8. *For any $g \in \mathcal{G}(i,j)$ and $h \in \mathcal{G}(j,k)$ with $i \neq j \neq k \neq i$, we have (cf. Figure 60):*

$$(T_{\overline{g}} \circ T_{\overline{g}}) \circ \Delta_{\overline{g}} \circ T_g = \Delta_g = \mathrm{rev}(\Delta_g); \tag{t4-5}$$

$$\mathrm{rot}(m_{g,h}) = T_{\overline{g}} \circ m_{h,\overline{gh}} \circ (\mathrm{id}_h \diamond T_{gh}); \tag{t6}$$

$$\mathrm{rev}(m_{g,h}) = T_{\overline{gh}} \circ m_{\overline{h},\overline{g}} \circ (T_h \diamond T_g). \tag{t7}$$

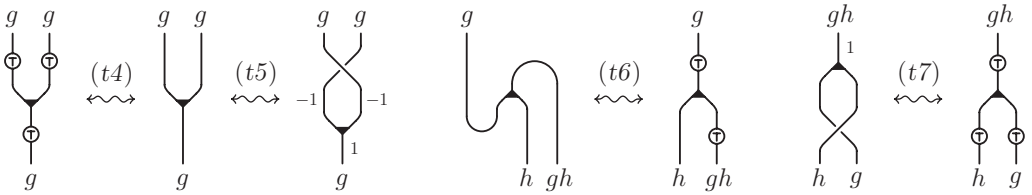

Figure 60. Additional relations for T_g – II ($g \in \mathcal{G}(i,j), h \in \mathcal{G}(j,k), i \neq j \neq k \neq i$).

Proof. $(t4)$ and $(t5)$ rewrite $(r12)$ and $(r10)$ (in Figures 57 and 51) when $g \in \mathcal{G}(i,j)$ with $i \neq j$, i.e. when $\sigma_{i,j}$ is trivial. $(t6)$ and $(t7)$ rewrite $(f5)$ and $(s4)$ (in Figures 42 and 39), under the further assumption that $h \in \mathcal{G}(j,k)$ and $i \neq k \neq j$. □

6.9. A ribbon Hopf $\mathcal{G}$-algebra H in a braided monoidal category $\mathcal{C}$ is called *selfdual* if

$$(l_i \diamond \mathrm{id}_{1_i}) \circ \sigma_{i,i} = L_{1_i} = (\mathrm{id}_{1_i} \diamond l_i) \circ \sigma_{i,i}. \tag{d1-1'}$$

A selfdual ribbon Hopf $\mathcal{G}$-algebra H is called *boundary* if

$$l_i \circ v_{1_i} \circ \eta_i = \mathrm{id}_{1_i} = l_i \circ v_{1_i}^{-1} \circ \eta_i. \tag{d2-2'}$$

We define $\partial^\star\mathcal{H}^r(\mathcal{G})$ (resp. $\partial\mathcal{H}^r(\mathcal{G})$) to be the quotient category of $\mathcal{H}^r(\mathcal{G})$ modulo the relation $(d1)$ presented in Figure 61 (resp. the relations $(d1)$ and $(d2)$ in the same figure). We call $\partial^\star\mathcal{H}^r(\mathcal{G})$ (resp. $\partial\mathcal{H}^r(\mathcal{G})$) the *universal selfdual* (resp. *boundary*) ribbon Hopf algebra.

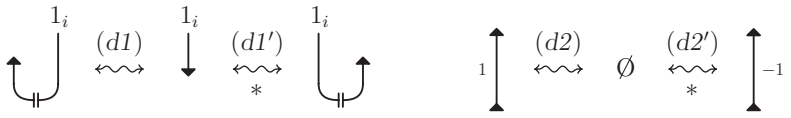

FIGURE 61. Axioms for $\partial^\star\mathcal{H}^r(\mathcal{G})$ and $\partial\mathcal{H}^r(\mathcal{G})$.

Actually $(d1')$ and $(d2')$ (marked with a star below the arrow) have been listed as axioms only for convenience. Indeed, $(d1')$ follows from $(d1)$ and $(p5\text{-}5')$ in Figure 55, while $(d2')$ follows from $(d2)$ and the relation shown in Figure 62.

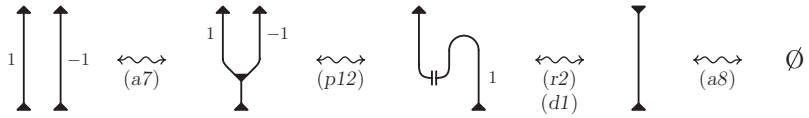

FIGURE 62. A relation in $\partial^\star\mathcal{H}^r(\mathcal{G})$ [a/29, d/43, p/40].

As it was observed by Kerler in [13], the relation $(d1)$ in Figure 61 implies the nondegeneracy of the copairing and the duality of the multiplication and comultiplication morphisms in $\partial^\star\mathcal{H}^r(\mathcal{G})$. In particular, if one defines pairing morphisms $H_{1_i} \diamond H_{1_j} \to \mathbf{1}$ as $(d3)$ in Figure 63, then the relations $(d4\text{-}4')$ and $(d5)$ presented in the same figure can be easily derived by using isotopy moves and move $(r8')$ in Figure 51.

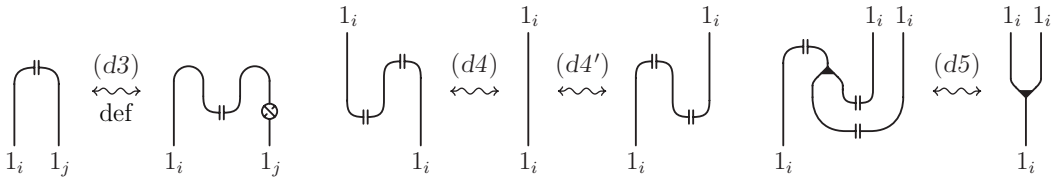

FIGURE 63. Some more relations in $\partial^\star\mathcal{H}^r(\mathcal{G})$.

7. From the algebra to the generalized Kirby diagrams

7.1. *Proof of Theorem 1.1.* The braided monoidal functor $\Phi_n : \mathcal{H}_n^r \to \mathcal{K}_n$ is defined by sending $H_{(i,j)}$ to the ordered pair (i, j) of labeled intervals, while the images of the elementary morphisms in $\mathcal{H}_n^r$ are presented in Figure 64.

The reader can check that the images of the form and the coform $\lambda_{(i,j)}$ and $\Lambda_{(i,j)}$ are equivalent in $\mathcal{K}_n$ to the ones presented in Figure 65.

The proof of the theorem is an extension of the well known fact that the category of admissible tangles contains a braided Hopf algebra object (see [13, 8]). In particular, here we work with the category of generalized tangles, i.e. tangles with dotted components and different labels, and correspondingly a groupoid Hopf algebra. Moreover we need to check the extra ribbon axioms in 6.2.

Most of the Hopf algebra axioms are very easy to check. For example $(a2\text{-}2')$, $(a6)$ and $(a8)$ in Figure 35 and $(i2)$, $(i3)$ in Figure 44 follow directly from the deletion of 1/2-canceling pairs (the bottom move in Figure 7). The same is true for $(a1)$, $(a3)$, $(a4\text{-}4')$, $(a7)$ and $(i1\text{-}1')$, but one needs to make one or two handle slides

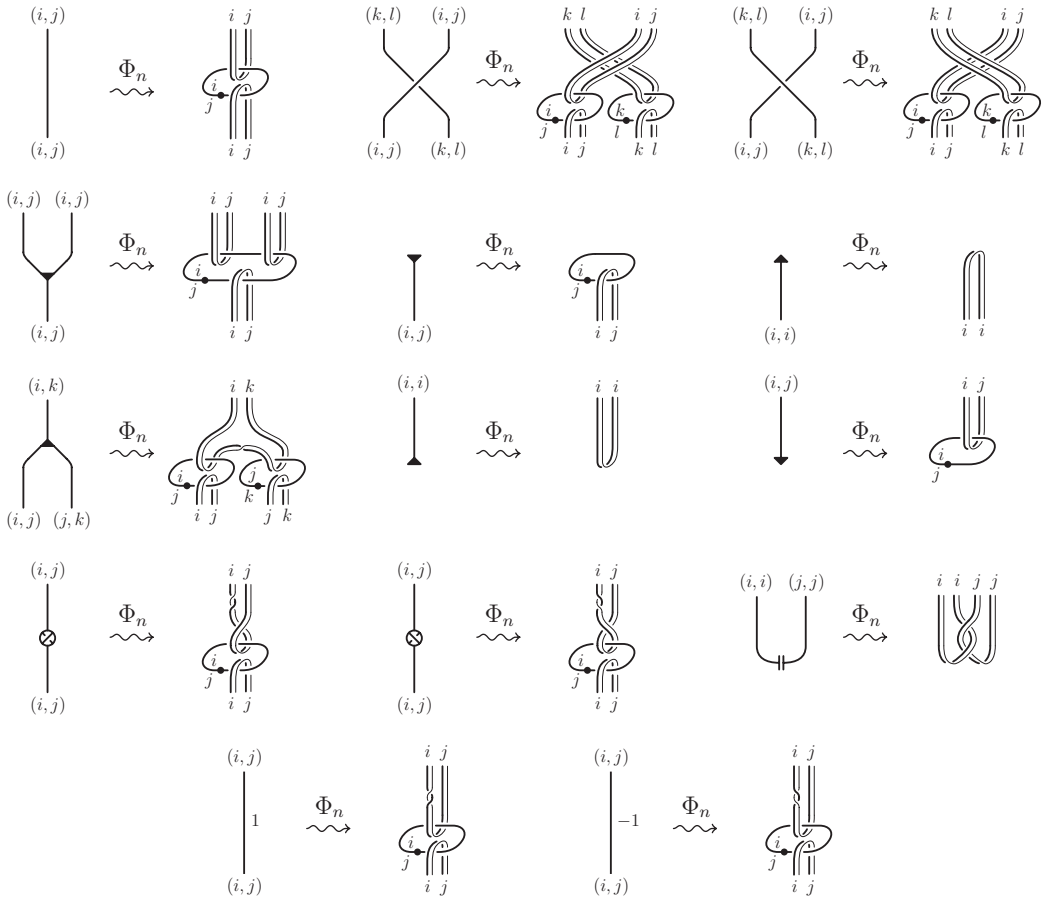

FIGURE 64. Definition of $\Phi_n : \mathcal{H}_n^r \to \mathcal{K}_n$.

FIGURE 65. $\Phi_n(\lambda_{(i,j)})$ and $\Phi_n(\Lambda_{(i,j)})$.

before deleting. (*s2-2′*) and (*i4*) reduce to an isotopy. (*a5*) in Figure 35 and (*s1*) in Figure 36 are shown in Figures 66 and 67 respectively ((*s1′*) is analogous).

The ribbon axiom (*r7*) in Figure 51 follows from the last move in Figure 6, which allows to change crossings between components with different labels. The

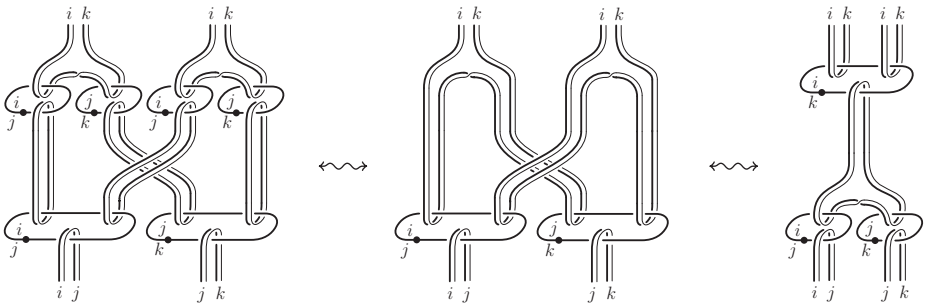

FIGURE 66. Proof of (*a5*) in Figure 35.

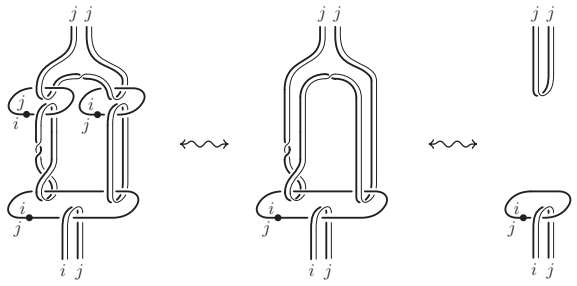

FIGURE 67. Proof of (*s1*) in Figure 36.

ribbon axioms (*r2*), (*r3*), (*r9*) and (*r9′*) follow from the deletion of 1/2-canceling pairs, while in showing (*r1*) and (*r4*) one needs to make a handle slide before deleting. The rest of the ribbon axioms are shown in Figures 68 to 72. □

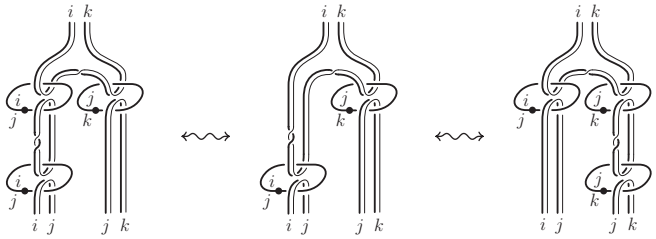

FIGURE 68. Proof of (*r5*-*5′*) in Figure 50.

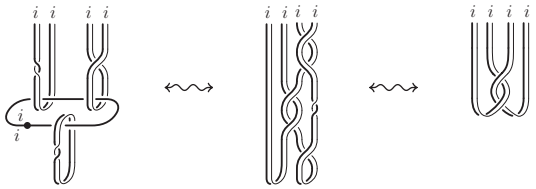

FIGURE 69. Proof of (*r6*) in Figure 51.

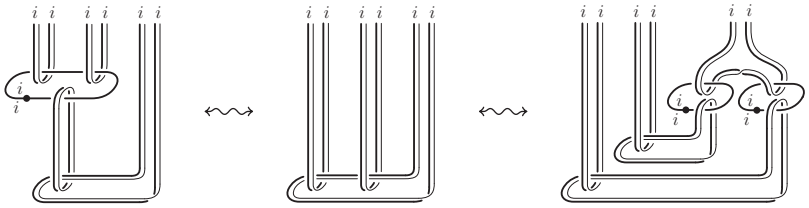

FIGURE 70. Proof of (*r8*) in Figure 51.

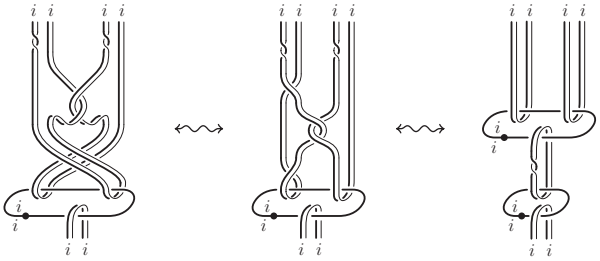

FIGURE 71. Proof of (*r10*) in Figure 51.

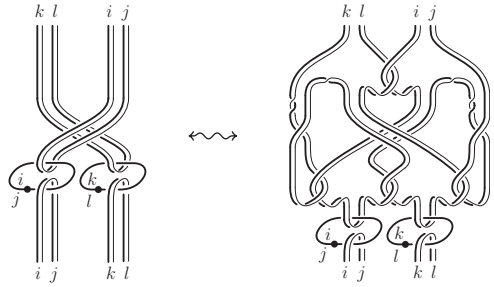

FIGURE 72. Proof of (*r11*) in Figure 51.

Observe that under the functor Φ_n, the relations (*d1*) and (*d2*) in Figure 61 translate directly in (*a*) and (*b*) in Figure 15. This leads to the following proposition.

PROPOSITION 7.2. *Φ_n induces functors on the quotient categories*

$$\partial^\star\Phi_n : \partial^\star\mathcal{H}_n^r \to \partial^\star\mathcal{K}_n \quad \textit{and} \quad \partial\Phi_n : \partial\mathcal{H}_n^r \to \partial\mathcal{K}_n.$$

7.3. The restriction of Φ_n to the set of complete closed morphisms in $\mathcal{H}_n^r$ is surjective, and this will follow from Theorem 1.4, once it is proved. Nevertheless, we sketch here the procedure which allows to find the preimage under Φ_1 of any Kirby diagram $K \in \widehat{\mathcal{K}}_1$. Obviously, this has a great practical value, since it allows to calculate invariants of 4-dimensional 2-handlebodies directly from their surgery presentation.

Let $K = \cup_j L_j$, where some of the L_j's form a trivial link of dotted unknots and the others are framed knots. Consider a planar diagram of K, where the dotted components project trivially, in such a way that the crossings are either between two framed components or between one framed and one dotted component. By changing a finite number of such crossings, say $C_1, \ldots, C_l$, one can obtain a new Kirby diagram $K' = \cup_j L'_j$ which is trivial as a link. Without loss of generality, K' can be assumed to coincide with K outside $E_1 \cup \ldots \cup E_l$, where each E_i is a cylinder projecting onto a small circular neighborhood of C_i. One of such cylinders E_i, together with the relative portions of the diagrams K and K', is depicted in Figure 73 (*a*) and (*b*), where j and k may or may not be distinct.

Now let $D = \cup_j D_j$ be a disjoint union of disks embedded in R^3 and bounded by $\cup_j L'_j$. Embed in each D_j a connected rooted uni/tri-valent tree whose uni-valent vertices (different from the root) are the preimages of the C'_i's in L'_i, and the rest of the tree lies in the interior of the disk. Then connect through a vertical (with respect to the projection plane) edge e_i the two preimages of each crossing C'_i (cf. Figure 73 (*b*)). Orient all edges of the trees in such a way that if L'_j is a dotted component, each tri-valent vertex has one incoming and two outgoing edges, and if L'_j is a framed component, each tri-valent vertex has two incoming and one outgoing edge. In this way one obtains a graph embedded in R^3 whose bi-valent vertices correspond to the preimages of C'_i. Remove these vertices from the graph. When the edges of the trees, attached to these preimages, are oriented in a consistent way as shown on the top in Figure 73 (*c*), this induces an orientation of the resulting edge. Otherwise divide this edge by a single bi-valent vertex as shown on the bottom in Figure 73 (*c*). In this way one obtains a graph G embedded in R^3 whose bi-valent vertices stay above those crossings C'_i which involve two framed components.

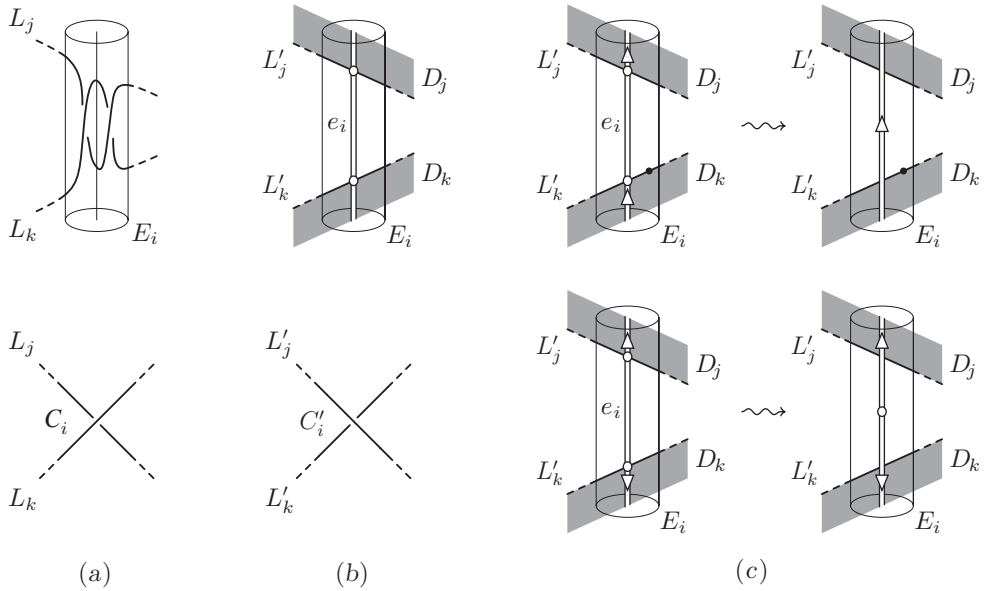

FIGURE 73.

At this point, consider a closed regular neighborhood N_G of G in R^3 extending the regular neighborhood $E = \cup_i E_i$ of the edges e_i and such that $J = N_G \cap D$ is a regular neighborhood of the trees in D. Let $I = \partial D \cap J$ be the set of intervals in which J intersects the boundary of the disks D_j. Then the link

$$K'' = (K \cap E) \cup (\partial J - \operatorname{Int} I)\,,$$

is isotopic to K through an isotopy which restricts to a deformation retraction on each D_j. Isotope further N_G (inducing an isotopy of G and K'') in such a way that G is in regular position with respect to the projection plane, and in a neighborhood of each root and tri-valent vertex the projection of the edges on the y-axis is increasing. Then isotope K'' in N_G, to put it in regular position with respect to the projection plane and transform its framing into blackboard framing. Finally, observe that, up to isotopy and creations of canceling pairs of 1/2-handles, K'' is composed by the elementary diagrams on the right in Figures 64 and 69, where the bi-valent vertices correspond to the images of the copairing morphism. An example (with blackboard framing) is presented in Figure 74 where the crossings C_i are encircled by a small gray disk.

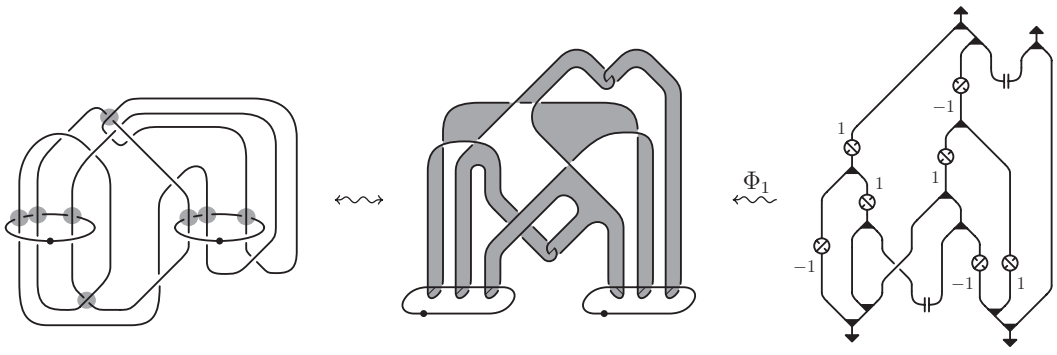

FIGURE 74. Surjectivity of Φ_1 on the set of closed morphisms.

8. The reduction map

This section is dedicated to the proof of Theorem 1.2, i.e. given $m < n$, we construct a bijective map $\downarrow^n_m : \widehat{\mathcal{H}}^{r,c}_n \to \widehat{\mathcal{H}}^{r,c}_m$ such that $\downarrow^n_m \circ \Phi_n = \Phi_m \circ \downarrow^n_m$. In other words, we realize in $\widehat{\mathcal{H}}^{r,c}_n$ (actually in $\widehat{\mathcal{H}}^{r,c}(\mathcal{G})$ for any $\mathcal{G}$) the algorithm for reducing the labels (0-handles) of a generalized Kirby diagram described in 2.2.

According to the algorithm in 2.2, in order to cancel the n-th 0-handle in a diagram K, one first separates the part of the diagram contained in this 0-handle by "pulling it up", and then slides it over an 1-handle U of label $x = (i_0, n)$ with $i_0 \neq n$. As a result the labels in the diagram change from j to j^x, where $\_^x : \mathcal{G}_n \to \mathcal{G}_{n-1}$ denotes the functor constructed in Paragraph 5.2; in particular, $n^x = i_0$ and $j^x = j$ for any $j \neq n$. Eventually, one cancels the n-th 0-handle and U. The resulting diagram $K^U \in \widehat{\mathcal{K}}_{n-1}$ does not contain the label n.

Observe that K^U can be thought as obtained from K through a sequence of the following local changes:

a) (if necessary) flip over in the projection plane any dotted components of label (i_0, n) in such a way that the upper face is labeled n;

b) change the sign of all crossings at which a component labeled n runs under a component labeled i_0;

c) change all labels from j to j^x;

d) cancel the component U.

The modifications *a*) and *b*) produce equivalent diagrams in $\widehat{\mathcal{K}}_n$, while *c*) replaces any label n with i_0, producing this way a diagram in $\Re^x_{\mathcal{K}}(K) \in \widehat{\mathcal{K}}_{n-1}$. Since $\Re^x_{\mathcal{K}}(K)$ is obtained from K through local changes which depend on x, but not on U, we may think of it as defining a map $\Re^x_{\mathcal{K}} : \mathcal{K}_n \to \mathcal{K}_{n-1}$. Figure 75 shows $\Re^x_{\mathcal{K}}(\Phi_n(\Delta_{(i_0,n)}))$, $\Re^x_{\mathcal{K}}(\Phi_n(S_{(i_0,n)}))$ and $\Re^x_{\mathcal{K}}(\Phi_n(\overline{S}_{(n,i_0)}))$ (here we apply the move described in Figure 32 to flip the dotted components). Observe that $\Re^x_{\mathcal{K}}$ respects the monoidal structures of the two categories, a structure which is violated by *d*).

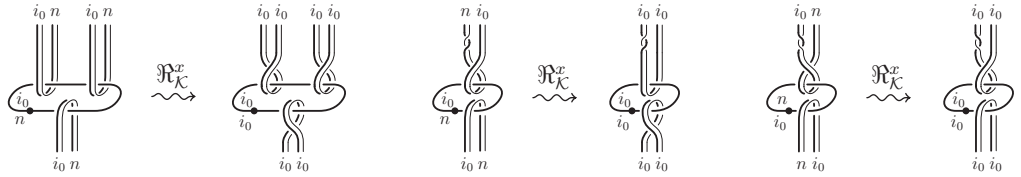

FIGURE 75. ($x \in \mathcal{G}(i_0, n)$ with $i_0 \neq n$)

On the other hand, given a different morphism $y = (j_0, n)$ with $i_0 \neq j_0 \neq n$, $\Re^x_{\mathcal{K}}(K)$ and $\Re^y_{\mathcal{K}}(K)$ may not be equivalent as diagrams in $\mathcal{K}_{n-1}$ even if K is closed. Indeed, if K is made out of a single 1-handle of label (n, n), then $\Re^x_{\mathcal{K}}(K)$ consists in a single 1-handle of index (i_0, i_0), while $\Re^y_{\mathcal{K}}(K)$ consists in a single 1-handle of index (j_0, j_0). Those two cannot be related unless it is present another 1-handle of label $y\overline{x} = (j_0, i_0)$, when $\Re^x_{\mathcal{K}}(K)$ can be slided over this 1-handle obtaining $\Re^y_{\mathcal{K}}(K)$. In particular, if K is a complete morphism in $\widehat{\mathcal{K}}^c_n$ and V is any dotted component of K with label $y = (j_0, n)$, then K^U can be transformed into K^V through 1-handle slides (cf. Figure 10). Therefore the reduction map $\downarrow^n_{n-1} K = K^U$ is well defined on the subset of closed complete morphisms.

Now we want to mimic the above reduction procedure in $\mathcal{H}^r(\mathcal{G})$ where $\mathcal{G}$ an arbitrary groupoid. Notice that in this case there is no natural order on $\operatorname{Obj}\mathcal{G}$, so the indices i_0 and n above will be replaced by two (possibly coinciding) objects $i_0, k_0 \in \operatorname{Obj}\mathcal{G}$.

Given $x \in \mathcal{G}(i_0, k_0)$, we extend the functor $\_^x : \mathcal{G} \to \mathcal{G}$ defined in Paragraph 5.2 to a map $\_^x : \operatorname{Obj}\mathcal{H}^r(\mathcal{G}) \to \operatorname{Obj}\mathcal{H}^r(\mathcal{G})$, by requiring that $(A \diamond B)^x = A^x \diamond B^x$ for any $A, B \in \operatorname{Obj}\mathcal{H}^r(\mathcal{G})$.

Our first goal is to prove the following theorem, where $\mathcal{G}^{\setminus i}$ denotes the full subgroupoid of $\mathcal{G}$ with $\operatorname{Obj}\mathcal{G}^{\setminus i} = \operatorname{Obj}\mathcal{G} - \{i\}$ (cf. Paragraph 5.2) and $\mathcal{H}^r(\mathcal{G}^{\setminus i}) \subset \mathcal{H}^r(\mathcal{G})$ are the universal ribbon Hopf algebras constructed respectively on $\mathcal{G}^{\setminus i}$ and $\mathcal{G}$, with the inclusion given by Proposition 6.4.

THEOREM 8.1. *Let $\mathcal{G}$ be a groupoid. For any $x \in \mathcal{G}(i_0, k_0)$ there exists a functor*

$$\Re^x : \mathcal{H}^r(\mathcal{G}) \to \mathcal{H}^r(\mathcal{G})$$

which coincides with $\_^x : \operatorname{Obj}\mathcal{H}^r(\mathcal{G}) \to \operatorname{Obj}\mathcal{H}^r(\mathcal{G})$ on the objects, such that:

a) *given any other $y \in \mathcal{G}(j_0, k_0)$ and any object A in $\mathcal{H}^r(\mathcal{G})$ there exists an invertible morphism*

$$\xi_A^{x,y} : H_{y\overline{x}} \diamond A^x \to H_{y\overline{x}} \diamond A^y,$$

such that for any morphism $F : A \to B$ in $\mathcal{H}^r(\mathcal{G})$ (cf. Figure 82):

$$\xi_B^{x,y} \circ (\mathrm{id}_{y\overline{x}} \diamond \Re^x(F)) = (\mathrm{id}_{y\overline{x}} \diamond \Re^y(F)) \circ \xi_A^{x,y}; \tag{$q1$}$$

b) *$\Re^x$ restricts to the identity on $\mathcal{H}^r(\mathcal{G}^{\setminus k_0})$ and to an equivalence of categories $\Re^x_| : \mathcal{H}^r(\mathcal{G}^{\setminus i_0}) \to \mathcal{H}^r(\mathcal{G}^{\setminus k_0})$ whose inverse is $\Re^{\overline{x}}_| : \mathcal{H}^r(\mathcal{G}^{\setminus k_0}) \to \mathcal{H}^r(\mathcal{G}^{\setminus i_0})$;*

c) *if $i_0 \neq k_0$ then $\Re^x(\mathcal{H}^r(\mathcal{G})) \subset \mathcal{H}^r(\mathcal{G}^{\setminus k_0})$, hence we have a retraction functor*

$$\Re^x : \mathcal{H}^r(\mathcal{G}) \to \mathcal{H}^r(\mathcal{G}^{\setminus k_0}).$$

Moreover, $\Re^x$ induces functors on the quotient categories

$$\partial^\star\Re^x : \partial^\star\mathcal{H}^r(\mathcal{G}) \to \partial^\star\mathcal{H}^r(\mathcal{G}) \quad \text{and} \quad \partial\Re^x : \partial\mathcal{H}^r(\mathcal{G}) \to \partial\mathcal{H}^r(\mathcal{G}).$$

We observe that in general $\Re^x$ and $\Re^y$ are not naturally equivalent, but a) can be interpreted as a weaker version of that.

In the next corollary we isolate two particular cases of ($q1$) which will be relevant for our purposes.

COROLLARY 8.2. *For any $x \in \mathcal{G}(i_0, k_0)$ and any morphism $F : A \to B$ in $\mathcal{H}^r(\mathcal{G})$, we have (cf. Figure 82):*

$$\xi_B^{1_{k_0},x} \circ (\mathrm{id}_x \diamond F) = (\mathrm{id}_x \diamond \Re^x(F)) \circ \xi_A^{1_{k_0},x}, \tag{$q2$}$$

$$\xi_B^{x,x} \circ (\mathrm{id}_{1_{i_0}} \diamond \Re^x(F)) = (\mathrm{id}_{1_{i_0}} \diamond \Re^x(F)) \circ \xi_A^{x,x}. \tag{$q3$}$$

DEFINITION OF ξ. As it is clear from the discussion above, ξ should be the algebraic analog of sliding over 1-handle or pushing through a dotted component. The definition itself is somewhat heavy and consists in the following steps. Given

$x \in \mathcal{G}(i_0, k_0)$ and $y \in \mathcal{G}(j_0, k_0)$, we define $\zeta_A^{x,y} : H_{y\overline{x}} \diamond A^x \to A^y$ for any object A in $\mathcal{H}^r(\mathcal{G})$ inductively by the following identities (cf. Figure 76) where $g \in \mathcal{G}(i, j)$:

$$\zeta_{H_g}^{x,y} = \zeta_g^{x,y} = \begin{cases} \epsilon_{y\overline{x}} \diamond \mathrm{id}_{g^x} & \text{if } i \neq k_0 \neq j, \\ m_{y\overline{x},g^x} & \text{if } i = k_0 \neq j, \\ m_{g^x,x\overline{y}} \circ (\mathrm{id}_{g^x} \diamond S_{y\overline{x}}) \circ \gamma_{y\overline{x},g^x} & \text{if } i \neq k_0 = j, \\ m_{y\overline{x},g^x x\overline{y}} \circ (\mathrm{id}_{y\overline{x}} \diamond m_{g^x,x\overline{y}}) \circ & \\ \quad \circ (\mathrm{id}_{y\overline{x}} \diamond ((\mathrm{id}_{g^x} \diamond S_{y\overline{x}}) \circ \gamma_{y\overline{x},g^x})) \circ (\Delta_{y\overline{x}} \diamond \mathrm{id}_{g^x}) & \text{if } i = k_0 = j; \end{cases} \tag{q4}$$

$$\zeta_{A \diamond H_g}^{x,y} = (\zeta_A^{x,y} \diamond \zeta_g^{x,y}) \circ (\mathrm{id}_{y\overline{x}} \diamond \gamma_{y\overline{x},A^x} \diamond \mathrm{id}_{g^x}) \circ (\Delta_{y\overline{x}} \diamond \mathrm{id}_{A^x \diamond g^x}). \tag{q5}$$

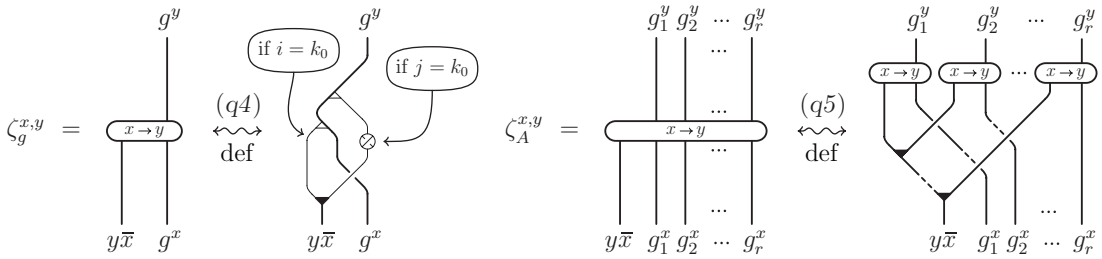

FIGURE 76. ($x \in \mathcal{G}(i_0, k_0)$, $y \in \mathcal{G}(j_0, k_0)$, $g \in \mathcal{G}(i, j)$ and $A = H_{g_1} \diamond H_{g_2} \diamond \ldots \diamond H_{g_r}$).

PROPOSITION 8.3. *If $x \in \mathcal{G}(i_0, k_0)$, $y \in \mathcal{G}(j_0, k_0)$ and $z \in \mathcal{G}(l_0, k_0)$, then for any object A in $\mathcal{H}^r(\mathcal{G})$ we have (cf. Figure 77):*

$$\zeta_A^{y,z} \circ (\mathrm{id}_{z\overline{y}} \diamond \zeta_A^{x,y}) = \zeta_A^{x,z} \circ (m_{z\overline{y},y\overline{x}} \diamond \mathrm{id}_{A^x}) : H_{z\overline{y}} \diamond H_{y\overline{x}} \diamond H_{A^x} \to H_{A^z}. \tag{q6}$$

In particular, $\zeta_{1_i}^{1_i,1_i} : H_{1_i} \diamond H_{1_i} \to H_{1_i}$ makes H_{1_i} into a H_{1_i}-module for any $i \in \mathrm{Obj}\,\mathcal{G}$.

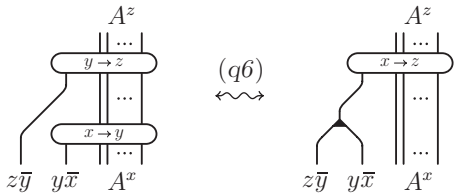

FIGURE 77. ($x \in \mathcal{G}(i_0, k_0)$, $y \in \mathcal{G}(j_0, k_0)$ and $z \in \mathcal{G}(l_0, k_0)$)

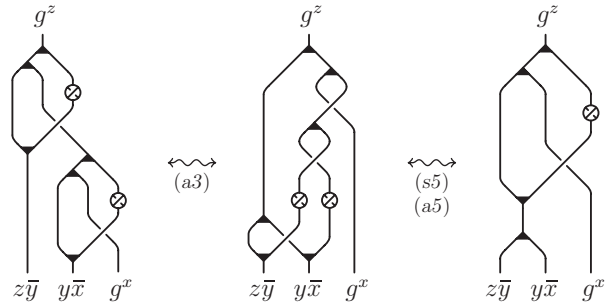

FIGURE 78. Proof of (*q6*) when $A = H_g$ with $g \in \mathcal{G}(k_0, k_0)$ [a/29, s/31].

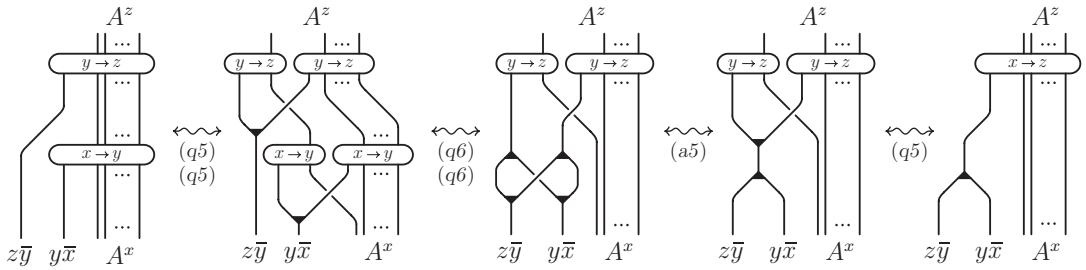

FIGURE 79. Proof of $(q6)$ – the inductive step [a/29, q/50-50]

Proof. First of all, let us consider the special case when $A = H_g$ with $g \in \mathcal{G}(i,j)$. If $j \neq k_0$, the statement is equivalent to $(a3)$ or $(a6)$ in Figure 35. If $j = k_0$ and $i \neq i_0$, it reduces to the antipode property $(s3)$ in Figure 39. Finally, the case when $i = j = k_0$ is shown in Figure 78. At this point, the general case follows by the inductive argument shown in Figure 79. □

Now we define the morphism $\xi_A^{x,y}$ and its inverse (cf. Figure 80):

$$\xi_A^{x,y} = (\mathrm{id}_{y\overline{x}} \diamond \zeta_A^{x,y}) \circ (\Delta_{y\overline{x}} \diamond \mathrm{id}_{A^x}) : H_{y\overline{x}} \diamond A^x \to H_{y\overline{x}} \diamond A^y,$$

$$(\xi_A^{x,y})^{-1} = (\mathrm{id}_{y\overline{x}} \diamond \zeta_A^{y,x}) \circ (((\mathrm{id}_{y\overline{x}} \diamond S_{y\overline{x}}) \circ \Delta_{y\overline{x}}) \diamond \mathrm{id}_{A^y}).$$

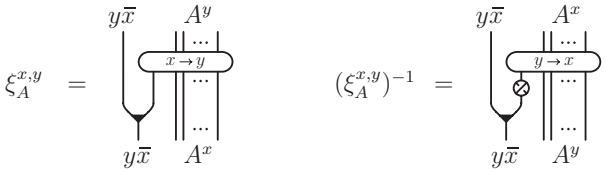

FIGURE 80.

The proof that $(\xi_A^{x,y})^{-1} \circ \xi_A^{x,y} = \mathrm{id}_{y\overline{x}} \diamond \mathrm{id}_{A^x}$ is given in Figure 81. In a similar way, using $(s1')$ instead of $(s1)$, one can prove that $\xi_A^{x,y} \circ (\xi_A^{x,y})^{-1} = \mathrm{id}_{y\overline{x}} \diamond \mathrm{id}_{A^x}$.

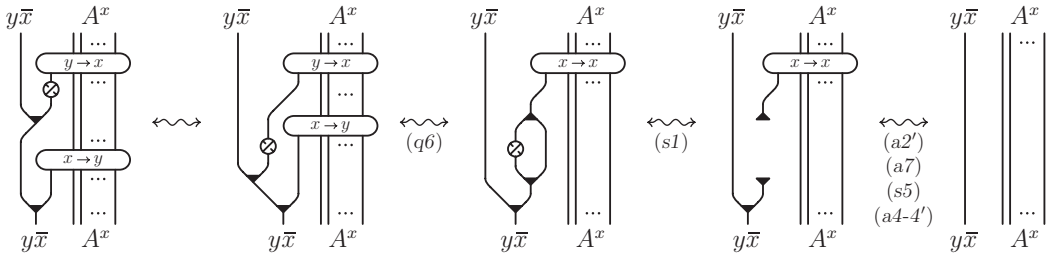

FIGURE 81. Invertibility of $\xi_A^{x,y}$ [a/29, q/50, s/30-31].

With the notation introduced in Figure 80, the relations of Theorem 8.1 and Corollary 8.2 look like in Figure 82.

We will need also the morphisms

$$\overline{\zeta}_A^{x,y} = \zeta_A^{x,y} \circ \overline{\gamma}_{A^x, y\overline{x}} : A^x \diamond H_{y\overline{x}} \to A^y,$$

$$\overline{\xi}_A^{x,y} = (\overline{\zeta}_A^{x,y} \diamond \mathrm{id}_{y\overline{x}}) \circ (\mathrm{id}_{A^x} \diamond \Delta_{y\overline{x}}) : A^x \diamond H_{y\overline{x}} \to A^y \diamond H_{y\overline{x}},$$

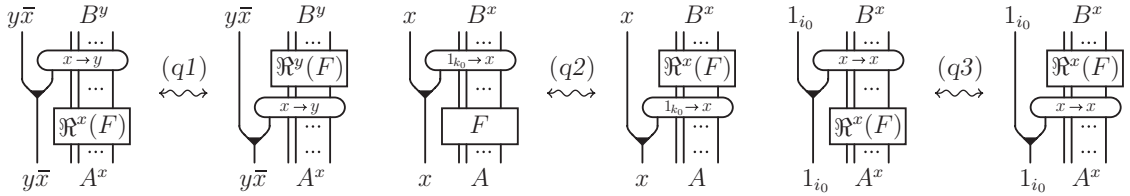

FIGURE 82. $(x \in \mathcal{G}(i_0,k_0),\ y \in \mathcal{G}(j_0,k_0),\ F : A \to B)$

which are obtained from $\zeta_A^{x,y}$ and $\xi_A^{x,y}$ by simply "pulling" the string labeled $y\overline{x}$ to the right as shown in Figure 83. $\bar{\xi}_A^{x,y}$ is invertible with

$$(\bar{\xi}_A^{x,y})^{-1} = (\bar{\zeta}_A^{y,x} \diamond \mathrm{id}_{y\overline{x}}) \circ (\mathrm{id}_{A^y} \diamond ((\overline{S}_{y\overline{x}} \diamond \mathrm{id}_{y\overline{x}}) \circ \Delta_{y\overline{x}})),$$

as shown in Figure 83.

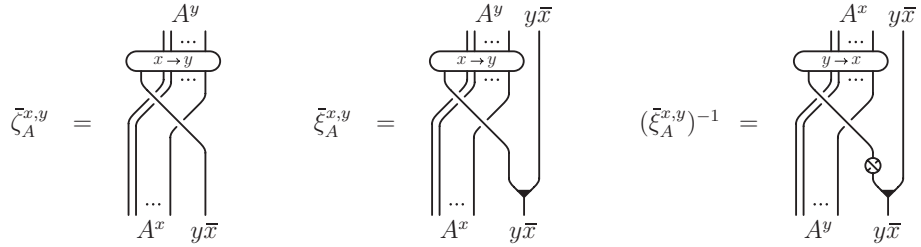

FIGURE 83.

In order to see that $\zeta_A^{x,y}$ and $\xi_A^{x,y}$ are the algebraic analog of sliding over 1-handles, in Figure 84 we represent the image $\Phi_n(\zeta_{g\diamond h}^{x,y})$ in $\mathcal{K}_n$ when $x = (i_0,k_0)$, $y = (j_0,k_0)$, $g = (k_0,k_0)$ and $h = (k_0,i)$ with $i \neq k_0$ are morphisms in $\mathcal{G}_n$. It should be obvious now that in terms of Kirby diagrams, $\zeta_A^{x,y}$ corresponds to a dotted component U of label $y\overline{x} = (j_0,i_0)$ embracing all framed strings of label $k_0^x = i_0$ and transforming these labels into $k_0^y = j_0$. The reader can see that $\Phi_n(\xi_A^{x,y})$ is the same, but there is an extra framed arc passing through U, which is a reflected image of the left most one of labels (i_0,j_0) with respect to a horizontal diameter of U.

Now we can interpret $(q2)$ and $(q3)$ in Figure 82 in terms of Kirby tangles. In particular, $(q2)$ implies that $\Re_{\mathcal{K}}^x(F)$ is obtained from F by pushing up the part contained in the k_0'th 0-handle through a dotted component of label $x = (i_0,k_0)$, changing this way the index k_0 to i_0. On the other hand, $(q3)$ states that if we have

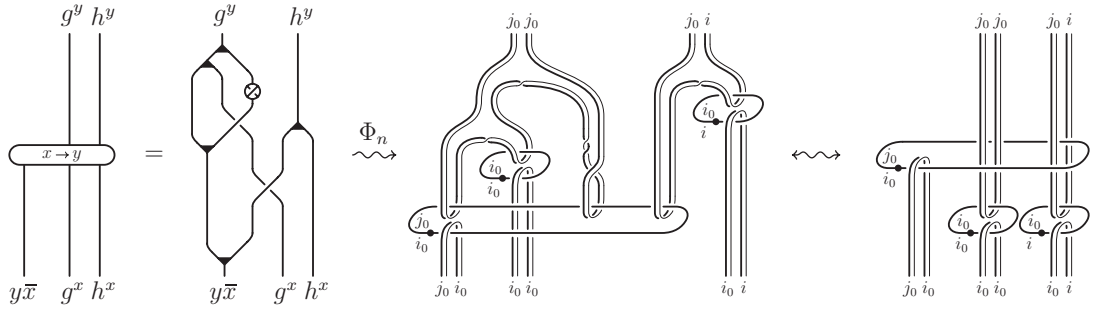

FIGURE 84. $\Phi_n(\zeta_{g\diamond h}^{x,y})$ for $x = (i_0,k_0)$, $y = (j_0,k_0)$, $g = (k_0,k_0)$, $h = (k_0,i)$, $i \neq k_0$.

already done this, the same part can be pushed through a dotted component of label (i_0, i_0) without further changes.

DEFINITION OF $\Re^x$. Let $x \in \mathcal{G}(i_0, k_0)$ as above. For $i_0 = k_0$ we define $\Re^x$ to be the formal extension of $\_^x$ to $\mathcal{H}^r(\mathcal{G})$, in the sense that $\Re^x(\Delta_g) = \Delta_{g^x}$, $\Re^x(\gamma_{g,h}) = \gamma_{g^x,h^x}$, $\Re^x(S_g) = S_{g^x}$ and so on.

However, when $i_0 \neq k_0$ such formal extension would run into problems. In fact the copairing $\sigma_{i,j}$ is defined to be trivial if $i \neq j$, so the axiom (r7) in Figure 51 would not be satisfied in the image if $i^x = j^x$. Thus we need to make some corrections in order to have a functor. Being $\Re^x$ the algebraic analog of $\Re^x_{\mathcal{K}}$, the nature of these corrections can be understood by reviewing the definition of $\Re^x_{\mathcal{K}}$ and Figure 75.

Namely, for $i_0 \neq k_0$ we define $\Re^x : \mathcal{H}^r(\mathcal{G}) \to \mathcal{H}^r(\mathcal{G})$ by putting, for any $i \in \operatorname{Obj}\mathcal{G}$ and any $g, h \in \mathcal{G}$ (assumed to be composable in $\mathcal{G}$ when dealing with $m_{g,h}$):

$$\Re^x(\Delta_g) = \begin{cases} \mu^{-1}_{g^x,g^x} \circ \Delta_{g^x} & \text{if } g \in \mathcal{G}(i_0, k_0), \\ \Delta_{g^x} & \text{otherwise;} \end{cases}$$

$$\Re^x(\gamma_{g,h}) = \begin{cases} \gamma_{g^x,h^x} & \text{if } g \in \mathcal{G}(k_0, k_0), \\ (\bar{\zeta}^{x,x}_h \diamond \mathrm{id}_{g^x}) \circ (\mathrm{id}_{h^x} \diamond \rho^l_{g^x,i_0}) \circ \gamma_{g^x,h^x} & \text{if } g \in \mathcal{G}(i, k_0),\ i \neq k_0, \\ \gamma_{g^x,h^x} \circ (\mathrm{id}_{g^x} \diamond \zeta^{x,x}_h) \circ & \\ \quad \circ (\mathrm{id}_{g^x} \diamond S_{1_{i_0}} \diamond \mathrm{id}_{h^x}) \circ (\rho^r_{g^x,i_0} \diamond \mathrm{id}_{h^x}) & \text{if } g \in \mathcal{G}(k_0, j),\ j \neq k_0, \\ (\bar{\zeta}^{x,x}_h \diamond \mathrm{id}_{g^x}) \circ (\mathrm{id}_{h^x} \diamond \rho^l_{g^x,i_0}) \circ \gamma_{g^x,h^x} \circ & \\ \quad \circ (\mathrm{id}_{g^x} \diamond \zeta^{x,x}_h) \circ (\mathrm{id}_{g^x} \diamond S_{1_{i_0}} \diamond \mathrm{id}_{h^x}) \circ (\rho^r_{g^x,i_0} \diamond \mathrm{id}_{h^x}) & \text{otherwise;} \end{cases}$$

$$\Re^x(\overline{\gamma}_{g,h}) = \begin{cases} \overline{\gamma}_{g^x,h^x} & \text{if } h \in \mathcal{G}(k_0, k_0), \\ (\mathrm{id}_{h^x} \diamond \zeta^{x,x}_g) \circ (\rho^r_{h^x,i_0} \diamond \mathrm{id}_{g^x}) \circ \overline{\gamma}_{g^x,h^x} & \text{if } h \in \mathcal{G}(k_0, l),\ l \neq k_0, \\ \overline{\gamma}_{g^x,h^x} \circ (\bar{\zeta}^{x,x}_g \diamond \mathrm{id}_{h^x}) \circ & \\ \quad \circ (\mathrm{id}_{g^x} \diamond \overline{S}_{1_{i_0}} \diamond \mathrm{id}_{h^x}) \circ (\mathrm{id}_{g^x} \diamond \rho^l_{h^x,i_0}) & \text{if } h \in \mathcal{G}(k, k_0),\ k \neq k_0, \\ (\mathrm{id}_{h^x} \diamond \zeta^{x,x}_g) \circ (\rho^r_{h^x,i_0} \diamond \mathrm{id}_{g^x}) \circ \overline{\gamma}_{g^x,h^x} \circ & \\ \quad \circ (\bar{\zeta}^{x,x}_g \diamond \mathrm{id}_{h^x}) \circ (\mathrm{id}_{g^x} \diamond \overline{S}_{1_{i_0}} \diamond \mathrm{id}_{h^x}) \circ (\mathrm{id}_{g^x} \diamond \rho^l_{h^x,i_0}) & \text{otherwise;} \end{cases}$$

$$\Re^x(S_g) = \begin{cases} \overline{S}_{g^x} v^2_{g^x} & \text{if } g \in \mathcal{G}(i_0, k_0), \\ S_{g^x} & \text{otherwise;} \end{cases}$$

$$\Re^x(\overline{S}_g) = \begin{cases} S_{g^x} v^{-2}_{g^x} & \text{if } g \in \mathcal{G}(k_0, i_0), \\ \overline{S}_{g^x} & \text{otherwise;} \end{cases}$$

$$\Re^x(\eta_i) = \eta_{i^x}; \qquad \Re^x(\epsilon_g) = \epsilon_{g^x};$$

$$\Re^x(l_i) = l_{i^x}; \qquad \Re^x(L_g) = L_{g^x};$$

$$\Re^x(m_{g,h}) = m_{g^x,h^x}; \qquad \Re^x(v_g) = v_{g^x};$$

$$\Re^x(\sigma_{i,j}) = \begin{cases} \sigma_{i^x,j^x} & \text{if } \{i, j\} \neq \{i_0, k_0\}, \\ \eta_{i_0} \diamond \eta_{i_0} & \text{otherwise.} \end{cases}$$

$\Re^x(\Delta_g)$, $\Re^x(\gamma_{g,h})$ and $\Re^x(\overline{\gamma}_{g,h})$ are presented in Figures 85 and 86. Moreover, up to equivalence in $\mathcal{H}^r(\mathcal{G})$, one can see that $\Re^x(\gamma_{g,A})$ and $\Re^x(\overline{\gamma}_{A,h})$ are given by

the same expressions for any object A in $\mathcal{H}^r(\mathcal{G})$ (cf. Figure 87). The proof of this statement for $\Re^x(\gamma_{g,A})$ with $A = h_1 \diamond h_2$ in the case when $g \in \mathcal{G}(i,j)$ with $i \neq k_0$ and $j \neq k_0$ is illustrated in Figure 88. The other cases are simpler and the generalization to an arbitrary A is straightforward. The proof for $\Re^x(\overline{\gamma}_{A,h})$ is similar.

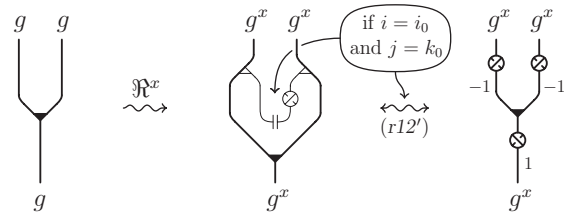

FIGURE 85. $\Re^x(\Delta_g)$ when $x \in \mathcal{G}(i_0, k_0)$ with $k_0 \neq i_0$ ($g \in \mathcal{G}(i,j)$) [r/41].

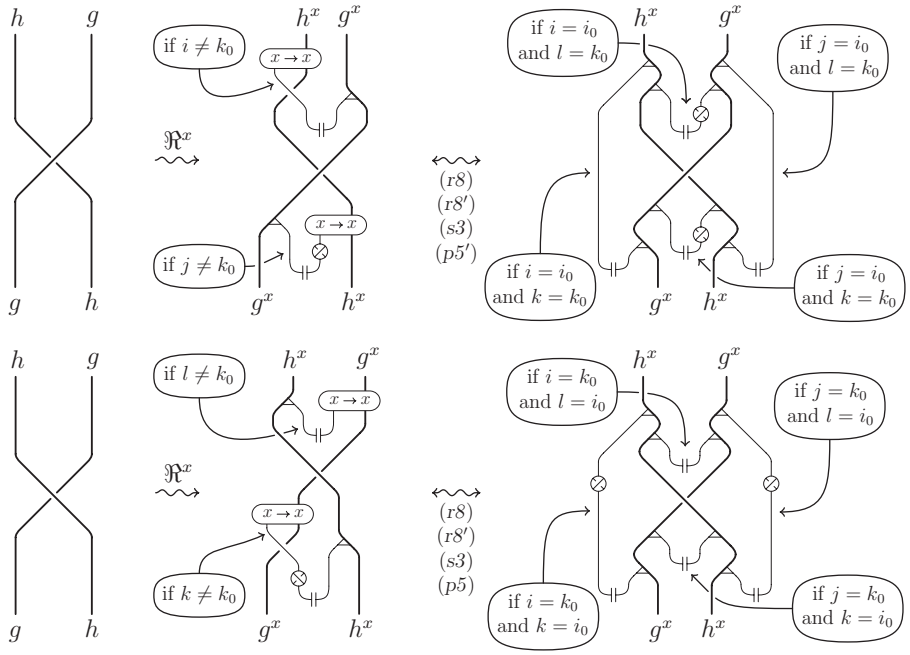

FIGURE 86. $\Re^x(\gamma_{g,h})$ and $\Re^x(\overline{\gamma}_{g,h})$ when $x \in \mathcal{G}(i_0, k_0)$ with $k_0 \neq i_0$ ($g \in \mathcal{G}(i,j)$ and $h \in \mathcal{G}(k,l)$) [p/40, r/37, s/31].

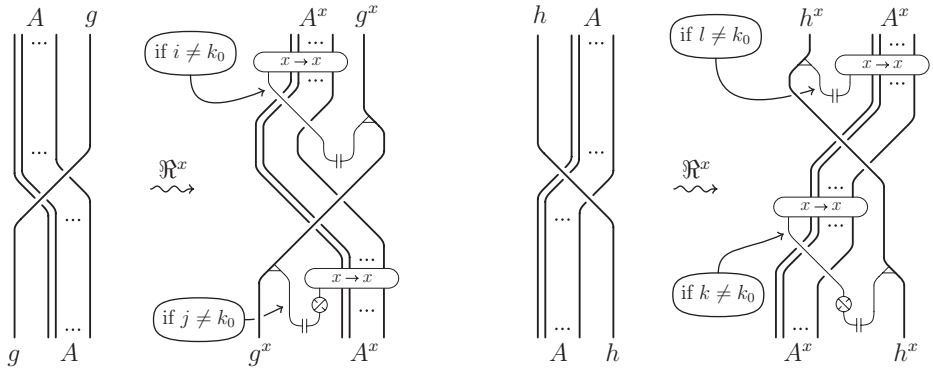

FIGURE 87. $\Re^x(\gamma_{g,A})$ and $\Re^x(\overline{\gamma}_{A,h})$ when $x \in \mathcal{G}(i_0, k_0)$ with $k_0 \neq i_0$ ($g \in \mathcal{G}(i,j)$ and $h \in \mathcal{G}(k,l)$).

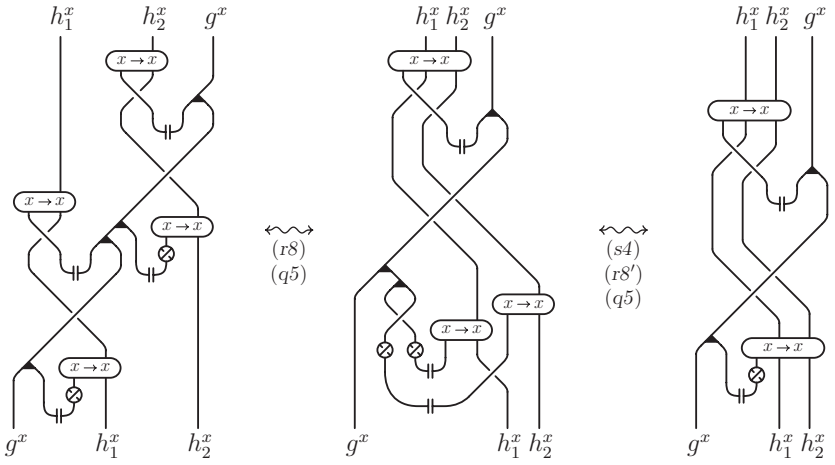

FIGURE 88. ($x \in \mathcal{G}(i_0, k_0)$, $k_0 \neq i_0$, $g \in \mathcal{G}(i, j)$, $i \neq k_0$, $j \neq k_0$) [q/50, r/37, s/31].

Proof of Theorem 8.1. First of all we prove that (*q1*) in a) holds for any $x \in \mathcal{G}(i_0, k_0)$, $y \in \mathcal{G}(j_0, k_0)$ and any elementary morphism $F : A \to B$, with $\xi_A^{x,y}$ and $\xi_B^{x,y}$ defined as above. More precisely, we will prove the identity

$$\zeta_B^{x,y} \circ (\mathrm{id}_{y\overline{x}} \diamond \Re^x(F)) = \Re^y(F) \circ \zeta_A^{x,y}, \tag{$q1'$}$$

which, by composing with $\Delta_{y\overline{x}} \diamond \mathrm{id}_{A^x}$, implies (*q1*).

Notice that if F is invertible then the relation ($q1'$) for F^{-1} follows from the one for F, once we know that $\Re^x(F^{-1})$ is the inverse of $\Re^x(F)$. It can be easily verified that this is true when F is $\gamma_{g,h}$ and S_g, by using ($p2$-$2'$) in Figure 53 and (*q6*) in Figure 77. Moreover, since the relations (*r6*) and (*r7*) in Figure 51 are trivially satisfied in the image, the identity ($q1'$) for $\sigma_{i,j}$ follows from the ones for the other elementary morphisms. Therefore, it suffices to prove that ($q1'$) holds for $F = \eta_{1_i}$, l_{1_i}, Δ_g, S_g, ϵ_g, L_g, v_g, $m_{g,h}$, $\gamma_{g,h}$.

$F = \eta_i, l_i$. If $i \neq k_0$ there is nothing to prove, being $\xi_{1_i}^{x,y}$ trivial and $\Re^x(F) = \Re^y(F) = F$. The case when $i = k_0$ is shown in Figure 89.

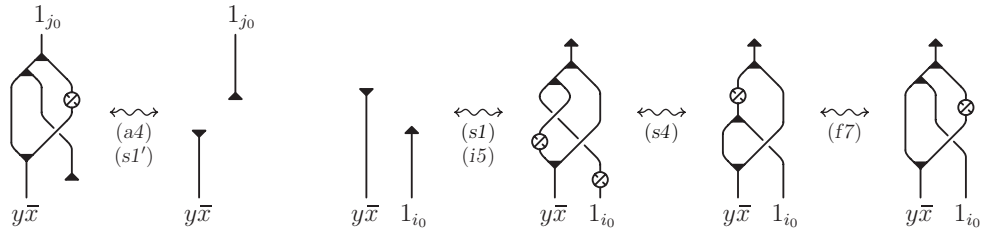

FIGURE 89. Proof of ($q1'$) for $F = \eta_{k_0}$ and $F = l_{k_0}$ ($x \in \mathcal{G}(i_0, k_0)$ and $y \in \mathcal{G}(j_0, k_0)$) [a/29, *i*/34, *f*/35, *s*/30-31].

$F = \Delta_g$. If $g \in \mathcal{G}(i, j)$ with $i, j \neq k_0$ there is nothing to prove, being $\xi_g^{x,y}$ trivial. For $g \in \mathcal{G}(k_0, j)$ with $j \neq k_0$, the statement essentially reduces to the relation (*a5*) in Figure 35. The proof for $g \in \mathcal{G}(i, k_0)$ with $i \neq k_0$ is presented in Figure 90, where one can see that the last diagram is exactly $\Re^y(\Delta_g) \circ \zeta_g^{x,y}$, by confronting it with Figure 85 when $i = i_0$, or applying (*t4*) in Figure 60 when $i \neq i_0$. The case $g \in \mathcal{G}(k_0, k_0)$ is shown in Figures 91 and 92.

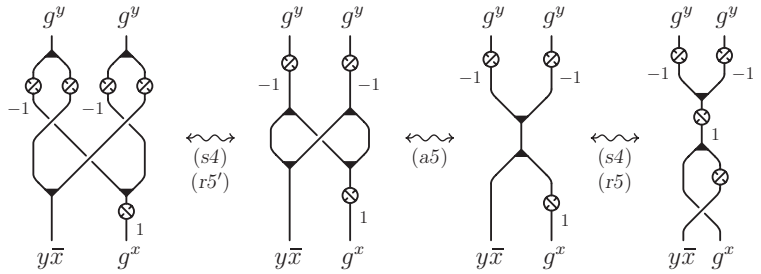

FIGURE 90. Proof of $(q1')$ for $F = \Delta_g$ with $g \in \mathcal{G}(i, k_0)$ and $i \neq k_0$ ($x \in \mathcal{G}(i_0, k_0)$ and $y \in \mathcal{G}(j_0, k_0)$) [a/29, r/37, s/31].

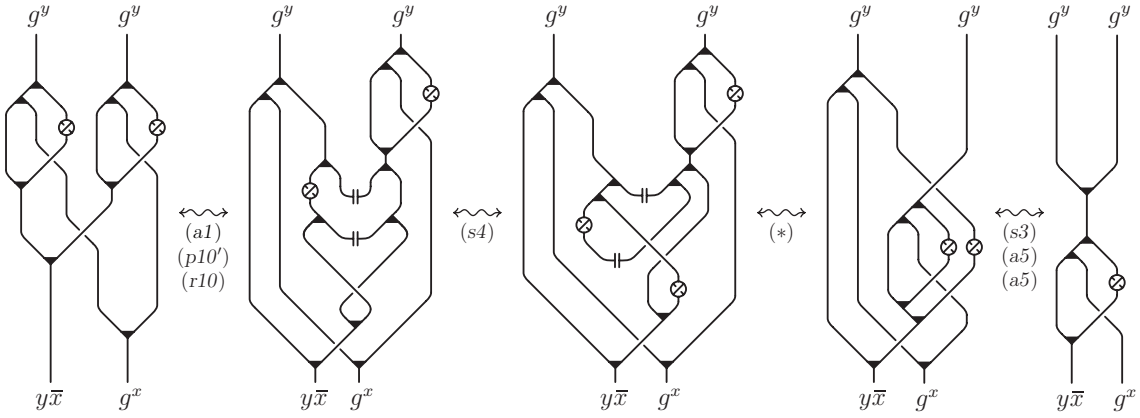

FIGURE 91. Proof of $(q1')$ for $F = \Delta_g$ with $g \in \mathcal{G}(k_0, k_0)$ ($x \in \mathcal{G}(i_0, k_0)$ and $y \in \mathcal{G}(j_0, k_0)$) [a/29, p/40, r/37, s/31, step $(*)$ in Figure 92].

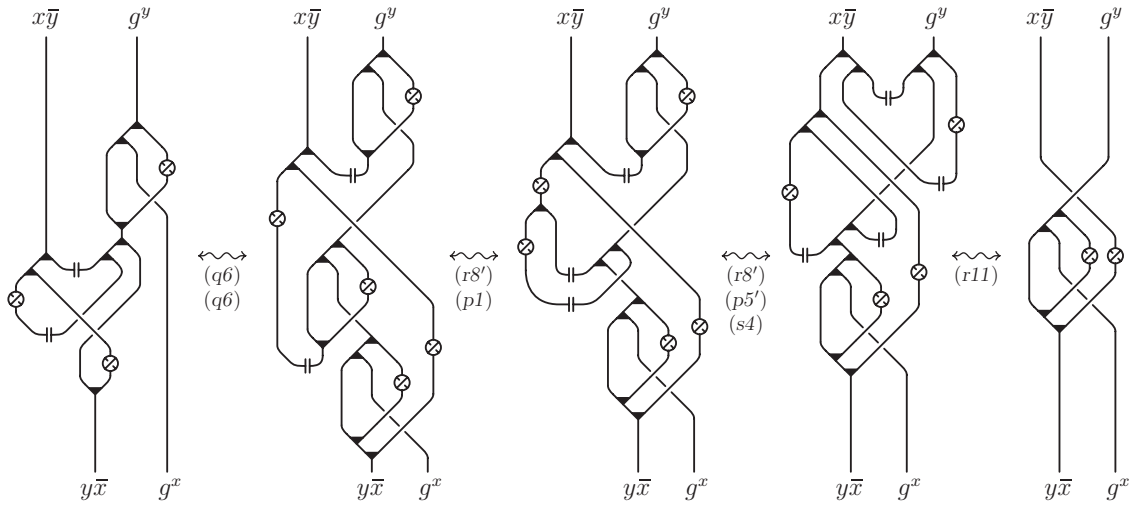

FIGURE 92. Proof of step $(*)$ in Figure 91 [p/39-40, q/50, r/37, s/31].

$F = S_g$. As above, there is nothing to prove for $g \in \mathcal{G}(i, j)$ with $i, j \neq k_0$. When $g \in \mathcal{G}(i, k_0)$ or $g \in \mathcal{G}(k_0, j)$ with $i, j \neq k_0$, the statement is equivalent to the property $(s4)$ of the antipode in Figure 39 (see Figure 93 for the former case). Figure 94 addresses the case of $g \in \mathcal{G}(k_0, k_0)$.

$F = \epsilon_g, L_g, v_g$. The statements follow respectively from $(a6)$ in Figure 35, $(i2\text{-}2')$ in Figure 44 and $(r5\text{-}5')$ in Figure 50.

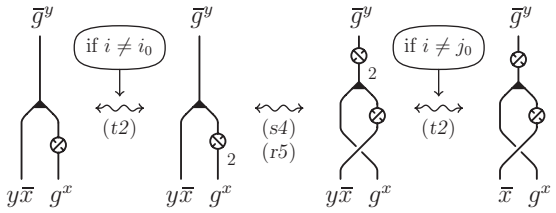

FIGURE 93. Proof of $(q1')$ for $F = S_g$ with $g \in \mathcal{G}(i, k_0)$ and $i \neq k_0$ ($x \in \mathcal{G}(i_0, k_0)$ and $y \in \mathcal{G}(j_0, k_0)$) [r/37, s/31, t/41].

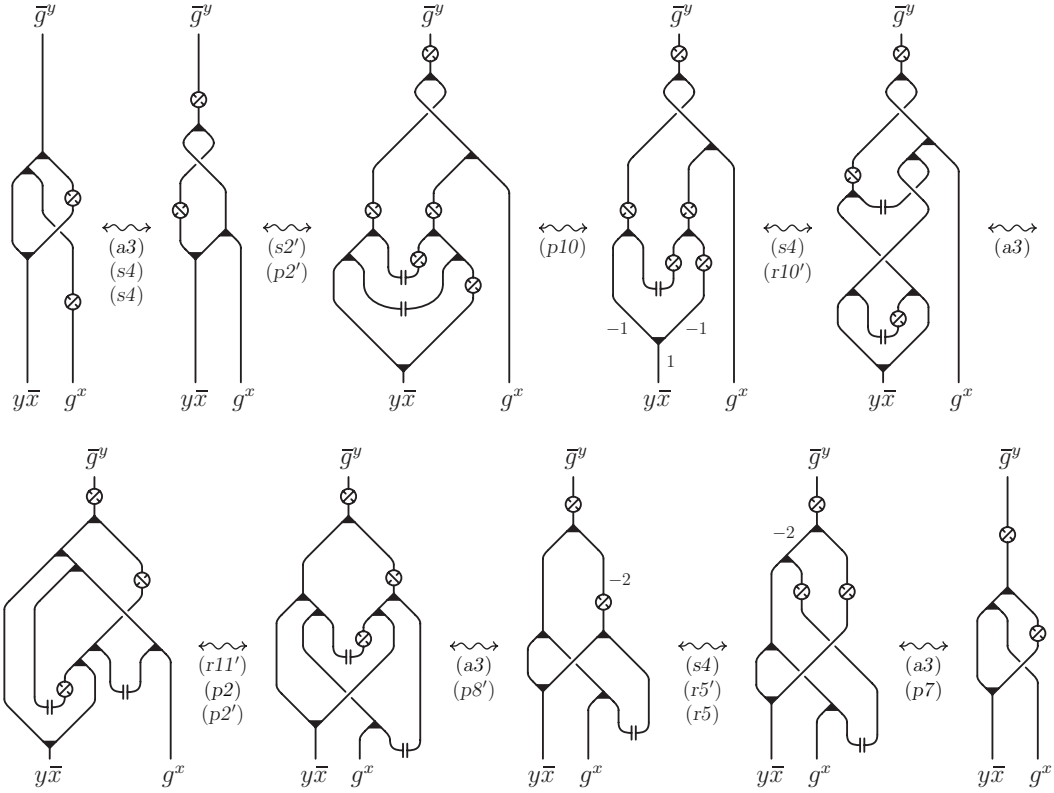

FIGURE 94. Proof of $(q1')$ for $F = S_g$ with $g \in \mathcal{G}(k_0, k_0)$ ($x \in \mathcal{G}(i_0, k_0)$ and $y \in \mathcal{G}(j_0, k_0)$) [a/29, p/39-40, r/37-41-41, s/31].

$F = m_{g,h}$. See Figure 95 for the case in which $g, h \in \mathcal{G}(k_0, k_0)$. The other cases are simpler and anologous.

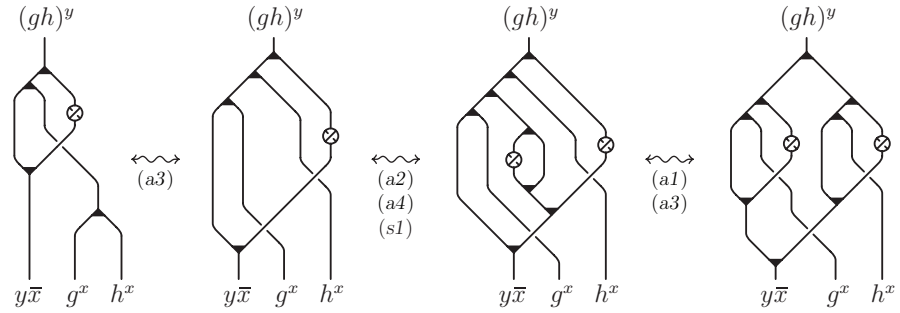

FIGURE 95. Proof of $(q1')$ for $F = m_{g,h}$ with $g, h \in \mathcal{G}(k_0, k_0)$ ($x \in \mathcal{G}(i_0, k_0)$ and $y \in \mathcal{G}(j_0, k_0)$) [a/29, s/30,].

$F = \gamma_{g,h}$. Let $g \in \mathcal{G}(i,j)$ and $h \in \mathcal{G}(k,l)$. We can transform the left side of $(q1')$ as shown in Figure 96. Now the idea is to change the "wrong" crossing between the edges labeled g^x and $y\overline{x}$, through move $(r13')$ in Figure 58, and then use the copairings that appear to transform $\gamma_{y\overline{x},y\overline{x}} \circ \Delta_{y\overline{x}}$ into $\Delta_{y\overline{x}}$. This is done separately for the four cases: $i \neq k_0$ and $j \neq k_0$ in Figures 97 and 98; $i = k_0$ and $j \neq k_0$ in Figure 99; $i \neq k_0$ and $j = k_0$ in Figure 100; $i = k_0$ and $j = k_0$ in Figure 101.

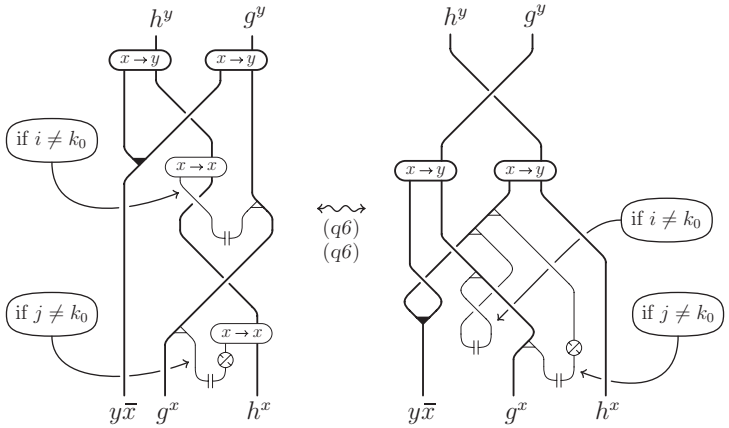

FIGURE 96. Proof of $(q1')$ for $F = \gamma_{g,h}$ – I ($g \in \mathcal{G}(i,j)$, $h \in \mathcal{G}(k,l)$, $x \in \mathcal{G}(i_0,k_0)$ and $y \in \mathcal{G}(j_0,k_0)$) [q/50].

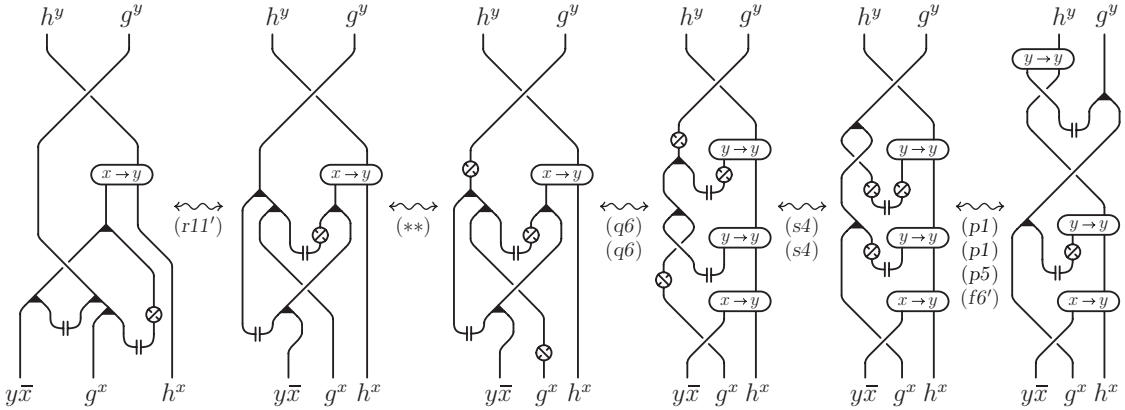

FIGURE 97. Proof of $(q1')$ for $F = \gamma_{g,h}$ with $g \in \mathcal{G}(i,j)$, $i \neq k_0$ and $j \neq k_0$ – II ($h \in \mathcal{G}(k,l)$, $x \in \mathcal{G}(i_0,k_0)$ and $y \in \mathcal{G}(j_0,k_0)$) [f/35, p/39-40, q/50, r/41, s/31, step $(**)$ follows from $(q1')$ for $F = S$ and $x, y = 1_{j_0}$ (cf. Figure 98)].

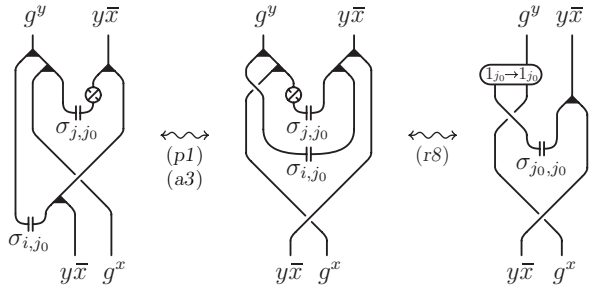

FIGURE 98. ($g \in \mathcal{G}(i,j)$, $x \in \mathcal{G}(i_0,k_0)$, $y \in \mathcal{G}(j_0,k_0)$, $i \neq k_0$ and $j \neq k_0$) [a/29, p/39, r/37].

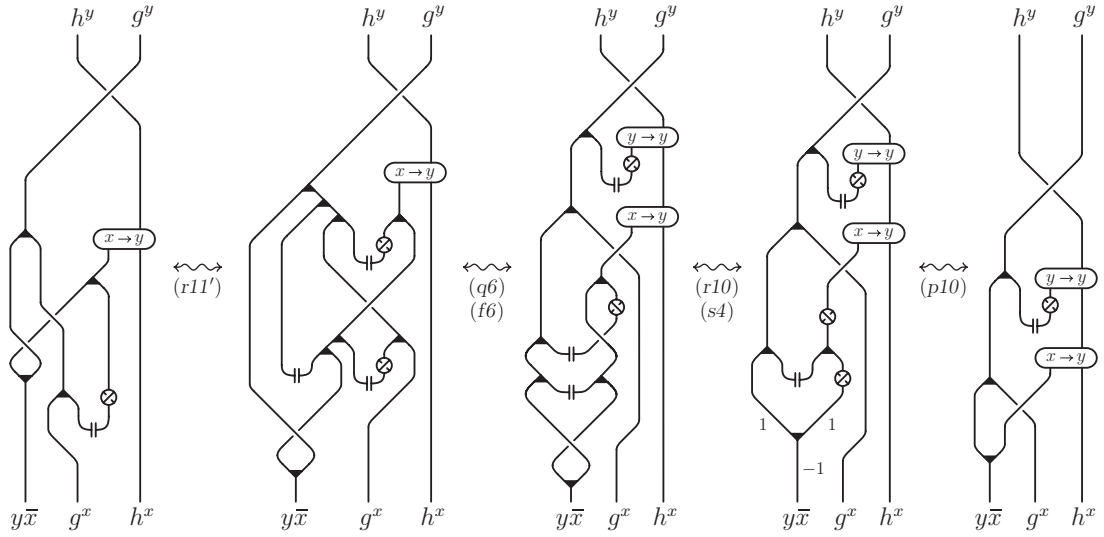

FIGURE 99. Proof of $(q1')$ for $F = \gamma_{g,h}$ with $g \in \mathcal{G}(k_0, j)$, $j \neq k_0$ – II ($h \in \mathcal{G}(k,l)$, $x \in \mathcal{G}(i_0, k_0)$ and $y \in \mathcal{G}(j_0, k_0)$) [f/35, p/40, q/50, r/37-41, s/31].

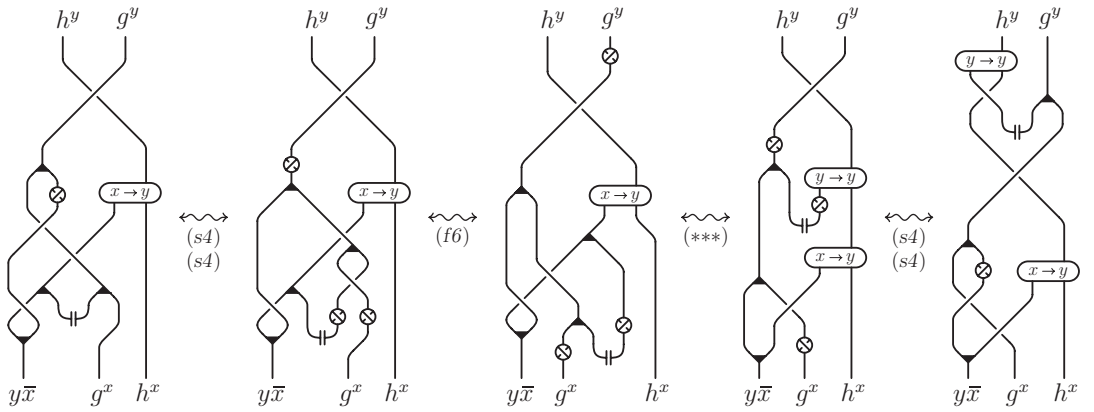

FIGURE 100. Proof of $(q1')$ for $F = \gamma_{g,h}$ with $g \in \mathcal{G}(i, k_0)$, $i \neq k_0$ – II ($h \in \mathcal{G}(k,l)$, $x \in \mathcal{G}(i_0, k_0)$ and $y \in \mathcal{G}(j_0, k_0)$) [f/35, s/31, step $(***)$ as in Figure 99].

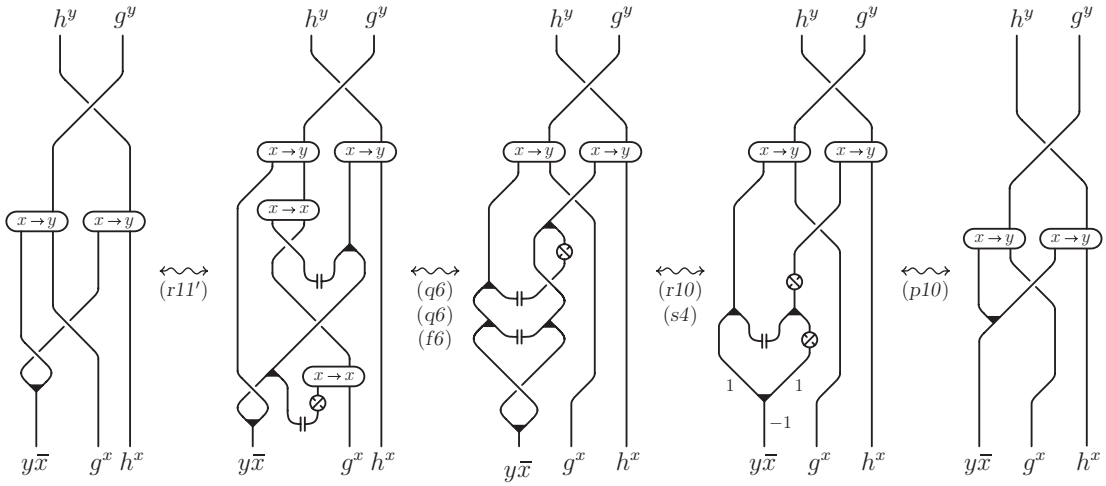

FIGURE 101. Proof of $(q1')$ for $F = \gamma_{g,h}$ with $g \in \mathcal{G}(k_0, k_0)$ – II ($h \in \mathcal{G}(k,l)$, $x \in \mathcal{G}(i_0, k_0)$ and $y \in \mathcal{G}(j_0, k_0)$) [f/35, p/40, q/50, r/37-41].

At this point, having established property *a*) for F being an elementary morphism, we are ready to show that $\Re^x$ is a functor, i.e. it preserves all the relations between the elementary morphisms in $\mathcal{H}^r(\mathcal{G})$ presented in Figures 34, 35, 36, 44, 50 and 51. This is trivially true when $x \in \mathcal{G}(k_0, k_0)$. Hence, we focus on the case when $x \in \mathcal{G}(i_0, k_0)$, $i_0 \neq k_0$.

We start with the isotopy moves in Figure 34. As it was already observed, moves (*b1-1'*) follow from (*p2-2'*) in Figure 53 and (*q6*) in Figure 77.

Moves (*b3*) and (*b4*) in Figure 34 need to be shown only when D is an elementary morphism $F : A \to B$. In this case, according to Figure 87, the statement follows from the identity $\zeta_B^{x,x} \circ (\mathrm{id}_{x\overline{x}} \diamond \Re^x(F)) = \Re^x(F) \circ \zeta_A^{x,x}$, which is equivalent to the specialization of the relation (*q1'*) proved above for $y = x$.

We continue with the bi-algebra axioms presented in Figure 35. The only non-trivial ones are (*a1*), (*a2*) and (*a5*) when g or h are in $\mathcal{G}(i_0, k_0)$. In this case, (*a1*) and (*a2*) follow directly from the fact that $\Re^x(\Delta_g) = (T_{\overline{g}^x} \diamond T_{\overline{g}^x}) \circ \Delta_{\overline{g}^x} \circ T_{g^x}^{-1}$ (cf. the definition of T in Paragraph 6.7 and the presentation of $\Re^x(\Delta_g)$ in Figure 85). The proof of (*a5*) for $g \in \mathcal{G}(i_0, k_0)$ and $h \in \mathcal{G}(k_0, k_0)$ is presented in Figure 102. The proofs for different choices of g and h are simpler or analogous.

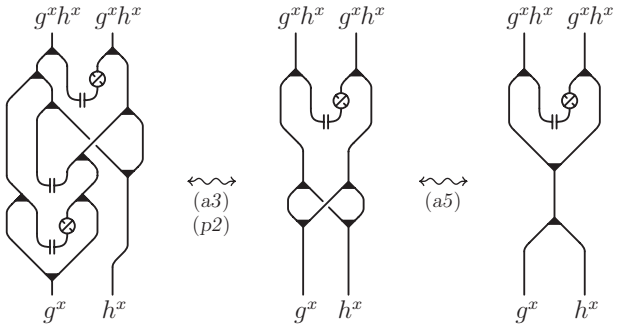

FIGURE 102. $\Re^x$ preserves (*a5*) when $g \in \mathcal{G}(i_0, k_0)$ and $h \in \mathcal{G}(k_0, k_0)$ ($x \in \mathcal{G}(i_0, k_0)$) [a/29,p/39].

From the antipode axioms in Figure 36 the only non-trivial ones are (*s1*) and (*s1'*) for $g \in \mathcal{G}(i_0, k_0)$. Figure 103 proves (*s1*) in this case, while the proof of (*s1'*) is obtained by reflecting all the diagrams in the same figure with respect to the y-axis.

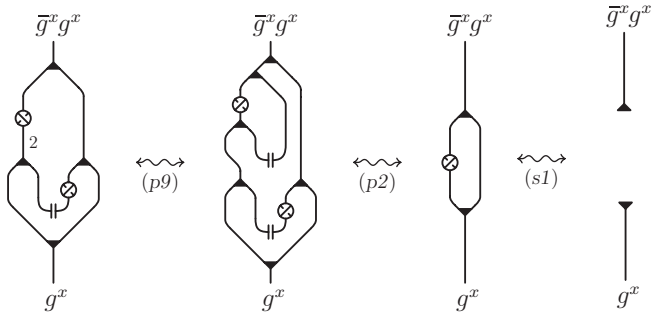

FIGURE 103. $\Re^x$ preserves (*s1*) when $g \in \mathcal{G}(i_0, k_0)$ ($x \in \mathcal{G}(i_0, k_0)$) [p/39-40, s/30].

The integral axioms in Figure 44 are trivially preserved because $\Re^x(m_{g,h}) = m_{g^x,h^x}$ and $\Re^x(\Delta_{1_i}) = \Delta_{1_i^x}$.

Also the axioms of the ribbon structure in Figure 50 are trivially preserved, while the only non-trivial ones from Figure 51 are (*r10*) when $g \in \mathcal{G}(i_0, k_0)$ and (*r11*) with $g \in \mathcal{G}(i, j)$ and $h \in \mathcal{G}(k, l)$ such that some of i, j are equal to k_0 and some of k, l are equal to i_0 or vice versa. Figure 104 deals with the above metioned case of (*r10*). Some of the cases of (*r11*) are presented in Figure 105 (cf. the expression for $\Re^x(\sigma_{i,j})$ on page 53) and the rest are analogous. This concludes the proof of the functoriality of $\Re^x$. Moreover, the functoriality together with the fact that *a*) holds for F being an elementary morphism, imply *a*) for any other morphism F.

Properties *b*) and *c*) derive from the definition of $\Re^x$; in particular, from the fact that $\Re^x$ coincides with the formal extension of $\_^x$ on the elementary morphisms of $\mathcal{H}^r(\mathcal{G})$ which do not involve i_0 or k_0 (see right side of Figure 86 for the crossings), taking into account 5.2 *e*).

Finally, the last part of the theorem follows from the fact that the additional relations defining the quotient categories $\partial^\star\mathcal{H}^r(\mathcal{G})$ and $\partial\mathcal{H}^r(\mathcal{G})$ involve only morphisms in H_{1_i} for $i \in \mathrm{Obj}\,\mathcal{G}$. □

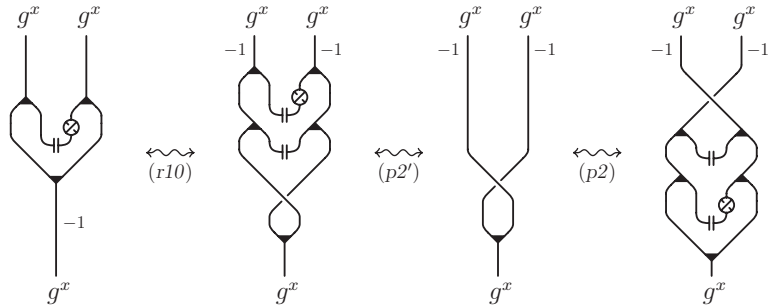

FIGURE 104. $\Re^x$ preserves (*r10*) when $g \in \mathcal{G}(i_0, k_0)$ ($x \in \mathcal{G}(i_0, k_0)$) [p/39, r/37].

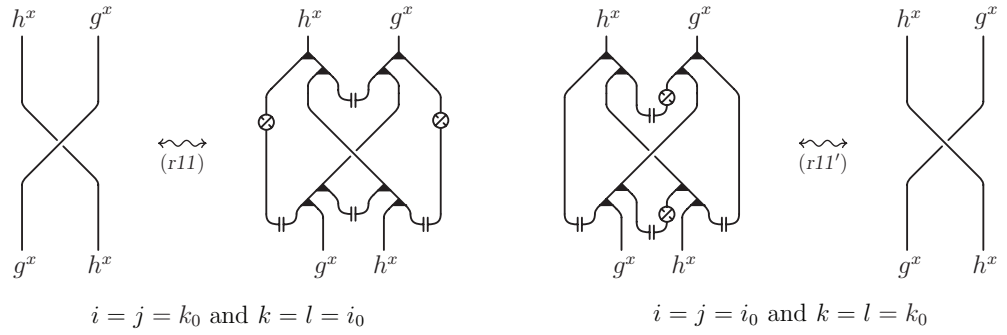

FIGURE 105. $\Re^x$ preserves (*r11*) ($g \in \mathcal{G}(i, j)$, $h \in \mathcal{G}(k, l)$, $x \in \mathcal{G}(i_0, k_0)$) [p/39, r/37-41].

Notice that, given any $x \in \mathcal{G}(i_0, k_0)$ and $y \in \mathcal{G}(j_0, l_0)$ with $i_0 \neq k_0 \neq l_0 \neq j_0$, both compositions of functors $\mathfrak{R}^{y^x} \circ \mathfrak{R}^x$ and $\mathfrak{R}^{x^y} \circ \mathfrak{R}^y$ retract $\mathcal{H}^r(\mathcal{G})$ to the subcategory $\mathcal{H}^r(\mathcal{G}^{\setminus k_0 \setminus l_0}) = \mathcal{H}^r(\mathcal{G}^{\setminus l_0 \setminus k_0})$, provided that $i_0 \neq l_0$ or $j_0 \neq k_0$ (if $i_0 = l_0$ and $j_0 = k_0$ one has $y^x \in \mathcal{G}(l_0, l_0)$ and $x^y \in \mathcal{G}(k_0, k_0)$).

The next proposition asserts that these two retractions are naturally equivalent. Since we will focus later on closed morphisms, this fact will not be used in the present work. Nevertheless, we include it for its significance, and also in view of a possible extension of what follows to non-closed morphisms.

PROPOSITION 8.4. *Given $i_0 \neq k_0 \neq l_0 \neq j_0$ in $\operatorname{Obj}\mathcal{G}$, such that either $i_0 \neq l_0$ or $j_0 \neq k_0$, and morphisms $x \in \mathcal{G}(i_0, k_0)$ and $y \in \mathcal{G}(j_0, l_0)$, there exists a natural transformation $\nu^{x,y} : \mathfrak{R}^{x^y} \circ \mathfrak{R}^y \to \mathfrak{R}^{y^x} \circ \mathfrak{R}^x$. In particular, for any morphism $F : A \to B$ in $\mathcal{H}^r(\mathcal{G})$, we have the following commutative diagram:*

$$\begin{array}{ccc} (A^x)^{y^x} & \xrightarrow{\nu_A^{x,y}} & (A^y)^{x^y} \\ {\scriptstyle \mathfrak{R}^{y^x}(\mathfrak{R}^x(F))}\downarrow & & \downarrow{\scriptstyle \mathfrak{R}^{x^y}(\mathfrak{R}^y(F))} \\ (B^x)^{y^x} & \xrightarrow[\nu_B^{x,y}]{} & (B^y)^{x^y}. \end{array}$$

Proof. Let x and y be as in the statement. To simplify the notation we put $\mathfrak{R}^{y,x} = \mathfrak{R}^{y^x} \circ \mathfrak{R}^x$ and $\mathfrak{R}^{x,y} = \mathfrak{R}^{x^y} \circ \mathfrak{R}^y$. Given any object A in $\mathcal{H}^r(\mathcal{G})$, it is easy to check that $\mathfrak{R}^{y,x}(A) = (A^x)^{y^x} = (A^y)^{x^y} = \mathfrak{R}^{x,y}(A)$, and we denote this image by A'. In particular, we have $H'_x = H_{1^y_{i_0}}$ and $H'_y = H_{1^x_{j_0}}$.

We define the morphism $\nu_A^{x,y} : A' \to A'$ as follows:

$$\nu_A^{x,y} = (\epsilon_{1^y_{i_0}} \diamond \epsilon_{1^x_{j_0}} \diamond \mathrm{id}_{A'}) \circ \mathfrak{R}^{y,x}(\Theta_A \circ \Xi_A^{-1}) \circ (\eta^{1^y_{i_0}} \diamond \eta^{1^x_{j_0}} \diamond \mathrm{id}_{A'}),$$

where $\Xi_A : H_x \diamond H_y \diamond A \to H_x \diamond H_y \diamond A'$ and $\Theta_A : H_x \diamond H_y \diamond A \to H_x \diamond H_y \diamond A'$ are the invertible morphisms given by

$$\Xi_A = ((\xi_{y^x}^{1_{i_0},x})^{-1} \diamond \mathrm{id}_{A'}) \circ (\mathrm{id}_x \diamond \xi_{A^x}^{1^x_{j_0},y^x}) \circ \xi_{H_y \diamond A}^{1_{i_0},x},$$

$$\Theta_A = ((\gamma_{x,y} \circ (\xi_{x^y}^{1_{j_0},y})^{-1}) \diamond \mathrm{id}_{A'}) \circ (\mathrm{id}_y \diamond \xi_{A^y}^{1^y_{i_0},x^y}) \circ \xi_{H_x \diamond A}^{1_{j_0},y} \circ (\overline{\gamma}_{x,y} \diamond \mathrm{id}_A).$$

Then, for any morphism $F : A \to B$ in $\mathcal{H}^r(\mathcal{G})$, the relation $(q2)$ implies that

$$\Xi_B \circ (\mathrm{id}_x \diamond \mathrm{id}_y \diamond F) = (\mathrm{id}_x \diamond \mathrm{id}_y \diamond \mathfrak{R}^{y,x}(F)) \circ \Xi_A,$$

$$\Theta_B \circ (\mathrm{id}_x \diamond \mathrm{id}_y \diamond F) = (\mathrm{id}_x \diamond \mathrm{id}_y \diamond \mathfrak{R}^{x,y}(F)) \circ \Theta_A.$$

From the former equality, it also follows that

$$\Xi_B^{-1} \circ (\mathrm{id}_x \diamond \mathrm{id}_y \diamond \mathfrak{R}^{y,x}(F)) = (\mathrm{id}_x \diamond \mathrm{id}_y \diamond F) \circ \Xi_A^{-1}.$$

Summing up, we have

$$\Theta_B \circ \Xi_B^{-1} \circ (\mathrm{id}_x \diamond \mathrm{id}_y \diamond \mathfrak{R}^{y,x}(F)) = (\mathrm{id}_x \diamond \mathrm{id}_y \diamond \mathfrak{R}^{x,y}(F)) \circ \Theta_A \circ \Xi_A^{-1}.$$

By applying $\mathfrak{R}^{y,x}$ to both the members of this identity in $\mathcal{H}^r(\mathcal{G})$, we get the following identity in $\mathcal{H}^r(\mathcal{G}^{\setminus k_0 \setminus l_0})$:

$$\mathfrak{R}^{y,x}(\Theta_B \circ \Xi_B^{-1}) \circ (\mathrm{id}_{1^y_{i_0}} \diamond \mathrm{id}_{1^x_{j_0}} \diamond \mathfrak{R}^{y,x}(F)) = (\mathrm{id}_{1^y_{i_0}} \diamond \mathrm{id}_{1^x_{j_0}} \diamond \mathfrak{R}^{x,y}(F)) \circ \mathfrak{R}^{y,x}(\Theta_A \circ \Xi_A^{-1}),$$

where we have used the fact that $\Re^{y,x} \circ \Re^{y,x} = \Re^{y,x}$ and $\Re^{y,x} \circ \Re^{x,y} = \Re^{x,y}$ (cf. Theorem 8.1 *b*) and *c*)).

Finally, we compose with $\epsilon_{1^y_{i_0}} \diamond \epsilon_{1^x_{j_0}} \diamond \mathrm{id}_{B'}$ on the left and with $\eta_{1^y_{i_0}} \diamond \eta_{1^x_{j_0}} \diamond \mathrm{id}_{A'}$ on the right, to obtain the desired identity: $\nu^{x,y}_B \circ \Re^{y,x}(F) = \Re^{x,y}(F) \circ \nu^{x,y}_A$. □

Now we proceed with the main result of this section, namely Theorem 8.6, which is a reformulation of the first part of Theorem 1.2, concerning reduction and stabilization maps, in the general context of the ribbon Hopf algebras $\mathcal{H}^r(\mathcal{G})$, where $\mathcal{G}$ is an arbitrary (finitely generated) connected groupoid $\mathcal{G}$ (cf. Paragraph 5.1). But before stating the theorem we need some preliminaries.

Recall that, given a connected groupoid $\mathcal{G}$, a morphism F in $\mathcal{H}^r(\mathcal{G})$ is called complete if the elements of $\mathcal{G}$ occurring as labels in a graph diagram of F together with the identities of $\mathcal{G}$ generate all $\mathcal{G}$, i.e. any element of $\mathcal{G}$ which is not an identity can be obtained as a product of such labels or their inverses. Observe that the definition is independent on the choice of the particular diagram representation of F, since the only new labels that can appear or disappear in the equivalence moves of $\mathcal{H}^r(\mathcal{G})$ are identities of $\mathcal{G}$ or products and inverses of labels already occuring.

On the other hand, given any $g \in \mathcal{G}$, we can use equivalence moves to change any diagram representing a complete morphism F, into a new one where g occurs as a label. Namely, move (*s2*) allows us to create a new edge whose label is the inverse of a preexisting one, while applying the move in Figure 106, possibly after isotopy, allows us to create a new edge whose label is the product of two preexisting labels. Since by the completeness of F, g is a product of labels which appear in the original diagram or their inverses, we can eventually create an edge labeled by g.

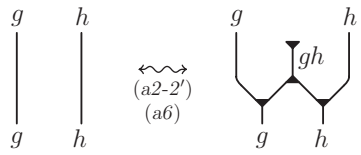

FIGURE 106. ($g \in \mathcal{G}(i,j)$, $h \in \mathcal{G}(j,k)$) [a/29].

We denote by $\widehat{\mathcal{H}}^{r,c}(\mathcal{G})$ the set of closed complete morphisms in $\mathcal{H}^r(\mathcal{G})$. Notice that the set $\widehat{\mathcal{H}}^{r,c}(\mathcal{G})$ of closed complete morphisms in $\mathcal{H}^r(\mathcal{G})$ is non-empty if and only if $\mathcal{G}$ is finitely generated, which in turn implies that $\mathrm{Obj}\,\mathcal{G}$ is finite.

LEMMA 8.5. *Let $\mathcal{G}$ be a connected groupoid and $F \in \widehat{\mathcal{H}}^{r,c}(\mathcal{G})$. Then for any $g \in \mathcal{G}$ there exists a morphism F' in $\mathcal{H}^r(\mathcal{G})$ such that $F = F' \circ L_g$.*

Proof. According to what was said above, we can assume that F contains an edge labeled g. Then F can be isotoped to the form $F' \circ L_g$, for a suitable morphism F' in $\mathcal{H}^r(\mathcal{G})$, as shown in Figure 107. □

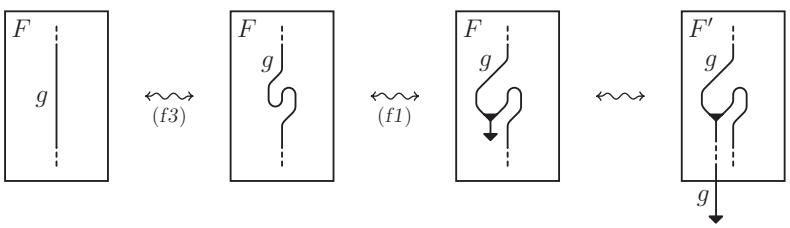

FIGURE 107. Isotoping F to $F' \circ L_g$.

THEOREM 8.6. *Any full inclusion $\mathcal{G} \subset \mathcal{G}'$ of finitely generated connected groupoids uniquely determines two bijective maps*

$$\uparrow_{\mathcal{G}}^{\mathcal{G}'} : \widehat{\mathcal{H}}^{r,c}(\mathcal{G}) \to \widehat{\mathcal{H}}^{r,c}(\mathcal{G}') \quad \text{and} \quad \downarrow_{\mathcal{G}}^{\mathcal{G}'} : \widehat{\mathcal{H}}^{r,c}(\mathcal{G}') \to \widehat{\mathcal{H}}^{r,c}(\mathcal{G}),$$

which we call respectively stabilization map and reduction map, such that:

a) $\uparrow_{\mathcal{G}}^{\mathcal{G}'}$ *and* $\downarrow_{\mathcal{G}}^{\mathcal{G}'}$ *are inverse of each other;*

b) $\uparrow_{\mathcal{G}}^{\mathcal{G}} = \downarrow_{\mathcal{G}}^{\mathcal{G}} = \mathrm{id}_{\widehat{\mathcal{H}}^{r,c}(\mathcal{G})}$ *and moreover*

$$\uparrow_{\mathcal{G}'}^{\mathcal{G}''} \circ \uparrow_{\mathcal{G}}^{\mathcal{G}'} = \uparrow_{\mathcal{G}}^{\mathcal{G}''} \quad \text{and} \quad \downarrow_{\mathcal{G}}^{\mathcal{G}'} \circ \downarrow_{\mathcal{G}'}^{\mathcal{G}''} = \downarrow_{\mathcal{G}}^{\mathcal{G}''}$$

for any other full inclusion $\mathcal{G}' \subset \mathcal{G}''$ of groupoids as above;

c) *if $x \in \mathcal{G}(i_0, k_0)$ with $i_0 \neq k_0$, then*

$$\uparrow_{\mathcal{G}^{\setminus k_0}}^{\mathcal{G}}(F) = F \diamond (\epsilon_x \circ L_x) \quad \text{for any } F \in \widehat{\mathcal{H}}^{r,c}(\mathcal{G}^{\setminus k_0}),$$
$$\downarrow_{\mathcal{G}^{\setminus k_0}}^{\mathcal{G}}(F) = \Re^x(F') \circ \eta_{1_{i_0}} \quad \text{for any } F = F' \circ L_x \in \widehat{\mathcal{H}}^{r,c}(\mathcal{G}).$$

Moreover, $\uparrow_{\mathcal{G}}^{\mathcal{G}'}$ and $\downarrow_{\mathcal{G}}^{\mathcal{G}'}$ induce bijective maps between the sets of closed complete morphisms of the quotient categories

$$\partial^\star\uparrow_{\mathcal{G}}^{\mathcal{G}'} : \partial^\star\widehat{\mathcal{H}}^{r,c}(\mathcal{G}) \to \partial^\star\widehat{\mathcal{H}}^{r,c}(\mathcal{G}') \quad \text{and} \quad \partial^\star\downarrow_{\mathcal{G}}^{\mathcal{G}'} : \partial^\star\widehat{\mathcal{H}}^{r,c}(\mathcal{G}') \to \partial^\star\widehat{\mathcal{H}}^{r,c}(\mathcal{G}),$$
$$\partial\uparrow_{\mathcal{G}}^{\mathcal{G}'} : \partial\widehat{\mathcal{H}}^{r,c}(\mathcal{G}) \to \partial\widehat{\mathcal{H}}^{r,c}(\mathcal{G}') \quad \text{and} \quad \partial\downarrow_{\mathcal{G}}^{\mathcal{G}'} : \partial\widehat{\mathcal{H}}^{r,c}(\mathcal{G}') \to \partial\widehat{\mathcal{H}}^{r,c}(\mathcal{G}).$$

Proof. We begin by verifying that c) gives a good definition for the two maps $\uparrow_{\mathcal{G}^{\setminus k_0}}^{\mathcal{G}} : \widehat{\mathcal{H}}^{r,c}(\mathcal{G}^{\setminus k_0}) \to \widehat{\mathcal{H}}^{r,c}(\mathcal{G})$ and $\downarrow_{\mathcal{G}^{\setminus k_0}}^{\mathcal{G}} : \widehat{\mathcal{H}}^{r,c}(\mathcal{G}) \to \widehat{\mathcal{H}}^{r,c}(\mathcal{G}^{\setminus k_0})$.

Concerning $\uparrow_{\mathcal{G}^{\setminus k_0}}^{\mathcal{G}}$, we have to prove that for any $F \in \widehat{\mathcal{H}}^{r,c}(\mathcal{G}^{\setminus k_0})$ the morphism $F \diamond (\epsilon_x \circ L_x)$ belongs to $\widehat{\mathcal{H}}^{r,c}(\mathcal{G})$ and does not depend on the choice of x. The only non-trivial point in the first assertion is the completeness of $F \diamond (\epsilon_x \circ L_x)$ in $\mathcal{H}^r(\mathcal{G})$. This follows from the completeness of F and from the fact that $\mathcal{G}^{\setminus k_0}$ together with x generate all $\mathcal{G}$ (cf. Paragraph 5.2). The independence on x is proved in Figure 108, where $y \in \mathcal{G}(j_0, k_0)$ with $j_0 \neq k_0$ and F'' is a morphism in $\mathcal{H}^r(\mathcal{G}^{\setminus k_0})$ such that $F = F'' \circ y\overline{x}$, whose existence is guaranteed by Proposition 8.5.

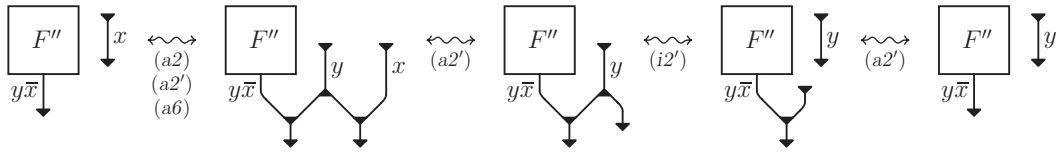

FIGURE 108. $F \diamond (\epsilon_x \circ L_x) = F \diamond (\epsilon_y \circ L_y)$ in $\mathcal{H}^r(\mathcal{G})$ [a/29, *i*/34].

Passing to $\downarrow_{\mathcal{G}^{\setminus k_0}}^{\mathcal{G}}$, we have to prove that for any $F \in \widehat{\mathcal{H}}^{r,c}(\mathcal{G})$ and any decomposition $F = F' \circ L_x$ the morphism $\Re^x(F) \circ \eta_{1_{i_0}}$ belongs to $\widehat{\mathcal{H}}^{r,c}(\mathcal{G}^{\setminus k_0})$ and does not depend on the choice of the decomposition. As above, for the first assertion it is enough to observe that $\Re^x(F) \circ \eta_{1_{i_0}}$ is complete in $\mathcal{H}^r(\mathcal{G}^{\setminus k_0})$, since the labels occurring in it include the images under the functor $\_^x$ of those occurring in F, so they generate all $\mathcal{G}^{\setminus k_0}$. To see that two different decompositions $F = F' \circ L_x$ with $x \in \mathcal{G}(i_0, k_0)$ and $F = F'' \circ L_y$ with $y \in \mathcal{G}(j_0, k_0)$ give rise to the same reduction of F,

without loss of generality, we may assume that those decompositions are obtained by isotoping edges, as in Figure 107, of two diagrams representing F. Assume first, that those two diagrams are the same, i.e that the decompositions are obtained by starting with the same diagram and making two different choices of an edge and an isotopy. By isotoping both edges simultaneously we obtain a third decomposition $F = F''' \circ (L_x \diamond L_y)$ (the center diagram in Figure 109) such that, up to isotopy, $F' = F''' \circ L_y$ and $F'' = F''' \circ L_x$. Then the functoriality of $\Re^x$ and $\Re^y$ implies that $\Re^x(F''') \circ (\eta_{1_{i_0}} \diamond L_{y\bar{x}})$ is equivalent to $\Re^x(F') \circ \eta_{1_{i_0}}$ and $\Re^y(F''') \circ (L_{x\bar{y}} \diamond \eta_{1_{j_0}})$ is equivalent to $\Re^y(F'') \circ \eta_{1_{j_0}}$ in $\mathcal{H}^{r,c}(\mathcal{G}^{\setminus k_0})$ (the equivalences on the left and on the right in Figure 109). Therefore it is enough to show that $\Re^x(F''') \circ (\eta_{1_{i_0}} \diamond L_{y\bar{x}})$ and $\Re^y(F''') \circ (L_{x\bar{y}} \diamond \eta_{1_{j_0}})$ are equivalent in $\mathcal{H}^{r,c}(\mathcal{G}^{\setminus k_0})$, which is done in Figure 110. Now the independence on the particular diagram representing F, follows from the fact that all elementary relations are local. So, by the argument above, when applying a relation to the diagram of F, we can always choose the isotoped edge producing the decomposition $F = F' \circ L_x$, away from the support of the relation and think of the relation as if it were applied to the diagram of F'. Now the statement follows from the functoriality of $\Re^x$. This concludes the proof that the stabilization and the reduction maps in c) are well defined.

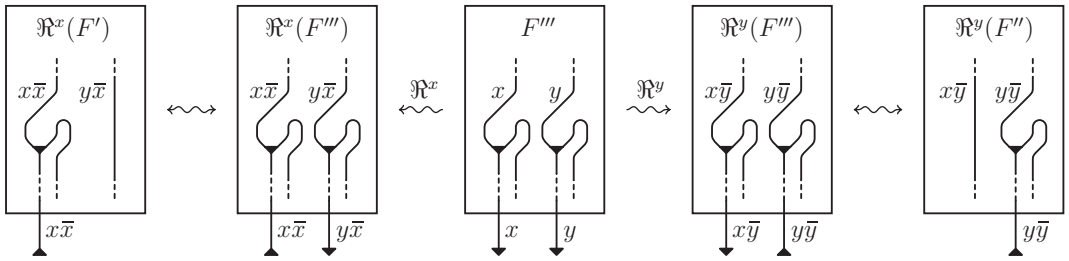

FIGURE 109. Two different reductions of $F = F''' \circ (L_x \diamond L_y)$.

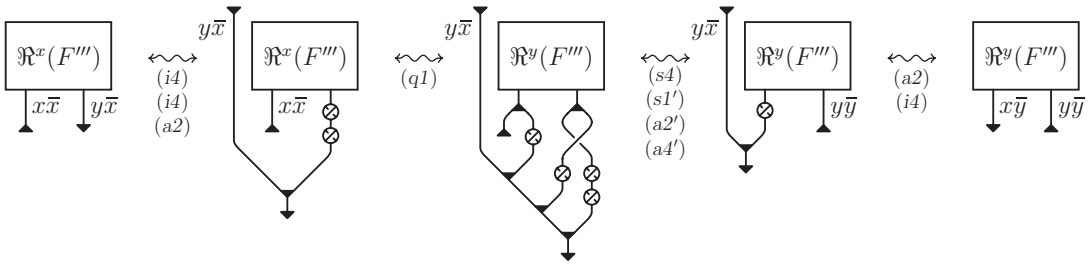

FIGURE 110. $\Re^x(F''') \circ (\eta_{x\bar{x}} \diamond L_{y\bar{x}}) = \Re^y(F''') \circ (L_{x\bar{y}} \diamond \eta_{y\bar{y}})$ [a/29, f/35, i/34, q/52, s/31].

Now we want to show that the maps $\uparrow^{\mathcal{G}}_{\mathcal{G}^{\setminus k_0}}$ and $\downarrow^{\mathcal{G}}_{\mathcal{G}^{\setminus k_0}}$ defined in c) are inverse of each other. Indeed, given $F \in \widehat{\mathcal{H}}^{r,c}(\mathcal{G}^{\setminus k_0})$ and $x \in \mathcal{G}(i_0, k_0)$ with $i_0 \neq k_0$, Theorem 8.1 b) implies that $\Re^x(F) = F$. Then $\downarrow^{\mathcal{G}}_{\mathcal{G}^{\setminus k_0}}(\uparrow^{\mathcal{G}}_{\mathcal{G}^{\setminus k_0}}(F)) = \downarrow^{\mathcal{G}}_{\mathcal{G}^{\setminus k_0}}(F \diamond (\epsilon_x \circ L_x)) = \Re^x(F \diamond \epsilon_x) \circ \eta_{1_{i_0}} = F \diamond (\epsilon_{1_{i_0}} \circ \eta_{1_{i_0}}) = F$. On the other hand, Figure 111 shows that $F = \uparrow^{\mathcal{G}}_{\mathcal{G}^{\setminus k_0}}(\downarrow^{\mathcal{G}}_{\mathcal{G}^{\setminus k_0}}(F))$ for any $F \in \widehat{\mathcal{H}}^{r,c}(\mathcal{G})$.

At this point, we define the maps $\uparrow^{\mathcal{G}'}_{\mathcal{G}}$ and $\downarrow^{\mathcal{G}'}_{\mathcal{G}}$ by iteration. Namely, given the full inclusion of groupoids $\mathcal{G} \subset \mathcal{G}'$ with $\operatorname{Obj}\mathcal{G}' - \operatorname{Obj}\mathcal{G} = \{k_1, \ldots, k_n\}$, we consider the sequence $\mathcal{G}' = G_n \supset G_n^{\setminus k_n} = G_{n-1} \supset \ldots \supset G_2^{\setminus k_2} = G_1 \supset G_1^{\setminus k_1} = \mathcal{G}$, and define

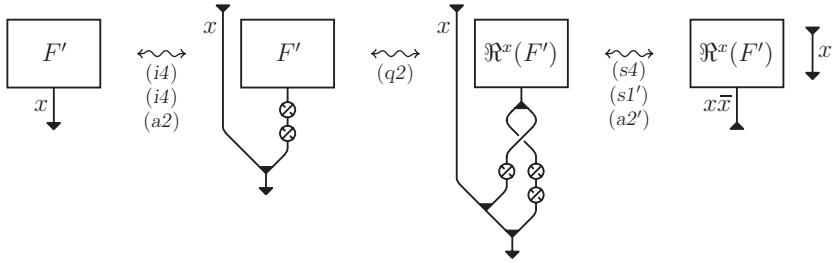

FIGURE 111. $F = \uparrow^{\mathcal{G}}_{\mathcal{G}\setminus k_0}(\downarrow^{\mathcal{G}}_{\mathcal{G}\setminus k_0}(F))$ [a/29, f/35, i/34, q/52, s/31].

$$\uparrow^{\mathcal{G}'}_{\mathcal{G}} = \uparrow^{G_n}_{G_n\setminus k_n} \circ \ldots \circ \uparrow^{G_2}_{G_2\setminus k_2} \circ \uparrow^{G_1}_{G_1\setminus k_1} \quad \text{and} \quad \downarrow^{\mathcal{G}'}_{\mathcal{G}} = \downarrow^{G_1}_{G_1\setminus k_1} \circ \downarrow^{G_2}_{G_2\setminus k_2} \circ \ldots \circ \downarrow^{G_n}_{G_n\setminus k_n}.$$

Observe that the maps $\uparrow^{\mathcal{G}'}_{\mathcal{G}}$ and $\downarrow^{\mathcal{G}'}_{\mathcal{G}}$ are inverses of each other and since the definition of first map is obviously independent on the choice of ordering of $\operatorname{Obj}\mathcal{G}' - \operatorname{Obj}\mathcal{G}$, the same must be true for the second one. Then properties *a*) and *b*) are trivially satisfied.

Finally, the induced maps between the sets of closed complete morphisms of the quotient categories are defined similarly to $\uparrow^{\mathcal{G}'}_{\mathcal{G}}$ and $\downarrow^{\mathcal{G}'}_{\mathcal{G}}$, by replacing $\Re^x$ with the induced functors $\partial^\star\Re^x$ and $\partial\Re^x$ (cf. Theorem 8.1). □

8.7. *Proof of Theorem 1.2.* We remind that $\mathcal{H}^r_n = \mathcal{H}^r(\mathcal{G}_n)$, where $\mathcal{G}_n$ is the groupoid with $\operatorname{Obj}\mathcal{G}_n = \{1, 2, \ldots, n\}$ and $\mathcal{G}_n(i,j) = \{(i,j)\}$ for any $1 \leq i, j \leq n$. Then Theorem 1.2 is essentially the specialization of Theorem 8.6 to the case when $\mathcal{G} = \mathcal{G}_m$, $\mathcal{G}' = \mathcal{G}_n$ and the full inclusion $\mathcal{G}_m \subset \mathcal{G}_n$ is the canonical one; moreover, the notations $\uparrow^n_m = \uparrow^{\mathcal{G}_n}_{\mathcal{G}_m}$ and $\downarrow^n_m = \downarrow^{\mathcal{G}_n}_{\mathcal{G}_m}$ have been used. Then the equality $\Phi_n \circ \uparrow^n_m = \uparrow^n_m \circ \Phi_m$ follows directly from the definitions of the functors Φ_k and of the stabilization maps. □

9. From surfaces to the algebra

This section is dedicated to the proof of Theorem 1.3. First of all, given a strict total order $<$ on $\operatorname{Obj}\mathcal{G}_n$, we define the functor $\Psi^<_n : \mathcal{S}_n \to \mathcal{H}^r_n$ in the following way: on the objects $\Psi^<_n$ is uniquely determined by the identities

$$\Psi^<_n((i\ j)) = H_{(i,j)} \ \text{ if } i < j,$$

$$\Psi^<_n(A \diamond B) = \Psi^<_n(A) \diamond \Psi^<_n(B),$$

while Figures 112 and 113 describe the images under $\Psi^<_n$ of the elementary morphisms of $\mathcal{S}_n$ (the image of any labeling of the morphism presented Figure 21 (e'), is defined through relation (*I6*) in Figure 22).

Then Theorem 1.3 states that $\Psi^<_n$ is a braided monoidal functor and if $<'$ is another strict total order, there is a natural equivalence $\tau : \Psi^<_n \to \Psi^{<'}_n$ which is identity on the empty set.

The proof of the theorem will make use of the relations (*t8*) and (*t9*), which are introduced in the next proposition for an arbitrary groupoid $\mathcal{G}$. Given $g \in \mathcal{G}(i,j)$ with $i \neq j$, let $T_g : H_g \to H_{\bar{g}}$ be defined as in Paragraph 6.7. We remind that $T_{\bar{g}} \circ T_g = \mathrm{id}_g$ (cf. (*t3*) in Figure 59).

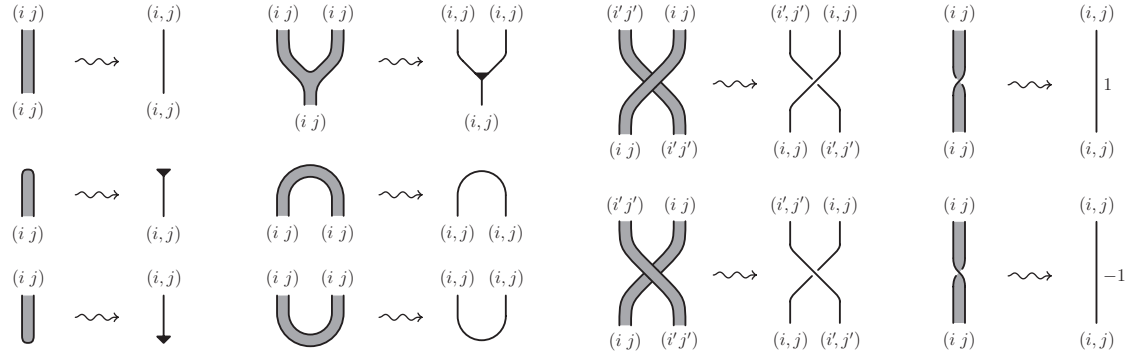

FIGURE 112. Definition of $\Psi_n^{\leq}$ – I ($i < j$, $i' < j'$).

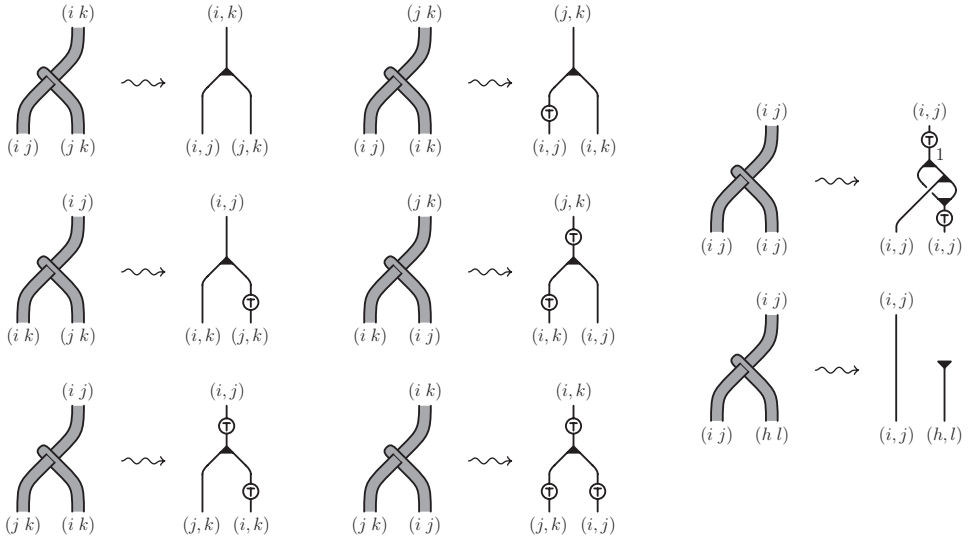

FIGURE 113. Definition of $\Psi_n^{\leq}$ – II ($i < j < k$, $h < l$ and $\{i,j\} \cap \{h,l\} = \emptyset$).

PROPOSITION 9.1. *Let $\mathcal{H}^r(\mathcal{G})$ be the universal ribbon Hopf $\mathcal{G}$-algebra. For any $g, h \in \mathcal{G}(i,j)$ with $i \neq j$, define the morphisms $c^{\pm}_{g,h} : H_g \diamond H_h \to H_{hgh}$ as follows:*

$$c^{+}_{g,h} = m_{h,gh} \circ (\mathrm{id}_h \diamond m_{g,h}) \circ (\gamma_{g,h} \diamond \mathrm{id}_h) \circ (\mathrm{id}_g \diamond \Delta_h),$$
$$c^{-}_{g,h} = m_{h,gh} \circ (\mathrm{id}_h \diamond m_{g,h}) \circ (\overline{\gamma}_{g,h} \diamond \mathrm{id}_h) \circ (\mathrm{id}_g \diamond \Delta_h).$$

Then (cf. Figure 114)

$$c^{+}_{g,h} \circ (\mathrm{id}_g \diamond v_h) = c^{-}_{g,h}, \tag{t8}$$
$$c^{+}_{g,h} = T_{\bar{h}\bar{g}\bar{h}} \circ c^{+}_{\bar{g},\bar{h}} \circ (T_g \diamond T_h). \tag{t9}$$

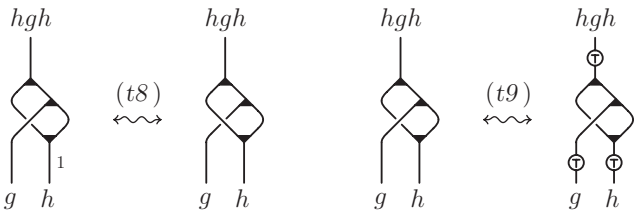

FIGURE 114. Relations of Proposition 9.1 ($g, h \in \mathcal{G}(i,j)$, $i \neq j$).

Proof. See Figure 115. □

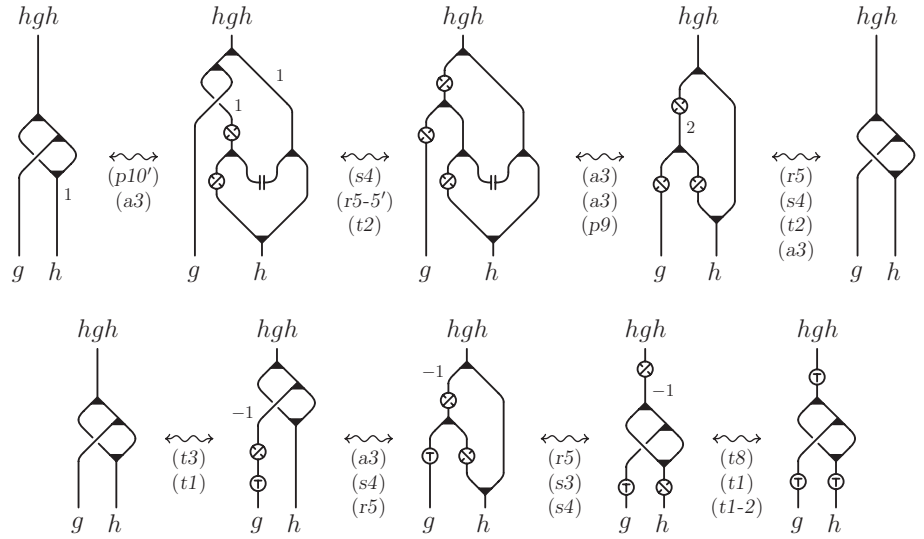

FIGURE 115. Proof of Proposition 9.1 [a/29, p/40, r/37, s/31, t/41-67].

Observe that, when $\mathcal{G} = \mathcal{G}_n$ and $g = h = (i, j)$, $S_{\bar{h}g\bar{h}} \circ c^{+}_{g,\bar{h}} \circ (\mathrm{id}_g \diamond T_h)$ is exactly the image of the uni-colored singular vertex under Ψ_n (cf. Figure 113).

9.2. *Proof of Theorem 1.3.* Given any two strict total orders $<$ and $<'$ on $\mathrm{Obj}\,\mathcal{G}_n$, for any object A in $\mathcal{S}_n$ we define the invertible morphism $\tau_A : \Psi_n^{<}(A) \to \Psi_n^{<'}(A)$ by induction, according to the relations

$$\tau_{(i,j)} = \begin{cases} \mathrm{id}_{(i,j)} : H_{(i,j)} \to H_{(i,j)} & \text{if } i < j \text{ and } i <' j, \\ T_{(i,j)} : H_{(i,j)} \to H_{(j,i)} & \text{if } i < j \text{ and } j <' i; \end{cases}$$

$$\tau_{\mathbf{1}} = \mathrm{id}_{\mathbf{1}}, \quad \tau_{A \diamond B} = \tau_A \diamond \tau_B.$$

Then for any morphism $F : A \to B$ in $\mathcal{S}_n$, represented as a fixed composition of products of elementary morphisms, we have the following commutative diagram:

$$\begin{array}{ccc} \Psi_n^{<}(A) & \xrightarrow{\tau_A} & \Psi_n^{<'}(A) \\ {\scriptstyle \Psi_n^{<}(F)}\downarrow & & \downarrow{\scriptstyle \Psi_n^{<'}(F)} \\ \Psi_n^{<}(B) & \xrightarrow[\tau_B]{} & \Psi_n^{<'}(B)\,. \end{array}$$

Indeed, the commutativity in the case when F is an elementary morphism can be easily derived from the definition of $\Psi_n^{<}$, by using the relations $(t3)$ in Figure 59, $(t4)$ in Figure 60 and $(t9)$ in Figure 114, while the extension to an arbitrary composition is allowed by the relation $(t3)$.

Now we have to show that $\Psi_n^{<}$ is well-defined on the level of morphisms. In other words, that it sends labeled rs-tangles related by any of the defining moves of $\mathcal{S}_n$ (the labeled versions of the moves in Figures 22, 23, 24 and 25 together with the moves in Figure 3) to labeled graph diagrams representing the same morphism in $\mathcal{H}_n^r$. In showing that, by the commutativity of the above diagram, we can choose the most convenient order $<$ for each single move.

We remind that move (*I6*) in Figures 22 was used to define the images under $\Psi_n^<$ of the morphisms on the left hand side, so there is nothing to prove for it. Analogously, for (*R2*) in Figure 3 it suffices to look at the definition of $\Psi_n^<$.

Here below we indicate how the verification goes for the remaining moves (actually, most of them essentially rewrite the algebra axioms and the relations in $\mathcal{H}_n^r$ proved in Sections 5 and 6).

(*I1*), (*I7-7′*) and (*I8-9*) follow from the braid axioms in Figure 34 (p. 29).

(*I2-2′*) correspond to axioms (*f3-3′*) in Figure 41 (p. 33).

(*I3*) follows from one of the botton-left duality moves in Figure 45 (p. 34).

(*I4*) follows from relation (*p4*) in Figure 55 (p. 40).

(*I5*) follows from move (*f4*) in Figure 42 (p. 33).

(*I10*), (*I12-12′*) and (*I13*) follow from the ribbon axioms in Figure 50 (p. 37).

(*I11*) follows from relations (*f6′*) in Figure 48 (p. 35) and (*t2*) in Figure 59 (p. 41).

(*I14-14′*) for a bi-colored singular vertex are trivial, while for a tri-colored singular vertex follow directly from (*t6*) and (*t7*) in Figure 60 (p. 42). The proof for a uni-colored singular vertex is presented in Figures 116 and 117, where Figure 116 shows that the image under $\Psi_n^<$ of the labeled rs-tangle in the middle of (*I14-14′*) is equivalent to the third graph diagram in Figure 117.

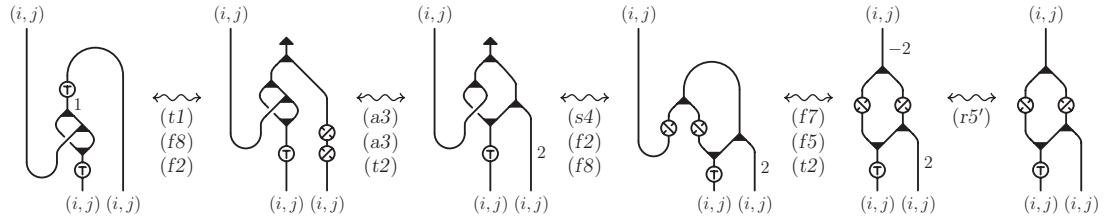

FIGURE 116. Proof of (*I14-14′*) in the uni-colored case – I ($i < j$) [a/29, f/33-33-35, p/40, r/37, s/31, t/41].

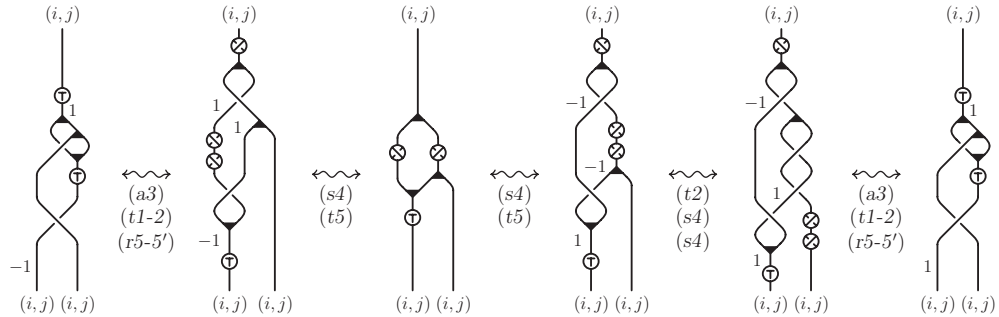

FIGURE 117. Proof of (*I14-14′*) in the uni-colored case – II ($i < j$) [a/29, r/37, s/31, t/41].

(*I15*) follows from relation (*t5*) in Figure 60 (p. 42).

(*I16*) follows from the definition of the coform (*f1*) in Figure 41 (p. 33).

(*I17*) for a bi-colored singular vertex reduces to a crossing change, so it follows from axioms (*r11*) in Figure 51 (p. 37). For a tri-colored singular vertex the proof is

presented in Figure 118, while for a uni-colored singular vertex it is presented in Figure 119.

(*I18*) corresponds to the bi-algebra axiom (*a1*) in Figure 35 (p. 29).

(*I19*) is presented in Figure 120.

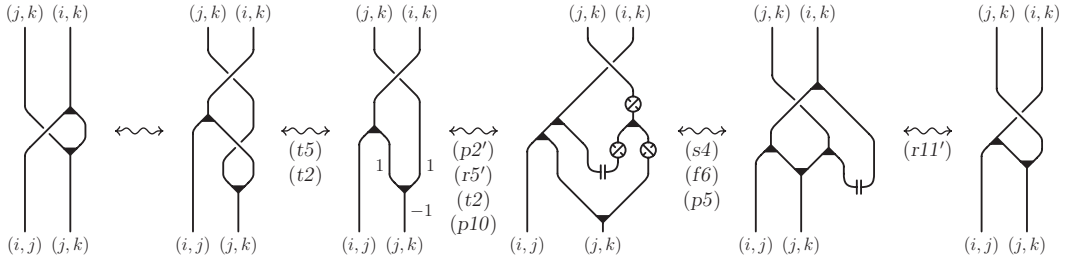

FIGURE 118. Proof of (*I17*) in the tri-colored case ($i < j < k$) [*f*/42, *p*/39-40, *r*/37-41, *s*/31, *t*/41].

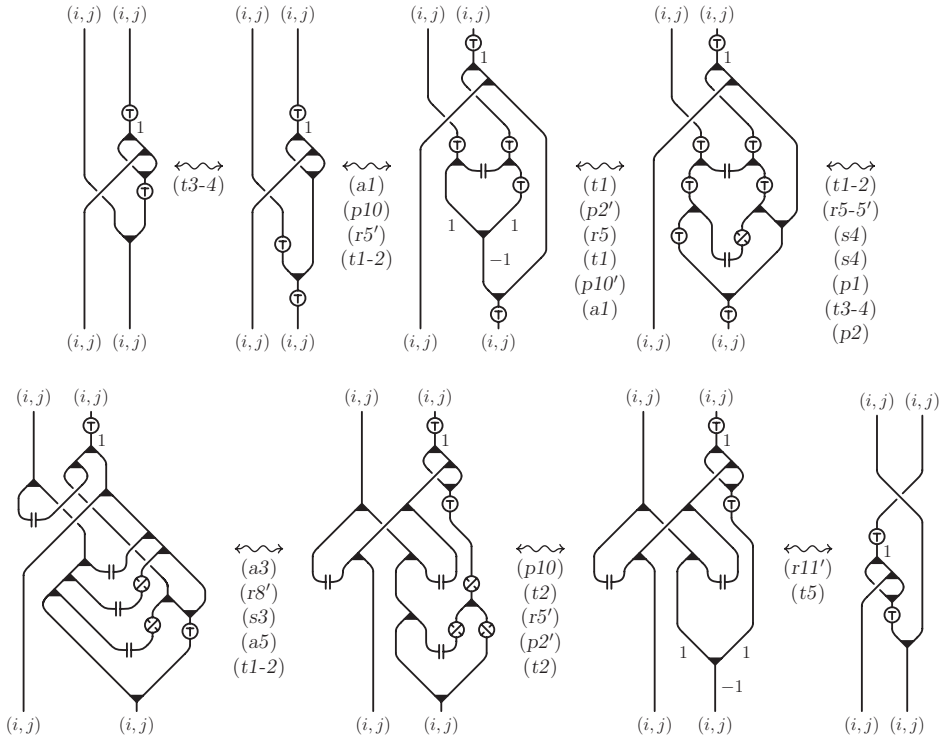

FIGURE 119. Proof of (*I17*) in the uni-colored case ($i < j$) [a/29, *p*/39-40, *r*/37-37-41, *s*/31, *t*/41].

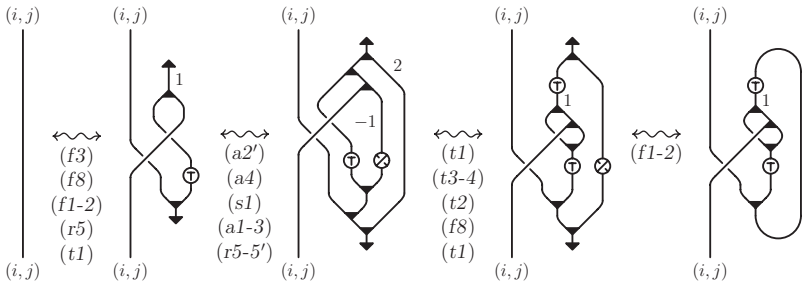

FIGURE 120. Proof of (*I19*) ($i < j$) [a/29, *f*/33-35, *r*/37, *s*/30, *t*/41].

(*I20*) follows from (*a6*), (*s6*) and (*r2*) respectively in Figures 35 (p. 29), 39 (p. 31) and 50 (p. 37).

(*I21*) for bi-colored singular vertices is trivial, while for tri-colored singular vertices, with the proper choice of the order $<$, it corresponds to the bi-algebra axiom (*a5*) in Figure 35 (p. 29). The proof for uni-colored singular vertices is presented in Figure 121.

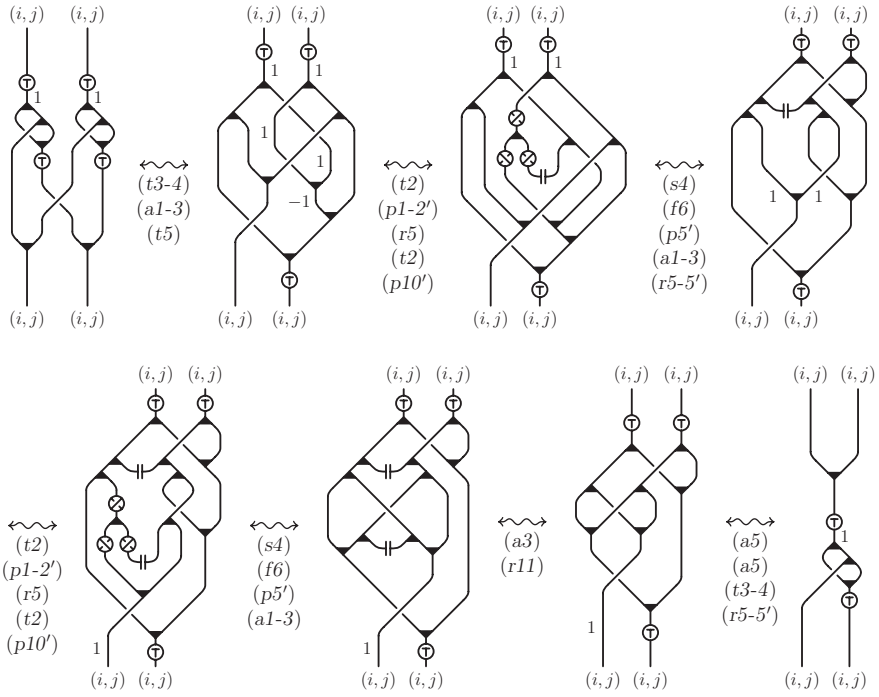

FIGURE 121. Proof (*I21*) in the uni-colored case ($i < j$) [a/29, p/40, r/37-37, s/31, t/42].

(*I22*) is the most complicated relation to deal with, since the source of the involved morphisms consists of three intervals which can be labeled independently from each other, so there are many different cases. First of all, we observe that the presence of disjoint labels allows us to simplify the relation by using move (*R2*) to remove the bi-colored singular vertices. In particular, such simplification makes (*I22*) trivial when the label of the rightmost interval is disjoint from the other two, while it makes (*I22*) easily reducible to other moves (namely (*I3*), (*I5*), (*I16*) and (*I20*)) when the leftmost and the rightmost intervals have disjoint labels. Up to conjugation, the only remaining labelings of the three intervals which include a pair of disjoint labels are given by the sequences $(i\ j)\,,(j\ k)\,,(k\ l)$ and $(i\ j)\,,(i\ k)\,,(i\ l)$ where i, j, k, l are all distinct. The first case corresponds, modulo move (*R2*), to the bi-algebra axiom (*a3*) in Figure 35 (p. 29), while the second case is treated in the top line of Figure 122. The bottom line of the same figure concerns the unique remaining case when a bi-colored singular vertex occurs (even if there is no pair of dijoint labels in the source). The rest of the cases are grouped depending on the number of uni-colored singular vertices: the three cases with only one such vertex are presented in Figure 123; the single case with two uni-colored vertices is considered in Figure 124; finally, the last

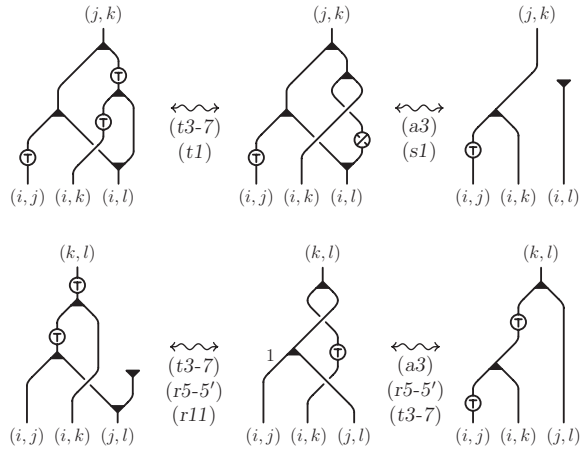

FIGURE 122. Proof of (*I22*) in the non trivial cases when a bi-colored singular vertex occurs, $(i < j < k < l)$ [a/29, r/37-37, s/30, t/41].

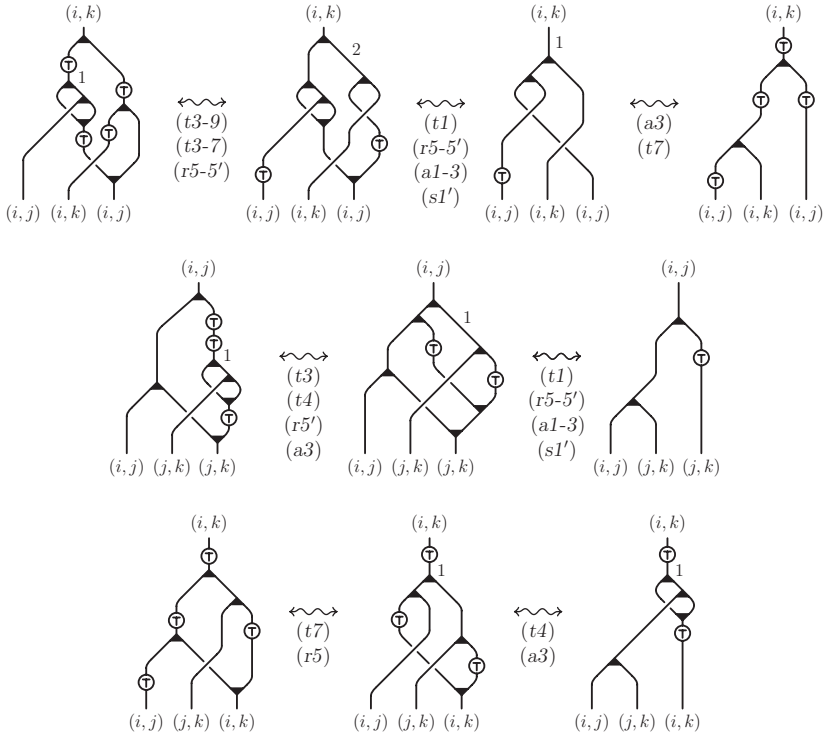

FIGURE 123. Proof of (*I22*) in the cases when one uni-colored singular vertex occurs $(i < j < k)$ [a/29, r/37, s/30, t/41-67].

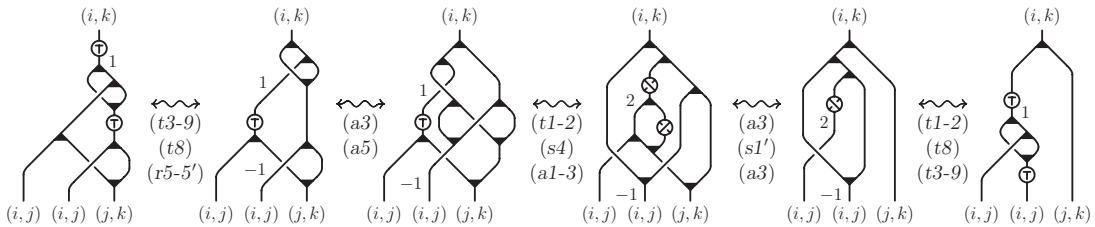

FIGURE 124. Proof of (*I22*) in the cases when two uni-colored singular vertices occur $(i < j < k)$ [a/29, r/37, s/30, t/41-67].

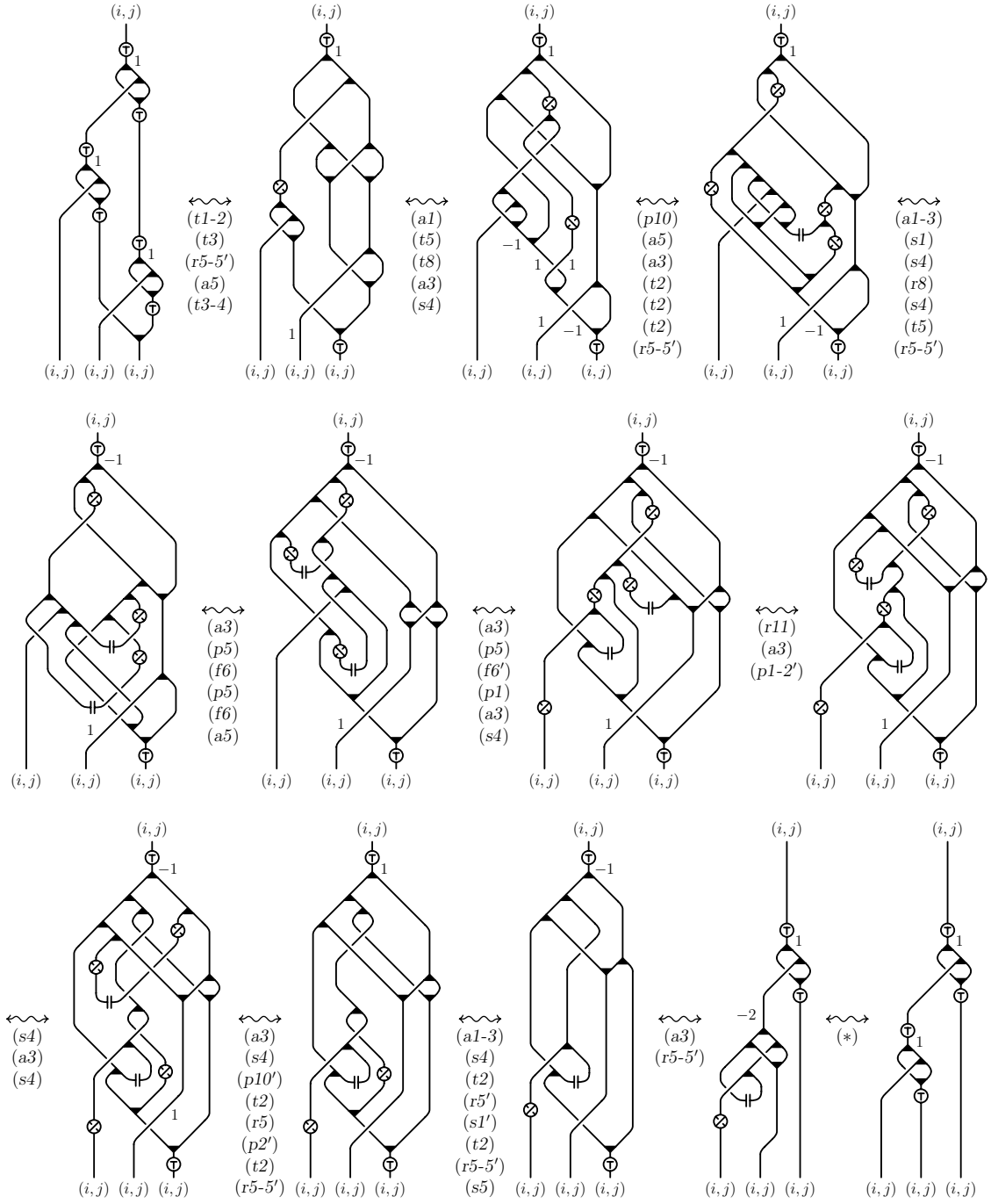

FIGURE 125. Proof of (*I22*) in the uni-colored case ($i < j$) [a/29, p/39-40, r/37-37, s/30-31, t/41-67].

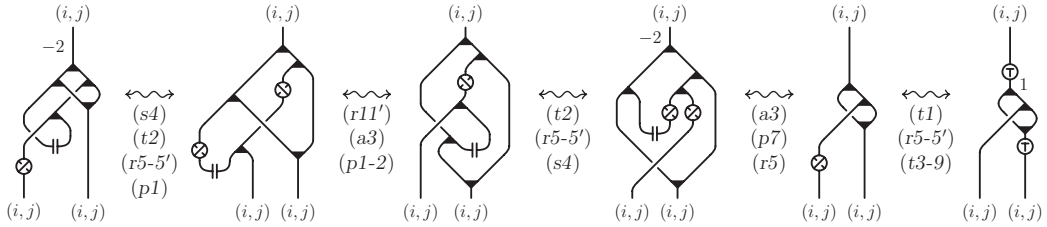

FIGURE 126. Proof of step (∗) in Figure 125 [a/29, p/40, r/37-37, s/31, t/41-67].

case in which all singular vertices are uni-colored is shown in Figures 125 and 126.

(*R1*) follows from the relations (*t3*) in Figure 59 (p. 41) and (*t6*) in Figure 60 (p. 42), taking into account that T propagates through the form and the coform, due to (*f7-8*) in Figure 46 (p. 35) and (*p3-4*) in Figure 55 (p. 40). □

9.3. *Proof of Theorem 1.4.* The fact that $\Phi_n(\Psi_n(F)) = K_F$ for any $F \in \widehat{\mathcal{S}}_n^c$ can be seen by comparing the definitions of Φ_n (cf. Figures 64 and 65) and Ψ_n (cf. Figures 112 and 113) with the description of K_F given in Section 4 (cf. Figures 29 and 30). Hence, as discussed after the statement of the theorem (at p. 7), it suffices to verify that the map $\Psi_n : \widehat{\mathcal{S}}_n^c \to \widehat{\mathcal{H}}_n^{r,c}$ is surjective for $n \geq 4$. Actually, we will do this for any $n \geq 3$.

Let F be an arbitrary morphism in $\widehat{\mathcal{H}}_n^{r,c}$ with $n \geq 3$, represented by a given diagram (without using copairings and form/coform notation). An edge of the diagram will be called an *i-edge*, $1 \leq i \leq n$, if it is labeled (i, i) and it is not attached to one positive tri-valent and one positive integral vertex. Moreover, a vertex will be called an *i-vertex* if it is not a positive integral vertex and all edges attached to it are labeled (i, i).

As a preliminary step, we will show how to transform the diagram representing F into an equivalent one, where no i-edges appear for any $1 \leq i \leq n$. Actually, the figures below deal only with edges of zero weight and not containing the antipode morphism, but the generalization to other weights or to the presence of the antipode is straightforward. Observe also that since F is complete and $n \geq 2$, we may assume that near a given i-edge there is a counit $\epsilon_{(i,j)}$ with $i \neq j$ (such a counit can be obtained by move (*a2*) from an edge labeled (i, j) and then isotoped everywhere).

We start by eliminating all uni-valent i-vertices as described in the first three moves in Figure 127. Then by applying, if necessary, the edge breaking shown in the fourth move in the same figure, we obtain a diagram where all i-edges connect two tri-valent vertices such that at most one of them is an i-vertex.

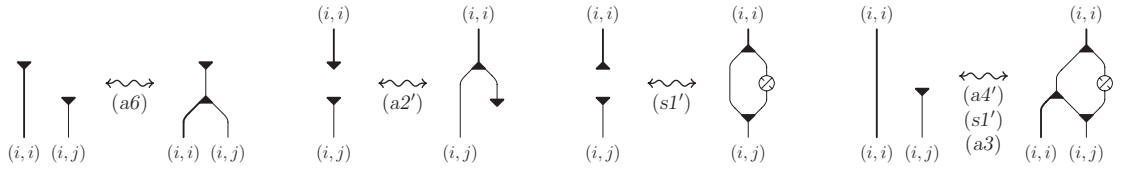

FIGURE 127. Eliminating uni-valent i-vertices ($i \neq j$) [a/29, s/30].

We proceed by eliminating the tri-valent i-vertices, starting with the negative ones as shown in the leftmost move in Figure 128 and then using the two other moves

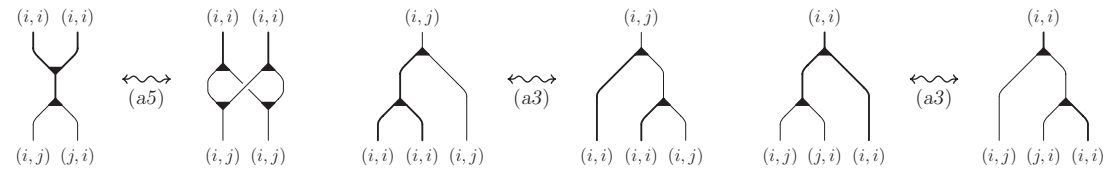

FIGURE 128. Eliminating tri-valent i-vertices ($i \neq j$) [a/29].

in the same figure (or their vertical reflections) to eliminate the positive i-vertices as well.

At this point, the only remaining i-edges, connect two positive tri-valent vertices none of which is an i-vertex. Such edges are eliminated through the moves shown in Figure 129 (or their vertical reflections), where, since $n \geq 3$ and F is complete, without loss of generality we have assumed that there exists close by a counit of label (j,k) with $i \neq j \neq k \neq i$.

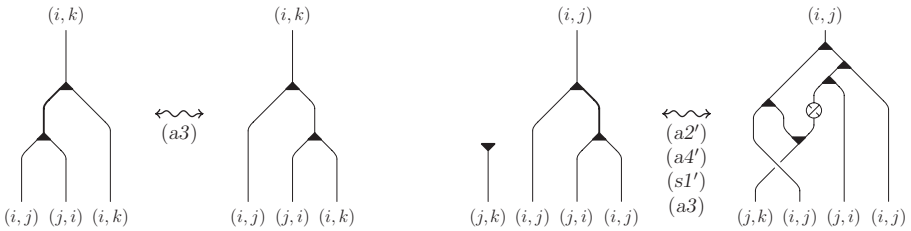

FIGURE 129. Eliminating i-edges connecting two tri-valent vertices none of which is an i-vertex ($i \neq j \neq k \neq i$) [a/29, s/30].

In this way we have represented the morphism F by a diagram in which any edge labeled (i,i) is attached to one positive tri-valent and one positive integral vertex. Then, by using the form notation introduced in Figure 41, we can eliminate those exceptional edges as well, obtaining a diagram of F whose labels are all of the type (i,j) with $i \neq j$.

Now, given any order $<$ on $\operatorname{Obj}\mathcal{G}_n$, we modify this last diagram of F in such a way that the labels (i,j) with $j < i$ are concentrated at short arcs of zero weight delimited on one end by a uni- or tri-valent vertex and on the other end by an antipode. This can be done by using relation (*t2*) in Figure 59 to convert all the inverses of antipodes into antipodes and to create/eliminate pairs of antipodes along the same edge (at the cost of adding some twists) and relations (*f7-8*) in Figure 46, (*p1-4*) in Figure 55 and (*r4*) in Figure 50 to slide antipodes and twists along edges.

Then, we remove those of the short arcs above, which are attached to uni-valent vertices and to negative tri-valent vertices by applying moves (*i4-5*) in Figure 44, (*s5-6*) in Figure 39 and (*t4*) in Figure 60. The antipodes still present in the diagram, bound short arcs attached to positive tri-valent vertices and using relation (*t1*) in Figure 59, we express them in terms of the morphisms $T_{(i,j)}$.

We finish the proof of Theorem 1.4 by observing that the resulting diagram of F is a composition of the diagrams on the left side of Figures 112 and 113, hence F is in the image of Ψ_n. □

9.4. *Proof of Theorem 1.5.* According to Proposition 7.2, Φ_n induces functors $\partial^\star\Phi_n : \partial^\star\mathcal{H}_n^r \to \partial^\star\mathcal{K}_n$ and $\partial\Phi_n : \partial\mathcal{H}_n^r \to \partial\mathcal{K}_n$ between the corresponding quotient categories. Moreover, by the last part of Theorem 8.6, $\downarrow_m^n$ and $\uparrow_m^n$ induce well defined bijective maps between the closed complete morphisms in these quotient categories for any $m < n$. In order to complete the proof of Theorem 1.5 we only need to show that the functor Ψ_n induces functors

$$\partial^\star\Psi_n : \partial^\star\mathcal{S}_n \to \partial^\star\mathcal{H}_n^r \quad \text{and} \quad \partial\Psi_n : \partial\mathcal{S}_n \to \partial\mathcal{H}_n^r,$$

in other words that the images under Ψ_n of the two sides of the relation (T) (resp. relations (T), (P) and (P')) in Figure 4 are equivalent in $\partial^\star\mathcal{H}^r_n$ (resp. $\partial\mathcal{H}^r_n$). This is done in Figures 130 (resp. 131). □

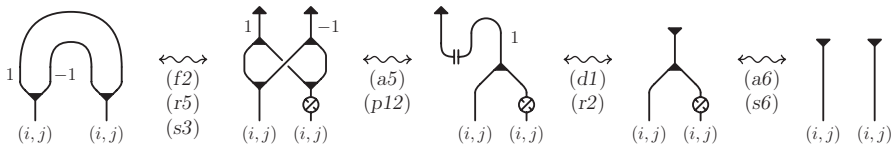

FIGURE 130. Proof of (T) in $\partial^\star\mathcal{H}^r_n$ $(i < j)$ [a/29, f/33-35, p/40, s/31].

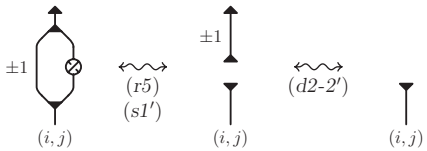

FIGURE 131. Proof of (P) and (P') in $\partial\mathcal{H}^r_n$ $(i < j)$ [d/43, r/37, s/30].

10. Appendix: proof of Proposition 3.1

We start with Proposition 10.1 which expresses 1-isotopy of ribbon surfaces through moves of planar diagrams. Namely, up to isotopy of planar diagrams, we have three types of moves: those which change the ribbon surface by 3-dimensional diagram isotopy while preserving the ribbon intersections and the core graph, described in Figure 23 (p. 20); those which change the core graph, depicted in Figure 24 (p. 21); those which interpret the 1-isotopy moves of Figure 17 in terms of planar diagrams, as shown Figure 25 (p. 21). Of course, in this context we disregard the moves of Figure 22 (p. 20), since isotopy of planar diagrams is not required to preserve y-coordinate. These last moves will become relevant when we will switch to the categorical point of view of Proposition 3.1.

PROPOSITION 10.1. *The ribbon surfaces represented by two planar diagrams are 1-isotopic if and only if their diagrams are related by a finite sequence of planar diagram isotopies (induced by ambient isotopies of the projection plane) and moves as in Figures 23, 24 and 25 (all considered up to planar diagram isotopy).*

Proof. The "if" part is trivial, since all the moves in Figures 23, 24 represent special 3-dimensional diagram isotopies, while the moves in Figure 25 are equivalent to the 1-isotopy moves in Figure 17 up to 3-dimensional diagram isotopy.

In order to prove the "only if" part, we consider two planar diagrams representing ribbon surfaces F_0 and F_1 as regular neighborhoods of their core graphs G_0 and G_1, such that there is a 3-dimensional diagram isotopy $H : (F, G) \times [0, 1] \to R^3$ taking (F_0, G_0) to (F_1, G_1). Contrary to our general convention, here we think of F as a 3-dimensional diagram, i.e a singular surface with ribbon self-intersections in R^3. Notice that the intermediate pairs $(F_t, G_t) = H((F, G), t)$ with $0 < t < 1$ do not necessarily project suitably into R^2 to give planar diagrams.

Of course, we can assume that H is smooth, as a map defined on a pair of smooth stratified spaces, and that the graph G_t regularly projects to a diagram in R^2 for every $t \in [0,1]$, except a finite number of t's corresponding to extended Reidemeister moves for graphs. For such exceptional t's, the lines tangent to G_t at its vertices are assumed not to be vertical.

We define $\Gamma \subset G \times [0,1]$ as the subspace of pairs (x,t) for which the plane $T_{x_t}F_t$ tangent to F_t at $x_t = H(x,t)$ is vertical (if $x \in G$ is a singular vertex, there are two such tangent planes and we require that one of them is vertical).

By a standard transversality argument, we can perturb H in such a way that:

a) Γ is a graph imbedded in $G \times [0,1]$ as a smooth stratified subspace of constant codimension 1 and the restriction $\eta : \Gamma \to [0,1]$ of the height function $(x,t) \mapsto t$ is a Morse function on each edge of Γ;

b) the edges of Γ locally separate regions consisting of points (x,t) for which the projection of F_t into R^2 has opposite local orientations at x_t;

c) the two planes tangent to any F_t at a singular vertex of G_t are not both vertical, and if one of them is vertical then it does not contain both the lines tangent to G_t at that vertex.

As a consequence of *b*), for each flat vertex $x \in G$ of valency one (resp. three) there are finitely many points $(x,t) \in \Gamma$, all of which have the same valency one (resp. three) as vertices of Γ. Similarly, as a consequence of *c*), for each singular vertex $x \in G$ there are finitely many points $(x,t) \in \Gamma$, all of which have valency one or two as vertices of Γ. Moreover, the above mentioned vertices of Γ of valency one or three are the only vertices of Γ of valency $\neq 2$.

Let $0 < t_1 < t_2 < \ldots < t_k < 1$ be the critical levels t_i at which one of the following facts happens:

1) G_{t_i} does not project regularly in R^2, since there is one point x_i along an edge of G such that the line tangent to G_{t_i} at $H(x_i,t_i)$ is vertical;

2) G_{t_i} projects regularly in R^2, but the projection of G_{t_i} is not a graph diagram, due to a multiple tangency or crossing;

3) there is one point $(x_i,t_i) \in \Gamma$ with x_i a uni-valent or a singular vertex of G;

4) there is one critical point (x_i,t_i) for the function η along an edge of Γ.

Without loss of generality, we assume that only one of the four cases above occurs for each critical level t_i. Notice that the points (x,t) of Γ such that $x \in G$ is a flat tri-valent vertex represent a subcase of *2*) and for this reason they are not included in *3*).

For $t \in [0,1] - \{t_1, t_2, \ldots, t_k\}$, there exists a sufficiently small regular neighborhood N_t of G_t in F_t, such that the pair (N_t, G_t) projects to a planar diagram, except for the possible presence of some ribbon intersections projecting in the wrong way, as in the left side of Figure 132 (notice the difference with the ribbon intersection

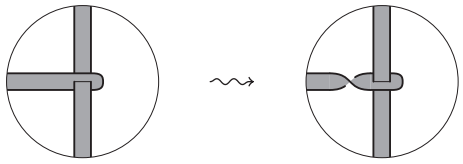

FIGURE 132. Reversing a wrong projection by an auxiliary half-twist.

in Figure 18). We fix this problem by inserting an auxiliary positive half-twists along the tounges containing those ribbon intersections, as shown in the right side of Figure 132. The resulting ribbon surfaces, still denoted by N_t, projects to a true planar diagram.

Actually, we modify the N_t's all together to get a new isotopy where no wrong projection of ribbon intersection occurs, so that N_t projects to a true planar diagram for each $t \in [0,1] - \{t_1, t_2, \dots, t_k\}$. Namely, at each critical level when a wrong projection of a ribbon intersection is going to appear in the original isotopy, we insert an auxiliary half-twis, to prevent the projection from becoming wrong. Such half-twist remains close to the ribbon intersection until the first critical level when the projection becomes good again in the original isotopy (remember that 3-dimensional diagram isotopy preserves ribbon intersections). At that critical level we remove the auxiliary half-twist. We remark that the second part of condition c) is violated when inserting/removing an auxiliary half-twist at critical points of type *2*), as it can be seen by looking at Figure 133.

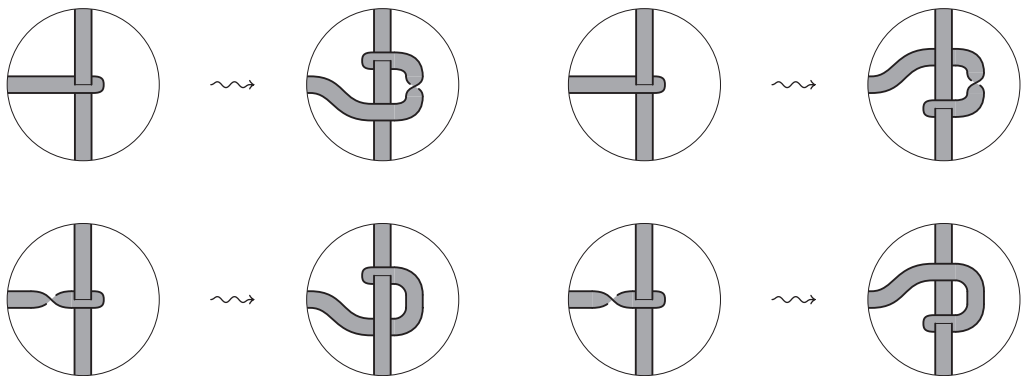

FIGURE 133.

We observe that the planar diagram of N_t is uniquely determined up to diagram isotopy by that of its core G_t and by the tangent planes of F_t at G_t. In fact, the half-twists of N_t along the egdes of G_t correspond to the transversal intersections of Γ with $G \times \{t\}$ and their signs, depend only on the local behaviour of the tangent planes of F_t. In particular, the planar diagrams of (N_0, G_0) and (N_1, G_1) coincide, up to diagram isotopy, with the original ones of (F_0, G_0) and (F_1, G_1).

If the interval $[t', t'']$ does not contain any critical level t_i, then each single half-twist persists between the levels t' and t'', and hence the planar isotopy relating the diagrams of $G_{t'}$ and $G_{t''}$ also relate the diagrams of $N_{t'}$ and $N_{t''}$, except for possible slidings of half-twists along ribbons over/under crossings. Therefore the planar diagrams of $(N_{t'}, G_{t'})$ and $(N_{t''}, G_{t''})$ are equivalent up to diagram isotopy and moves (*I8-9*) in Figure 23.

On the other hand, if the interval $[t', t'']$ is a sufficiently small neighborhood of a critical level t_i, then the planar diagrams of $N_{t'}$ and $N_{t''}$ are related by the moves in Figure 23, depending on the type of t_i as follows.

If t_i is of type *1*), then a positive/negative kink is appearing (resp. disappearing) along an edge of the core graph. When the kink is positive and (x_i, t_i) is a local maximum (resp. minimum) point for η, i.e. two positive half-twists along the ribbon

corresponding to the edge are being converted into a kink (resp. viceversa), the diagrams of $N_{t'}$ and $N_{t''}$ are directly related by move (*I11*). The cases when (x_i, t_i) is not a local maximum (resp. minimum) point for η, that is one or two negative half-twists appear (disappear) together with the kink, can be reduced to the previous case by means of move (*I12*). On the other hand, by using the regular isotopy moves (*I7-9*) in order to create or delete in the usual way a pair of canceling kinks (without introducing any half-twist) along the ribbon, we can reduce the case of a negative kink to that of a positive one.

If t_i is of type *2*), then either a regular isotopy move is occurring between $G_{t'}$ and $G_{t''}$ or two tangent lines at a tri-valent vertex x_i of the graph project to the same line in the plane. In the first case, the regular isotopy move occurring between $G_{t'}$ and $G_{t''}$, trivially extends to one of the moves (*I7-9*). In the second case, x_i may be either a flat or a singular vertex. If x_i is a flat vertex, then the tangent plane to F_t at $H(x_i, t)$ is vertical for $t = t_i$ and its projection reverses the orientation when t passes from t' to t''. Move (*I15*) (modulo moves (*I7*) and (*I12*)) describes the effect on the diagram of such a reversion of the tangent plane. If x_i is a singular vertex, then $N_{t'}$ changes into $N_{t''}$ in one of the four ways shown in Figure 132. In the top (resp. bottom) line auxiliary half-twists are inserted (resp. removed) according to what we have said above, while left and right columns differ for the edges which present the common tangency at the critical level. All these modifications can be reduced to moves (*I14-14'*) by using moves (*I7*) and (*I12*).

If t_i is of type *3*), then either a half-twist is appearing/disappearing at the tip of the tongue of surface corresponding to a uni-valent vertex or one of the two bands at the ribbon intersection corresponding to a singular vertex is being reversed in the plane projection. The first case corresponds to move (*I13*) (here we have a positive half-twist, for dealing with a negative one we combine this move with (*I12*)). The second case may happen in two different ways, depending on which band is being reversed. If such band is the one passing through the other in the ribbon intersection, then, we can transform $N_{t'}$ into $N_{t''}$ by applying moves (*I10*) and (*I12*). Otherwise, the projection of the ribbon intersection is changing from good to wrong one or viceversa, and the appearing/disappearing half-twist is compensated by the auxiliary one up to move (*I12*).

Finally, if t_i is of type *4*), a pair of canceling half-twists is appearing or disappearing along an egde of the graph. This is just move (*I12*).

At this point, in order to conclude that the moves in the statement of the theorem suffice to realize 3-dimensional diagram isotopy between any two planar diagrams of a given ribbon surface F, it is left to prove that, given two different core graphs G', G'' of F as above, the planar diagrams F' and F'' determined respectively by G' and G'', are related by those moves. This is quite straightforward. In fact, by cutting F along the ribbon intersection arcs, we get a new surface $\widehat{F}$ with some marked arcs. This operation also makes the graphs G' and G'' into two simple spines T' and T'' of $\widehat{F}$ relative to those marked arcs (Figure 134 shows the effect of the cut at the ribbon intersections in Figure 20).

From intrinsic point of view, that is considering $\widehat{F}$ as an abstract surface and forgetting its inclusion in R^3, the theory of simple spines tells us that the moves in Figures 20 and 24 suffice to transform T' into T''. In particular, the first and last

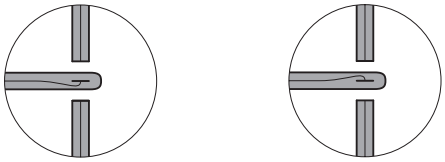

FIGURE 134.

moves in Figure 24 correspond to the well known moves for simple spines of surfaces, while the one in the midle relates the different positions of the spine with respect to the marked arcs in the interior of $\widehat{F}$. It remains only to observe that, up to a 3-dimensional diagram isotopy preserving the core graph, hence up to the moves in Figure 23, the portion of the surface involved in each single spine modification can be isolated in the planar diagram as in Figure 24.

An analogous observation holds for the moves in Figure 25, which realize in terms of planar diagrams the 1-isotopy moves of Figure 17, up to 3-dimensional diagram isotopy. □

Now we need to restrict ourselves to planar diagrams which are oriented in a special way with respect to the y-axis. This requires an explicit description of the ambient isotopy in the projection plane in terms of moves.

A planar diagram of an rs-tangle is said to be in *normal position* with respect to the y-axis if its core graph satisfies the following properties:

a) each edge projects to a regular smooth arc immersed in $R \times [0, 1]$, such that the y-coordinate restricts to a Morse function on it;

b) vertices, half-twists, crossings and local minimum/maximum points for the y-coordinate along the edges have all different y-coordinate (in particular, there are no horizontal tangencies at vertices, half-twists and crossings).

Figure 135 shows the different ways, up to plane isotopy preserving y-coordinate, to put the spots of Figures 18 (p. 18) and 19 (p. 19) in normal position with respect to the y-axis, by planar diagram isotopies wich do not introduce any local minimum/maximum for the y-coordinate along the edges of the core graph.

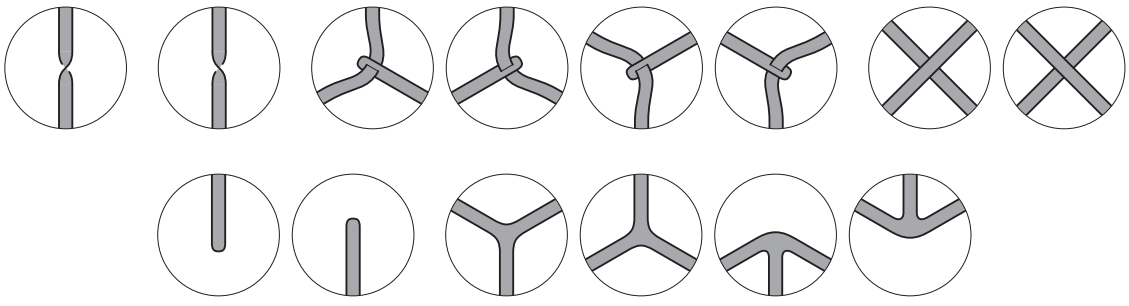

FIGURE 135.

We notice that all such local configurations appear among the elementary rs-tangle diagrams in Figure 21 (p. 20), except for some of those at tri-valent vertices of the core graph. Namely, only the first two of those at a singular vertex (that means at a ribbon intersection) and the first of those at a flat tri-valent vertex are

considered as elementary rs-tangle diagrams. The others can be expressed in terms of them as in Figure 136.

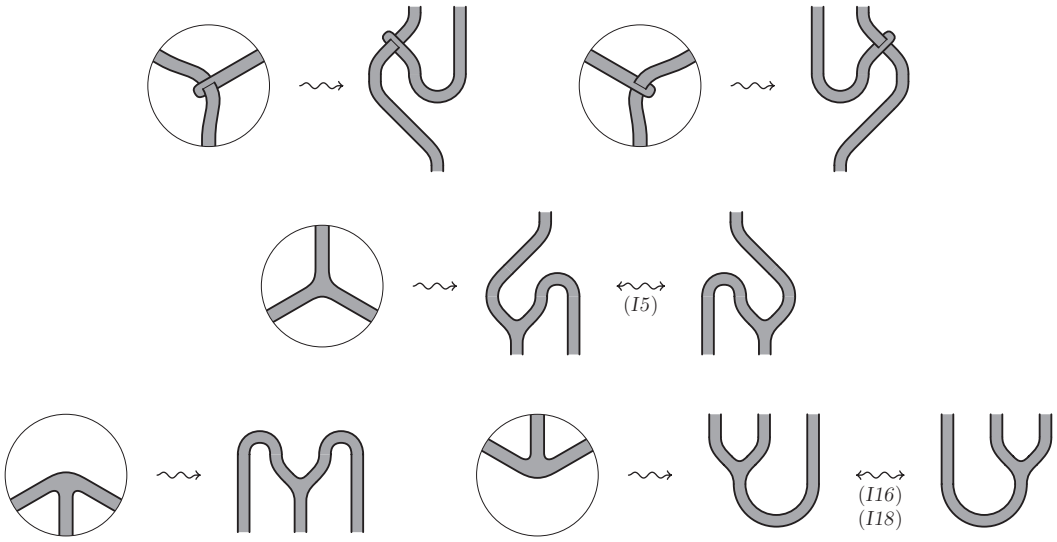

FIGURE 136.

On the other hand, all the elementary rs-tangle diagrams in Figure 21 are in normal position with respect to the y-axis. Hence, this is also true for any iterated product/composition of them, up to vertical perturbations to get property b).

LEMMA 10.2. *Through planar diagram isotopy, any planar diagram of an rs-tangle can be presented as an iterated product/composition of the elementary ones of Figure 21 in normal position with respect to the y-axis. Moreover, any two such presentations of the same rs-tangle are related by a finite sequence of plane isotopies preserving the y-coordinate, moves as in Figures 22 and 137 (all considered up to plane isotopy preserving the y-coordinate).*

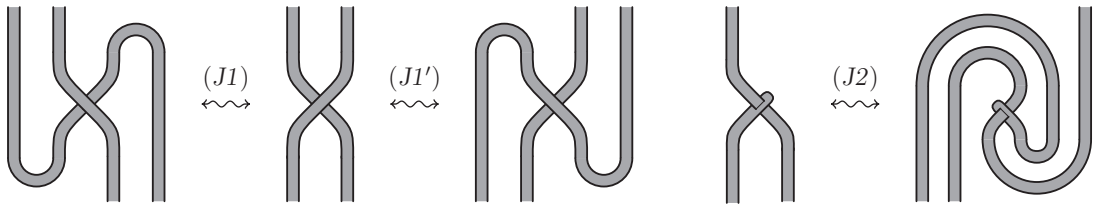

FIGURE 137.

Proof. Here we think of a planar diagram of the core graph of an rs-tangle as a planar graph in itself, whose vertices, other than the uni- and tri-valent flat ones and the singular tri-valent ones, also include bi- and four-valent vertices respectively at the half-twists and at the crossings.

In the light of the discussion above, the first part of the statement is essentially trivial. In fact, any planar diagram can be perturbed to get normal position with respect to the y-axis and then made into an iterated product/composition of the elementary rs-tangle diagrams by local isotopies as in Figure 136.

The proof of the second part is analogous to the proof of the previous Proposition. We start with an arbitrary smooth planar diagram isotopy relating any two given presentions as in the stament. Then we use transversality to perturb this isotopy in such a way the diagram is in normal position with respect to the y-axis at all the levels except a finite number of critical ones. At these critical levels the planar diagram of the core graph presents exactly one of the following properties:

1) the y-coordinate on one edge is not a Morse function;
2) one of the vertices (including half-twists and crossings) has a horizontal tangent;
3) two points among the extremal ones along edges and the vertices (including half-twists and crossings) have the same y-coordinate.

Away from critical levels the isotopy can be assumed to preserve the y-coordinate, while, as it is argued below, the moves of Figures 22 and 137 allow us to realize all the changes occurring in the planar diagram when passing through one critical level.

In fact, the cases of critical levels of types *1*) and *3*) are respectively covered by moves (*I2-2′*) and (*I1*). At critical levels of type *2*) the vertex with horizontal tangency is swiching from one to another of its normal positions depicted in Figure 135. At the same time one extremal point (resp. one pair of canceling extremal points) for the y-coordinate is appearing/disappearing along the edge (resp. the opposite edges) presenting the horizontal tangency. The cases when the vertex we are considering is a uni-valent flat vertex, a half-twists or a crossing correpond respectively to moves (*I3*), (*I4*) and (*J1-1′*), modulo moves (*I1*) and (*I2-2′*). On the other hand, in order to deal with singular and tri-valent flat vertices, we need to replace the normal positions which are missing in the elementary diagrams as indicated in Figure 136. After that, modulo moves (*I1*) and (*I2-2′*), all the cases reduce to moves (*I6*) and (*J2*) for singular vertices, and to move (*I5*) for tri-valent vertices. □

Proof of Proposition 3.1. First of all we observe that in Proposition 10.1 the moves of Figures 23–25 are considered up to plane isotopy, disregarding their normal position with respect to the y-axis. On the contrary, here those moves need to be interpreted in a more restrictive way, assuming that they are in the preferred normal position given in the figures, up to plane isotopy preserving the y-coordinate. However, as a consequence of Lemma 10.2, the two points of view coincide in the presence of the moves of Figures 22 and 137.

Then Proposition 3.1 immediately follows from Proposition 10.1 and Lemma 10.2, once the auxiliary moves in Figure 137 are shown to be consequences of those in Figures 22–25. Actually, move (*J1-1′*) can be easily derived from the moves (*I2-2′*), (*I7-7*) and (*I8-9*), while Figure 138 describes how to get (*J2*). □

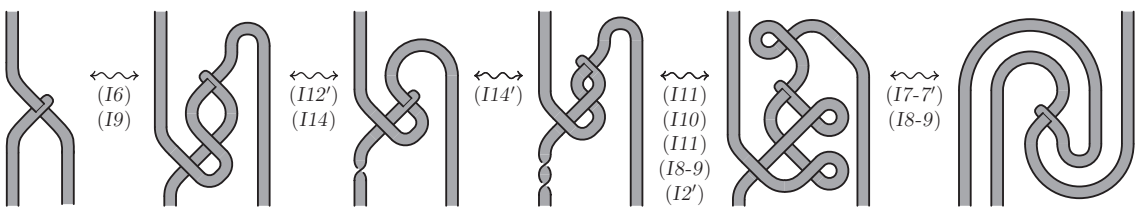

FIGURE 138.

11. Appendix: proof of some relations in $\mathcal{H}^r(\mathcal{G})$

Here we prove the relations in Figures 55 and 56 and show that $(r8')$ is a consequence of the rest of the axioms for $\mathcal{H}^r(\mathcal{G})$.

We start with the "easy" isotopy moves in Figure 55, postponing the proof of $(p3)$ to the end. $(p4)$ is a direct consequence of the definition $(f2)$ in Figure 41 and of the axioms $(r4)$ and $(r5\text{-}5')$ in Figure 50. Concerning $(p5)$ and $(p5')$, they can be seen to be equivalent by using $(f6\text{-}6')$ in Figure 46 and $(p1)$ in Figure 53. On the other hand, they are trivial when $i \neq j$, due to the definition $(r7)$ and the duality moves in Figure 45, while the proof of $(r5')$ for $i = j$ is given in Figure 139.

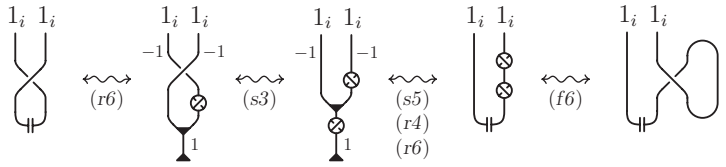

FIGURE 139. Proof of $(p5')$ for $i = j$ [f/35, r/37, s/30-31].

As already mentioned, $(p5)$ and $(p5')$ are particular cases of a more general set moves which allow to interchange the positions of any coform and copairing appearing on the same string connecting two polarized vertices. We want to show that $(p5)$ and $(p5')$ actually imply all such moves. Since the braid axioms in Figure 34 allow coforms and copairings to pass crissings when we slide them along strings, we can assume that the coform and the copairing which we want to exchange are contiguous as in Figure 140. Now, the first move in this figure is a trivial consequence of move $(f3\text{-}3')$ in Figure 41, while the other two are equivalent to $(p5)$ and $(p5')$ up to $(f3\text{-}3')$ and the braid axioms.

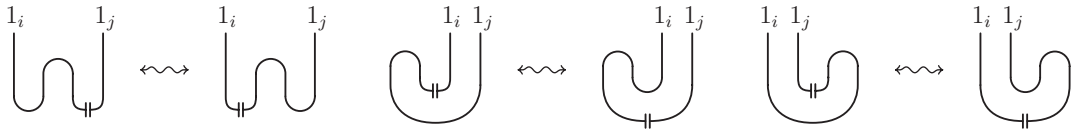

FIGURE 140.

Observe that the proof of $(p5')$ and therefore of the moves interchanging coforms copairings appearing on the same string, uses only two of the ribbon axioms: the definition of copairing ($(r6)$ in Figure 51) and the commutativity of the ribbon morphism with the antipode ($(r4)$ in Figure 50). It is easy to see that $(r8')$ can be obtained from $(r8)$ through such interchangings and the braid axioms. Therefore $(r8')$ is a consequence of the rest of the axioms of $\mathcal{H}^r(\mathcal{G})$.

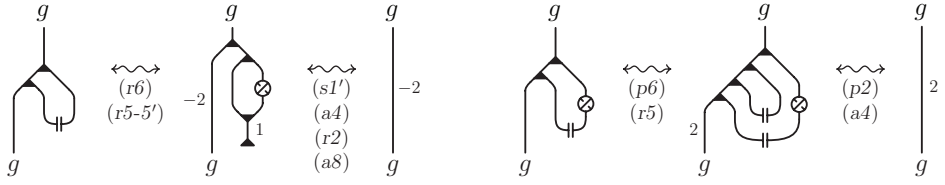

FIGURE 141. Proof of $(p6)$ and $(p7)$ [p/40, r/37-37, s/30].

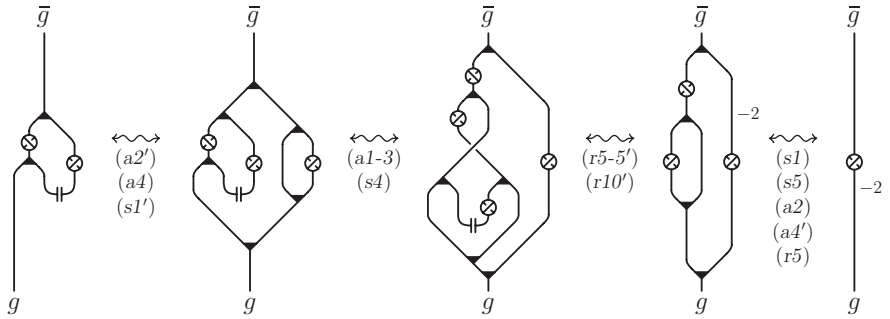

FIGURE 142. Proof of (*p8*) [a/29, *p*/39, *r*/37-41, *s*/30-31].

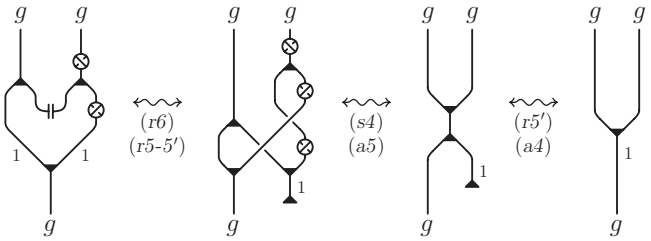

FIGURE 143. Proof of (*p10*) [a/29, *r*/37-37, *s*/30].

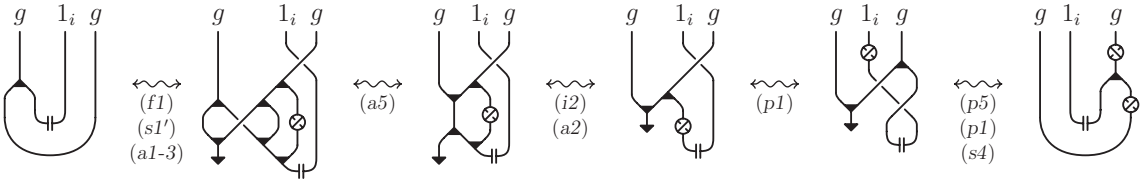

FIGURE 144. Proof of (*p11*) [a/29, *f*/33, *i*/34, *s*/30-31, *p*/39-40].

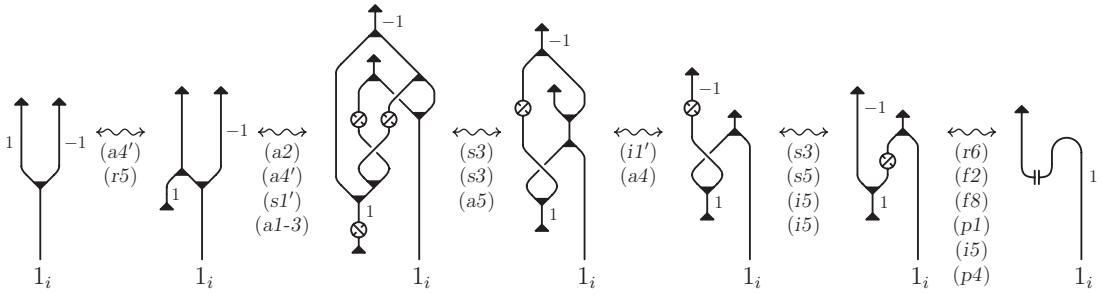

FIGURE 145. Proof of (*p12*) [a/29, *f*/35, *i*/34, *p*/39, *r*/37-37, *s*/31].

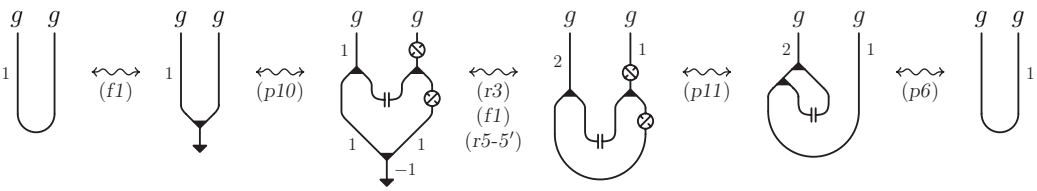

FIGURE 146. Proof of (*p3*) [*f*/33, *p*/40, *r*/37].

The proof of the moves in Figure 56 is given in Figures 141–145. We limits ourselves to consider the moves (*p6*)–(*p10*), being the proof of the corresponding

moves $(p6')$–$(p10')$ analogous. Observe that $(p9)$ follows from $(p8)$ in the same way as $(p7)$ follows from $(p6)$ (cf. Figure 141) and we leave the proof to the reader.

Finally, we prove $(p3)$ in Figure 146.

References

[1] I. Bobtcheva, M.G. Messia, *HKR-type invariants of 4-thickenings of 2-dimensional CW-complexes*, Algebraic and Geometric Topology **3** (2003), 33–87.

[2] I. Bobtcheva, R. Piergallini, *Covering Moves and Kirby Calculus*, preprint ArXiv:math.GT/0407032.

[3] I. Bobtcheva, F. Quinn, *The reduction of quantum invariants of 4-thickenings*, Fundamenta Mathematicae **188** (2005), 21–43.

[4] Y. Bespalov, T. Kerler, V. Lyubashenko, V. Turaev, *Integrals for braided Hopf algebras*, preprint ArXiv:q-alg/9709020.

[5] R. Fenn, C. Rourke, *On Kirby's calculus of links*, Topology **18** (1979), 1–15.

[6] R.E. Gompf, A.I. Stipsicz, *4-manifolds and Kirby calculus*, Grad. Studies in Math. **20**, Amer. Math. Soc. 1999.

[7] M. Iori, R. Piergallini, *4-manifolds as covers of S^4 branched over non-singular surfaces*, Geometry & Topology **6** (2002), 393–401.

[8] K. Habiro, *Claspers and finite type invariants of links*, Geometry & Topology, **4** (2000), 1–83.

[9] M. Hennings, *Invariants from links and 3-manifolds obtained from Hopf algebras*, J. London Math. Soc. (2) **54** (1996), 594–624.

[10] T. Kerler, *Genealogy of nonpertrubative quantum invariants of 3-manifolds – The surgical family*, in "Geometry and Physics", Lecture Notes in Pure and Applied Physics **184**, Marchel Dekker 1997, 503–547.

[11] T. Kerler, *Bidged links and tangle presentations of cobordism categories*, Adv. Math **141** (1999), 207–281.

[12] T. Kerler, V.V. Lyubashenko, *Non-semisimple topological quantum field theories for 3-manifolds with corners*, Lecture Notes in Mathematics **1765**, Springer Verlag 2001.

[13] T. Kerler, *Towards an algebraic characterization of 3-dimensional cobordisms*, Contemporary Mathematics **318** (2003), 141–173.

[14] R. Kirby, *The topology of 4-manifolds*, Lecture Notes in Mathematics **1374**, Springer-Verlag 1989.

[15] G. Kuperberg, *Non-involutory Hopf algebras and 3-manifold invariants*, Duke Math. J. **84** (1996), 83–129.

[16] G. Lusztig, *Introduction to quantum groups*, Progress in Mathematics **110**, Birkhäuser 1993.

[17] S. MacLane, *Natural associativities and commutativities*, Rice Univ. Studies **49** (1963), 28–46.

[18] J.M. Montesinos, *4-manifolds, 3-fold covering spaces and ribbons*, Trans. Amer. Math. Soc. **245** (1978), 453–467.

[19] S. Matveev, M. Polyak, *A geometrical presentation of the surface mapping class group and surgery*, Comm. Math. Phys. **160** (1994), 537–550.

[20] M. Mulazzani, R. Piergallini, *Lifting braids*, Rend. Ist. Mat. Univ. Trieste **XXXII** (2001), Suppl. 1, 193–219.

[21] T. Ohtsuki, *Problems on invariants of knots and 3-manifolds*, Geom. Topol. Monogr. **4**, in "Invariants of knots and 3-manifolds (Kyoto, 2001)", Geom. Topol. Publ. 2002, 377–572.

[22] R. Piergallini, *Covering Moves*, Trans Amer. Math. Soc. **325** (1991), 903–920.

[23] R. Piergallini, *Four-manifolds as 4-fold branched covers of* S^4, Topology **34** (1995), 497–508.

[24] R. Piergallini, D. Zuddas, *A universal ribbon surface in* B^4, Proc. London Math. Soc. **90** (2005), 763–782.

[25] N.Yu. Reshetikhin, V.G. Turaev, *Invariants of 3-manifold via link polynomials and quantum groups*, Invent. Math. **103** (1991), 547–597.

[26] L. Rudolph, *Special position for surfaces bounded by closed braids*, Rev. Mat. Ibero-Americana **1** (1985), 93–133; revised version: preprint 2000.

[27] M.C. Shum, *Tortile tensor categories*, Journal of Pure and Applied Algebra **93** (1994), 57–110.

[28] T. Standford, *Finite type invariants of knots, links and graphs*, Topology **35** (1996), 1027–1050.

[29] A. Virelizier, *Algébres de Hopf graduées et fibrés plats sur les 3-variétés*, PhD thesis, Institut de recherche mathématique avancée, Université Louis Pasteur et CNRS 2001.